

**MOLECULAR AND BIOCHEMICAL CHARACTERIZATION OF THE T
LYMPHOCYTE TYPE *N* POTASSIUM CHANNEL**

by

Yun-Cai Cai

A DISSERTATION

Presented to the Department of Microbiology and Immunology
Oregon Health Sciences University
School of Medicine

in partial fulfillment of
the requirements for the degree of

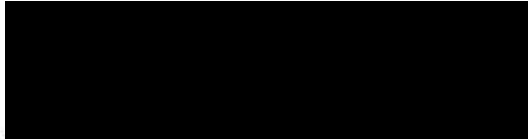
Doctor of Philosophy

March 1993

Approved:

A black rectangular box redacting a signature.

(Professor in Charge of Thesis)

A black rectangular box redacting a signature.

(Chairman, Graduate Council)

ACKNOWLEDGEMENTS

I would like to give my special thanks to Dr. Douglass for his encouragement and support during the entire course of my project. In addition, I also appreciate his effort to teach me the English language.

I am indebted to many people in the Vollum Institute and Microbiology Department, who contributed their ideas, technical expertise, and friendship. Among them, I would like to mention Dr. Adelman, a devoted scientist, for his critical advice and great help; and Dr. Wilkinson, for his valuable advice.

I would like to share my enjoyment with those people (especially those in the Douglass and Adelman labs), who create so much happiness and fun out of science and daily life. And I also appreciate their teaching me so much great American slang.

This thesis is a special gift to my parents for their encouragement, and full support of all my educational seeking.

Finally, I would like to devote my thesis to Xiaowen for her consistent support and love.

TABLE OF CONTENTS

Abbreviations.....	i
List of Figures and Tables.....	iii
Abstract.....	v
Introduction.....	1
1. Molecular basis underlying the diversity of voltage-gated potassium channels.....	2
2. Voltage-gated potassium channels and T lymphocyte functions.....	8
3. Regulation of voltage-gated potassium channel function by protein phosphorylation.....	15
4. Specific aims of the thesis.....	17
5. Historical aspects of the thesis regarding research performed.....	18
Results and Manuscripts	
1. Characterization and Functional Expression of a Rat Genomic DNA Clone Encoding a Lymphocyte Potassium Channel.....	22
2. Characterization and Functional Expression of Genomic DNA Encoding the Human Lymphocyte Type <i>n</i> Potassium Channel.....	42
3. <u>In vivo</u> and <u>in vitro</u> Phosphorylation of the T Lymphocyte type <i>n</i> (Kv1.3) Potassium Channel.....	60
4. Functional Significance of a Highly Conserved Serine Residue Within the Intracellular S4/5 Loop of Mammalian Potassium Channels.....	85

Summary and Discussion.....	97
References.....	105

ABBREVIATIONS

4-AP	4-Aminopyridine
C-	carboxyl-
ConA	Concanavalin A
CFTR	cystic fibrosis transporter
CTX	charybdotoxin
α -DTX	α -dendrotoxin
EAE	experimentally-induced encephalomyelitis
FCS	fetal calf serum
GABA	γ -aminobutyric acid
IL-2	interleukin-2
IPTG	isopropyl- β -D-thiogalactoside
IP3	inositol trisphosphate
Mal-E	maltose binding protein
MBP	myelin basic protein
mRNA	messenger RiboNucleic Acids
ms	milliseconds
mV	milliVolts
N-	amino-
NK	natural killer cells
pS	picoSiemens
PCR	polymerase chain reaction
PKA	cAMP-dependent protein kinase
PKC	protein kinase C
PMSF	phenylmethylsulfonyl fluoride

Tc	cytotoxic T cells
Th	helper T cells
TPA	12- <i>O</i> -tetradecanoylphorbol-13-acetate
Ts	suppressor T cells
TEA	tetraethylammonium

LIST OF FIGURES AND TABLES

Figure 1.1	The proposed topological structure of voltage-gated potassium channels.....	118
Figure 2.1	Diagram of rat genomic DNA clones RCK1 and RGK5.....	119
Figure 2.2	Nucleotide and predicted translation product sequences of the RGK5 clone.....	120
Figure 2.3	Amino acid sequence alignment of the cloned rat potassium channels RGK5, RBK1, RBK2, and DRK1.....	121
Figure 2.4	Rat genomic Southern blot analysis of the RGK5 clone.....	122
Figure 2.5	Rat Northern blot analysis of RGK5 transcripts.....	123
Figure 2.6	Expression of the RGK5 clone in <i>Xenopus</i> oocytes.....	124
Table 2.1	Comparison of biophysical properties of RGK5, RCK3, and murine T lymphocyte type <i>n</i> potassium channels.....	125
Figure 3.1	Diagram and nucleotide and deduced amino acid sequences of the HGK5 clone.....	127
Figure 3.2	Human genomic Southern and Northern blot analysis of the HGK5 clone.....	128
Figure 3.3	Expression of the HGK5 clone in <i>Xenopus</i> oocytes	129
Figure 3.4	Inactivation properties of expressed HGK5 channels.....	130
Figure 3.5	The effects of blocking drugs on expressed HGK5 currents.....	131
Figure 3.6	[³ H] thymidine incorporation plot of ConA stimulation of human T cells.....	132
Figure 3.7	Effects of ConA treatment on cellular levels of HGK5 mRNA in human T lymphocytes.....	133
Table 3.1	Comparison of functional properties of HGK5 and human T	

	lymphocyte type <i>n</i> potassium channels.....	134
Figure 4.1	Amino acid sequence alignment of mouse, rat, and human Kv1.3 potassium channels.....	135
Figure 4.2	Amino acid sequence of hKv1.3 regions used to generate MalE fusion proteins.....	136
Figure 4.3	Characterization of antisera against MalE - hKv1.3 fusion proteins.....	137
Figure 4.4	Immunoprecipitation of 65-kDa, ³² P radiolabeled hKv1.3 from metabolically labeled Jurkat cells.....	138
Figure 4.5	Phosphoamino acid analysis of 65-kDa, ³² P radiolabeled Jurkat hKv1.3 following immunoprecipitation with MalE-H1 antiserum..	139
Figure 4.6	<u>In vitro</u> phosphorylation/immunoprecipitation of 65-kDa Jurkat hKv1.3 by PKA.....	140
Figure 4.7	<u>In vitro</u> phosphorylation/immunoprecipitation of 65-kDa Jurkat hKv1.3 by PKC.....	141
Figure 5.1	Amino acid sequence comparison of S4/5 loops between <i>ShB</i> and hKv1.3 and rKv1.2, as well as a list of different mutants.....	142
Figure 5.2	Mutation of hKv1.3 ³⁴² Ser to ³⁴² Ala abolishes ionic currents....	143
Figure 5.3	Gating currents of hKv1.3 ³⁴² Ser and ³⁴² Ala potassium channels.....	144
Figure 5.4	TEA sensitivity of expressed potassium currents indicates functional polymerization between ³⁴² Ala and ³⁹⁹ Tyr subunits...	145
Figure 6.1	Amino acid alignment of the S4/5 loops among voltage-gated and calcium-activated potassium channels.....	146

ABSTRACT

The type *n* voltage-gated potassium channel plays important functional roles in the development and activation of T lymphocytes. Screening of a rat genomic DNA library at low stringency with a rat Kv1.1 coding sequence has resulted in the characterization of a rat Kv1.3 potassium channel clone, RGK5, which was used to generate a human Kv1.3 clone, HGK5, from a human genomic DNA library. Sequence analysis reveals uninterrupted nucleotide sequences encoding polypeptides of 525 and 523 amino acids in length, respectively. RNAs transcribed in vitro from these two clones direct expression of functional voltage-gated potassium currents in *Xenopus* oocytes. The functional characteristics of the expressed Kv1.3 channels are strikingly similar to those of the type *n* channels on murine and human T lymphocytes, respectively. This, together with the presence of significant levels of Kv1.3 transcripts in both murine and human T lymphocytes, supports the notion that both Kv1.3 clones encode the type *n* voltage-gated potassium channels. Activation of both murine and human T cells with ConA induced a time-dependent decrease in Kv1.3 mRNA levels, suggesting that previously observed increases in potassium current density following mitogen activation are not due to increased transcriptional activity of the type *n* potassium channel gene.

Several polyclonal antisera against different regions of Kv1.3 have been developed. A 65-kDa protein is identified by immunoprecipitation with these antisera in both murine and human T cell lines. The size of the endogenous type *n* channel protein is larger than the in vitro translated product of 58-kDa, indicating in vivo posttranslational modification events. Whole cell labeling studies revealed that the type *n* channel is phosphorylated by endogenous kinases in Jurkat cells. Phosphoamino acid analysis of the metabolically labeled type *n* channel reveals phosphorylation of serine residues exclusively. In vitro studies also describe the ability of both PKA and PKC to phosphorylate the Jurkat type *n*

channel. However, PKC phosphorylation requires pre-treatment with phosphatase, indicating basal phosphorylation on PKC sites in Jurkat cells. Additionally, PKA also phosphorylates a 40-kDa protein which co-immunoprecipitates with the type *n* channel. Thus, phosphorylation of channel-associated proteins may also serve as a means by which the channel activity is regulated, in addition to phosphorylation of the type *n* channel itself.

The intracellular S4/5 loop has been suggested to mediate potassium channel gating and/or potassium permeation. Conservative mutation of ³⁹²Ser within this region has been reported to inhibit the channel conductance of the *ShB* potassium channel by 40%. The results presented here reveal that the corresponding serine mutation to alanine produces similar but more dramatic effects on the channel conductance of two mammalian potassium channels (rKv1.2 and hKv1.3), with complete elimination of potassium currents. Studies of gating currents and coexpression analysis of hKv1.3 ³⁴²Ala and ³⁹⁹Tyr further indicate that the hKv1.3 ³⁴²Ser mutation does not disrupt gating charge movement or subunit assembly.

INTRODUCTION

Ions are essential for living cells. The cellular membranes are lipid bilayers which form an impermeable barrier to ions. Thus, special membrane proteins such as pumps and channels are required for the exchange of ions between the internal and external environments. Pumps are energy-driven transporters which are involved in generation and maintenance of ion concentration gradients; high potassium and chloride, and low sodium and calcium concentrations within the cytoplasm of eukaryocytes. Ion channels, on the other hand, form an aqueous pore for ions to passively pass through the lipid bilayer (Hille, 1984; Rudy, 1988). When compared to ion transporters, the flow rates through ion channels are remarkably fast, with more than 1 million ions passed per second. The normal resting membrane potential of many cell types is negative intracellularly, around -60 mV, contributing to high permeability of potassium ions. The direction of ion flow through ion channels is, thus, determined by electrochemical gradient. The net influx of positive charge decreases intracellular negative potential which is called depolarization; the efflux causes hyperpolarization. The primary functions of ion channels involve the regulation of intracellular ion concentrations (biochemical signaling) and cell membrane potentials (electrical signaling). Ion channels are also involved in mediating numerous cellular functions, including excitation of neuronal cells, contraction of muscle cells, secretion in endocrine cells, and mitogen induced cell responses (Jan and Jan, 1989).

Ion channels fluctuate between opened and closed states. Various factors (including membrane potential, chemical messengers, and mechanical stimuli) are known to affect the opening of ion channels, thus serving as the basis by which to distinguish ion channels into subfamilies such as ligand-, voltage-, and stretch-gated ion channels. Ion channels can also be subgrouped based on their ion selectivity. For example, the

potassium channel family consists of voltage-, calcium-, ATP-, and G protein-gated channels, to name a few.

Voltage-gated ion channels are those that open in response to alteration of membrane potentials. The principal members among voltage-gated cationic channels are voltage-gated sodium, potassium, and calcium channels. Each species of ion channel contains a very selective pore permeable to a restrictive spectrum of ions.

Voltage-gated potassium channels are membrane potential-dependent ion channels specialized in potassium ion translocation across the membrane. They are also involved in repolarization and maintenance of the cell membrane. These ion channels are ubiquitously distributed and have been detected in almost every eukaryotic cell type examined (Rudy, 1988). However, potassium channels are not uniform; a variety of potassium channels with variant properties in channel dynamics have been described. Furthermore, unique combinations of different types of potassium channels have been described in cell- and tissue-specific patterns. Thus, potassium channels play very diverse roles in cell functions. In neuronal cells, for example, a great diversity of potassium channels are used to control the timing, frequency, and number of action potentials, which in turn regulate neuronal excitability and neurotransmitter release.

1. Molecular basis underlying the diversity of voltage-gated potassium channels

Molecular characterization of voltage-gated potassium channels

Molecular cloning -- Sodium and calcium channels exist in large quantities in specialized neuronal tissues, and were purified to near homogeneity with high affinity ligands. The availability of purified proteins provided the basis to generate antibodies for the initial cloning of these channels (Ellis et al., 1988; Noda et al., 1984). However, isolation of a large amount of purified potassium channels was not successful because of

the relatively low degree of expression of potassium channels in various tissues. With the availability of genetic mutants in *Drosophila*, the *Shaker* potassium channel gene was first localized to a segment of X chromosome (Tanouye et al., 1981). Subsequent chromosomal walking, genomic DNA isolation, and cDNA isolation coupled with nucleotide sequence analysis eventually defined the coding region of the *Shaker* gene (Papazian et al., 1987). The coding region spans approximately 130 kb and contains at least 20 exons. Additionally, multiple potassium channel mRNAs are generated by alternative splicing at the *Shaker* locus (Papazian et al., 1987; Pongs et al., 1988; Schwarz, et al., 1988; Tempel et al., 1987). Potassium channels encoded by these mRNAs share a core sequence with variation at N- and C-termini. Several *Shaker* potassium channels have been functionally expressed in *Xenopus* oocytes (Iverson et al., 1988; Timpe et al., 1988a; Timpe et al., 1988b). The expressed currents exhibit properties of the family of A-type potassium channels, with each manifesting unique electrophysiological and pharmacological properties. Employing low stringency hybridization screening of *Drosophila* genomic DNA libraries, additional potassium channel genes have been identified, which include the *Shab*, *Shaw*, and *Shal* loci (Butler et al., 1989; Wei et al., 1990). Additionally, a potential voltage-gated potassium channel gene, the *eag* locus, has been identified by genetic cloning in *Drosophila* (Warmke et al., 1991). Like the *Shaker* gene locus, the *Shal* gene produces at least two different potassium channels by alternative mRNA splicing. Expression in *Xenopus* oocytes indicates that the different *Shal* transcripts encode functional potassium channels. The *Shal* channels exhibit features of A-type potassium channels, similar to those of the *Shaker* channels. In contrast, both the *Shab* and *Shaw* genes encode delayed rectifier potassium channels. In summary, gene duplication contributes to the diversity of potassium channels in *Drosophila*, in addition to extensive mRNA splicing mechanisms.

Many mammalian potassium channels have been identified by employing *Drosophila* potassium channel nucleotide sequences as hybridization probes, as well as by

expression cloning (Christie et al., 1989; Douglass et al., 1990; Frech et al., 1989; McCormack et al., 1990a; McKinnon, 1989; Pak et al., 1991a, 1991b; Stuhmer et al., 1989; Swanson et al., 1990; Tempel et al., 1988; Wei et al., 1990; Yokoyama et al., 1989). These channels all exhibit unique functional properties when expressed in *Xenopus* oocytes. Mammalian voltage-gated potassium channels have been subdivided into four subfamilies based on homology with the four distinct potassium channel encoding loci in *Drosophila*, and a nomenclature has since been adopted (Chandy et al., 1991). The Kv1 group corresponds to the *Shaker* family, while the Kv2, Kv3, and Kv4 groups represent the *Shab*, *Shaw*, and *Shal* families, respectively. Approximately 40% homology at the amino acid level is observed between different subfamilies, while 50% to 70% homology is observed between members of the same family. In contrast to *Drosophila*, mammalian Kv1 potassium channels are encoded by distinct genes, with no intron located within protein coding regions. Although alternative splicing of coding region exons has been discovered for the Kv3 subfamily (Luneau et al., 1991), it appears to be a relatively rare event in the mammalian potassium channel genes characterized to date. Therefore, duplication and divergence of potassium channel genes appears to be the major mechanism underlying the generation of multiple species of voltage-gated potassium channels in mammals.

In addition to six membrane domain-spanning potassium channels (the Kv family) described above, a single membrane domain-spanning voltage-gated potassium channel (the IsK channel) has been identified in both rat and human (Murai et al., 1989; Takumi et al., 1988). The amino acid sequence shares little homology with those of the Kv family, and does not contain a positively charged motif similar to that of the Kv family. The current from this potassium channel when expressed in *Xenopus* oocytes is very slow in activation, and exhibits properties which are quite different from those of the Kv family. Therefore, IsK represents a distinct family from the Kv family. Nearly all voltage-gated potassium channels mentioned within this thesis are those belonging to the Kv family.

Membrane orientation -- Voltage-gated ion channels are membrane proteins. Hydrophobic plot analysis suggests the presence of six putative membrane-spanning segments (S1 - S6) in Kv potassium channels. There are four homologous repeats of the six membrane-spanning domain motif in sodium and calcium channels; however, a single motif is utilized by Kv potassium channels. The C-terminus and the protein loops connecting the four homologous repeats were first localized intracellularly in the sodium channel using peptide-specific antibodies as probes for channel orientation; the same topology was thus proposed for voltage-gated potassium channels, with both N- and C-termini located intracellularly (reviewed by Catterall, 1988). The intracellular location of the N-terminus was also determined for the *Shaker* potassium channel (Zagotta et al., 1990). Furthermore, TEA can block potassium channel currents when applied from either side of the membrane, and such binding sites have been identified on the loop between S5 and S6 membrane-spanning regions (MacKinnon et al., 1990; Yellen et al., 1991). Thus, the loop between S5 and S6 regions must span the lipid bilayer. Fig. 1.1 represents the best knowledge about the topological structure for voltage-gated potassium channels.

Voltage-gated potassium channels form a tetramer structure -- The voltage-gated potassium channel pore is created by the close association of four homologous transmembrane domains, as suggested for sodium and calcium channels. Thus, functional potassium channels appear to result from the formation of a tetramer structure through the association of individual potassium channel subunits. Several approaches have been used to test the theory of tetramer formation. First, co-expression of two potassium channel subunits with distinct properties in *Xenopus* oocytes resulted in the generation of a pool of heterooligomeric potassium channels, with features distinct from the algebraic summation of those from two homomeric channels (Christie et al., 1990; Isacoff et al., 1990; McCormack et al., 1990; Ruppersberg et al., 1990). Additionally, expression of non-functional truncated potassium channels interfered with normal potassium channel functions in transgenic *Drosophila melanogaster* (Gisselmann et al., 1989). Thus,

individual subunits must interact with each other in order to form functional potassium channels. Furthermore, the tetramer structure was deduced from co-expression studies, in which the interaction of CTX with co-expressed wild-type and toxin-insensitive mutant *Shaker* potassium channel subunits was analyzed (MacKinnon, 1991). Taken together, these studies provide support for the notion that four channel subunits constitute a functional potassium channel, resembling the structure of sodium and calcium channels.

Structural features of voltage-gated potassium channels

Several structural components have been characterized which are important to voltage-gated potassium channel function. These include a voltage sensor which is involved in monitoring membrane potential; an aqueous pore for the selection and passage of potassium ions; and gates for channel inactivation (Aldrich, 1989; Guy and Conti, 1990; Jan and Jan, 1992; MacKinnon, 1991).

The voltage sensor -- Voltage dependent activation is a prominent feature of voltage-gated ion channels. A potential voltage sensor was first described in sodium channels, and later was found to be conserved in calcium and potassium channels. It is a positively-charged motif with lysine or arginine residues located at every third position in the S4 region. Conversion of these positively charged residues to neutral or negatively-charged residues reduces voltage dependence as well as gating charges during activation (Liman et al., 1991; Logothetis et al., 1992; Papazian et al., 1991; Stuhmer et al., 1989). The steepness of voltage dependence and the number of gating charges are directly correlated with the number of basic residues. Thus, this motif represents a voltage sensor determining voltage-dependent activation. Furthermore, observed differences between time constants of activation can be attributed to the number of basic residues in this voltage sensor in different channels. However, basic residues at different positions are not equivalent in their contributions towards determining voltage-dependence of activation;

mutation of some basic residues in the voltage sensor have been found to exert no effect at all (Logothetis et al., 1992; Papazian et al., 1991). In contrast, nonpolar residue substitutions in the S4 region and S4/5 loop of sodium and potassium channels greatly altered voltage dependence of activation (Auld et al., 1990; McCormack et al., 1991; Lopez et al., 1991). Therefore, the voltage dependence of activation can not be simply attributed to the positively-charged residues in the S4 region.

The hydrophilic pore -- Potassium channels contain an aqueous pore selectively permeable to potassium ions. A sequence of approximately 20 amino acids between S5 and S6 has been suggested to line the wall of the channel pore. It is divided into two short segments, SS1 and SS2, each of which spans the lipid bilayer. The external mouth of the channel consists of areas between S5 and SS1 and between SS2 and S6. Mutational and chimeric studies support this model. Several binding sites for channel blockers have been identified. Charybdotoxin (CTX) and tetraethylammonia (TEA) bind to the external mouth and reduce potassium channel currents (MacKinnon and Miller, 1989). Most interestingly, TEA also binds to a single amino acid residue between SS1 and SS2 of the potassium channel when applied intracellularly (Yellen et al., 1991). Thus, the region between SS1 and SS2 must constitute the internal mouth of the pore. Furthermore, mutations of several residues within the potassium channel pore region alter ion selectivity, single channel conductance, and binding affinity for channel blockers (Kirsch et al., 1992; Yool and Schwarz, 1991). Similarly, single mutations within the SS2 sequence in the sodium channel alter ion selection from sodium to calcium (Heinemann et al., 1992). Therefore, residues within SS1 and SS2 determine ion selectivity and ion flow rate for voltage-gated potassium channels.

Inactivation domains -- Voltage-gated potassium channels open with membrane depolarization; however, they inactivate afterwards even when the membrane is still depolarized. Inactivation of *Shaker* potassium channels is relatively fast and consists of several biophysical processes. At least two types of inactivation processes have been

described. The so-called N-type process can be prevented by intracellular application of proteases, indicating that the N-type inactivation gate is located in the cytoplasm (Hoshi et al., 1990; Zagotta et al., 1989). Such a gate has since been characterized on the N-terminus of the *Shaker* potassium channel (Stocker et al., 1990; Zagotta et al., 1990). This domain interacts with the intracellular mouth of the channel in the region between S4 and S5 to induce fast inactivation (Isacoff et al., 1991). The second classification of inactivation process is referred to as the C-type inactivation. Different C-termini in *Shaker* potassium channels are responsible for the diverse kinetics of C-type inactivation; in addition, a single amino acid within the S6 region also affects the inactivation process (Hoshi et al., 1991). Similarly, sodium channels also inactivate very fast. A region between repeats III and IV within sodium channels has thus far been identified as the fast inactivation gate (Stuhmer et al., 1989; Vassilev et al., 1989). Removal of this segment markedly prolongs the inactivation time.

In summary, voltage-gated potassium channels of the Kv family contain six transmembrane regions with both N- and C- termini located intracellularly. A functional potassium channel represents the formation of a complex consisting of four potassium channel subunits, of either homopolymeric or heteropolymeric composition. A positively-charged motif in the S4 region acts as a part of the voltage sensor to determine voltage dependence of channel activation. The SS1 and SS2 regions line the channel pore and determine ion selectivity and ion flow rate. The regions between S5 and SS1 as well as SS2 and S6 constitute the extracellular mouth of potassium channels, and the internal portions of SS1 and SS2 plus the regions between S4 and S5 become at least a part of the internal mouth. The N-terminus of the *Shaker* potassium channels acts as a ball-and-chain structure (Armstrong and Bezanilla, 1977) to block the internal mouth of the channel, thus inactivating channel currents.

2. Voltage-gated potassium channels and T lymphocyte functions

The immune system consists of mainly two types of effector cells; T and B lymphocytes. B cells are activated to secrete antibodies, while T cells are involved in diverse functions. A subset of T lymphocytes, T helper cells (Th), are required to assist T and B cell activation; cytotoxic (Tc) and natural killer cells (NK) to kill infected cells and tumor cells; and suppressor cells (Ts) to regulate and coordinate immune responses.

Similar to other cell types, ion translocation is also important and required for maintenance of T cell functions. A variety of techniques have been used to study ion flux across the cytoplasmic membrane of T cells. During the last decade, patch-clamp recording has revealed a diverse set of ion channels on T lymphocytes (Lewis and Cahalan, 1990). These ion channels are classified based on ion selectivity and physiological properties. There are two species of potassium channels activated by depolarization or calcium. Sodium channels are not usually observed and are apparently present at very low numbers. Calcium channels are observed only following mitogen-induced T cell activation, and no voltage-gated calcium channels have been detected to date (Cahalan et al., 1985; Fukushima et al., 1984). Chloride channels found on T lymphocytes can be divided into three types. Maxi-chloride channels have a single channel conductance of 300-400 pS and open in response to calcium binding; midi-chloride channels have a single channel conductance of 40 pS and are activated by phosphorylation by cAMP-dependent protein kinase; and mini-chloride channels have a single channel conductance of 1-2 pS and appear to open in response to osmotic alterations. The expression of a species of mRNA encoding a slow activating potassium channel (HIsK) has recently been detected in human T cells (Attali et al., 1992). Of all these ion channels, however, only voltage-gated potassium channels are active in resting T cells. The exact roles these ion channels play are largely unknown; however, limited information suggests that they are important for proper T cell development and function.

Expression of voltage-gated potassium channels in T cells

There are three distinct types of voltage-gated potassium channels found on mammalian T lymphocytes, referred to as the type *n* (stands for "normal"), *n'* ("n-like"), and *l* ("large") channels (Lewis and Cahalan, 1988). These three species of potassium channels are found on resting lymphocytes, and serve to maintain a resting membrane potential of approximately -60 mV. The type *n* potassium channel is the most commonly observed species of voltage-gated potassium channel, and is found on a variety of T cell subtypes. It has a single channel conductance of 12-16 pS, and is sensitive to a unique profile of ion channel blockers. These include classical blockers for voltage-gated potassium channels such as TEA and 4-aminopyridine (4-AP) (DeCoursey et al., 1984; Grissmer and Cahalan, 1989); for calcium-activated potassium channels such as CTX and quinine (DeCoursey et al., 1984; Matteson and Deutsch, 1984; Sands et al., 1989); and for voltage-gated calcium channels such as verapamil and nifedipine (DeCoursey et al., 1985). The type *n* channel is also blocked by calmodulin antagonists, such as trifluoperazine and chlorpromazine (DeCoursey et al., 1985). The type *n'* potassium channel shares many properties with those of the type *n* channel. However, it does contain several unique features; it opens at a more positive potential, does not manifest accumulative inactivation, and is less sensitive to TEA. The type *l* channel is different from these two types in many aspects. It has a large single channel conductance (approximately 21-27 pS), inactivates faster, is more sensitive to TEA, and is unaffected by CTX.

The type *n* potassium channel is expressed in a variety of T cells, including human and murine thymocytes, peripheral T cells, and many T cell clones. In addition, it has also been characterized on B lymphocytes, macrophages, and platelets (reviewed by Lewis and Cahalan, 1990). Conversely, type *n'* and *l* channels are restricted in their expression to murine thymocytes and peripheral T cells which are of CD4⁻/CD8⁺ lineage (Lewis and Cahalan, 1988). They have not been detected in human T cells or human T cell lines.

Interestingly, abnormal expression of the type *I* channel is closely associated with autoimmune diseased mice (Chandy et al., 1986; Grissmer et al., 1988). The type *I* channel is present in large quantities on CD4⁺/CD8⁻ T cells of mice with systemic lupus erythematosus (SLE), non-obese diabetic (NOD), or myelin basic protein-induced encephalomyelitis (MBP-induced EAE).

Calcium signalling is partially controlled by potassium channels during T cell activation

T lymphocytes are activated by occupancy of cell surface receptors with antigens. They can also be activated in vitro by lectins and antibodies (MacDonald and Nabbolz, 1986). Alteration of ion translocation across the membrane is among one of the earliest events observed following T lymphocyte activation. Both influx of calcium and efflux of potassium have been observed and are required for T cell activation (Segel et al., 1979; Weiss and Imboden, 1987). Calcium ions play crucial roles during T cell activation (Gardner, 1989). In human Jurkat leukemic cells, an initial rise of intracellular calcium levels has been recorded immediately following activation (Lewis and Cahalan, 1989). This increase involves 1,4,5-trisphosphate (IP3) mobilization of calcium from internal stores (Berridge and Irvine, 1989). IP3-gated calcium channels have been detected on the endoplasmic reticular membrane in brain cells (Ross et al., 1989), which suggests IP3-gated calcium channels on the endoplasmic reticular membrane in T cells are responsible for the initial rise of intracellular calcium levels. However, sustained increases in calcium levels are also required for cell activation, which requires influx of calcium across the cell membrane (Weiss et al., 1984; Oettgen et al., 1985). IP3-gated calcium channels have also been discovered on the T cell membrane (Kuno et al., 1986; Kuno and Gardner, 1987). Thus, IP3-gated calcium channels are involved in mobilization of calcium from both the endoplasmic reticula and extracellular medium; however, IP3-independent mitogen-induced calcium channels may also be required for calcium influx (Cahalan and Lewis, 1990).

Additionally, potassium channels are required for maintenance of calcium channel activity and sustained calcium increase. Influx of calcium ions causes depolarization of the cell membrane, which activates voltage-gated potassium channels. Intracellular calcium ions also activate calcium-gated potassium channels. Both of these types of potassium channels are present on the T cell membrane. The efflux of potassium thus causes repolarization and slight hyperpolarization of the membrane, which maintains an electrical driving force for calcium influx. On the other hand, calcium ions in very high concentration inactivate voltage-gated potassium channels by becoming trapped inside open potassium channel pores (Bregestovski et al., 1986). Therefore, both calcium-activated and voltage-gated potassium channels are involved in regulating calcium channel activity, and are required for sustained intracellular calcium signalling following T cell activation.

Regulation of voltage-gated potassium channels in T cell development and activation

Voltage-gated potassium channels play an important role regarding the onset of various intracellular events associated with T cell development and activation (Lewis and Cahalan, 1990). The three species of voltage-gated potassium channels expressed on T lymphocytes are associated with distinct T cell subtypes in the mouse. Immature thymocytes (CD4⁻/CD8⁻) express only the type *n* channel, while mature thymocytes are associated with all three types of channels (Lewis and Cahalan, 1988). However, mature thymocytes and peripheral T cells can be further classified based on the presence or absence of specific cell surface proteins; Th cells express the CD4 surface marker, while Tc/Ts cells express the CD8 surface marker. CD4⁺ cells associate exclusively with the type *n* channel, while CD8⁺ cells express predominantly the type *n'* and *l* channels. Thus, T helper cells are associated with the exclusive expression of the type *n* channel. Furthermore, regulation of the type *n*, *n'*, and *l* potassium channel genes more than likely accompanies the

maturation of Tc and Ts cells (n' and l channel expressing) from immature thymocytes (n channel expressing).

There also exists a correlation between the surface density of voltage-gated potassium channels and the state of T cell proliferation in the mouse. Immature thymocytes, which are highly proliferative and double negative or positive for CD4 and CD8 molecules, express relatively high numbers of the type n potassium channel, exclusively; typically 100-500 channels per cell (Lewis and Cahalan, 1988). Mature thymocytes and resting peripheral Th cells, however, contain 10-fold lower levels of type n potassium channels. The number of type n channels, though, increases 10-20-fold in activated and proliferating Th cells (DeCoursey et al., 1987; Sutro et al., 1989). This latter observation also extends to a murine IL2-dependent Th cell clone, and B cells following mitogen-induced activation (Lee et al., 1986; Sutro et al., 1988). Additionally, there is a switch of channel species from predominant type n' and l to n following activation of Tc/Ts cells (DeCoursey et al., 1987).

A similar correlation has also been demonstrated for human T cells. Although resting human T cells express a relatively high density of the type n channel comparable to that found on activated murine T cells (Cahalan et al., 1985), the density of the type n channel still increases approximately 2-fold following stimulation with Concanavalin A (ConA) (Matteson and Deutsch, 1984); some variation has also been observed with other mitogens (DeCoursey et al., 1987). Thus, increased expression of the type n channel is closely associated with, and may be required for, T cell proliferation in both mouse and human.

Voltage-gated potassium channels are required during T cell activation

Further evidence from studies employing channel blockers supports the notion that the type n channel is required during T cell activation. Both mouse and human T cell

activation is suppressed by a wide variety of voltage-gated potassium channel blockers in a dose-dependent manner. Concentrations similar to those which reduce the type *n* channel current block activation; however, doses required to block the *l* channel do not have any effect (Chandy et al., 1984; DeCoursey et al., 1984 and 1985; Deutsch et al., 1986). This inhibition has also been extended to activation of B cells (Sutro et al., 1988). Non-specific inhibitions have been ruled out, in that viability of suppressed cells is not affected (Cahalan et al., 1987). The T cell properties inhibited by potassium channel blockers are quite broad, including suppression of metabolite uptake of nucleotides and amino acids, overall protein synthesis, IL-2 production, and cell proliferation; however, expression of the IL-2 receptor is not affected (Chandy et al., 1984; Sabath et al., 1986; Schell et al., 1987). Apparently, proper functional activity of the type *n* channel is required for various steps associated with T cell activation. However, exactly how the type *n* channel exerts its role(s) remains to be determined.

Voltage-gated potassium channels are required for the generation of Tc and NK cells

Cytotoxic and natural killer lymphocytes are activated by infected cells expressing foreign antigens, followed by the killing of these cells by the activated lymphocytes. Following activation, potassium efflux is observed in these effector cells, which is primarily due to voltage-gated potassium channels (Fukushima et al., 1984; Russell and Dobos, 1983). Activation of these effector cells is also inhibited by channel blockers specific to voltage-gated potassium channels, suggestive of a requirement for these channels (Sharma, 1988). Furthermore, application of IL2 to the culture medium abolishes this inhibitory effect, indicating that the inhibition could be simply due to the blockage of IL2 secretion from Th cells which was reduced significantly by channel blockers. In addition, calcium influx is also required for the activation of Tc and NK cells (Poenie et al., 1987).

Voltage-gated potassium channels play a role in regulatory volume decrease (RVD)

Voltage-gated potassium channels are involved in regulatory volume decrease (RVD). T lymphocytes swell when exposed to hypotonic solutions; and shrink back to their original volume in about half an hour. The efflux of potassium and chloride ions across the membrane has been observed in RVD (Sarkadi et al., 1984). A model has thus been proposed by Cahalan and Lewis (1990) whereby the expansion of T cell volume stimulates a type of chloride channel, specifically the mini-chloride channel (1-2 pS), resulting in depolarization of the membrane. This, in turn, activates voltage-gated potassium channels. Activation of both chloride and potassium channels causes the efflux of chloride and potassium ions. The loss of H₂O accompanying the efflux of chloride and potassium ions results in shrinkage of cell volume.

3. Regulation of voltage-gated potassium channel function by protein phosphorylation

The efficacy of a variety of distinct types of ion channels can be controlled by protein modification events. Phosphorylation represents such an event, is common to a variety of ion channel species, and modulates numerous channel properties including single channel conductance and open probability (Levitan, 1985; Rossie and Catterall, 1987).

Biochemical studies have revealed that both sodium and calcium channels can be phosphorylated directly (Catterall, 1988). The α subunit of calcium channels is phosphorylated in vitro by cAMP-dependent kinase (PKA); in addition, the β subunit is also phosphorylated. Similarly, the purified α subunit of sodium channels is phosphorylated by both PKA and PKC in vitro. It is also phosphorylated by endogenous kinases in intact neuronal cells. Moreover, both sodium and calcium channel activities are modulated by phosphorylation events (Catterall, 1988). Reconstituted calcium channels

show prolonged opening if incubated with the α catalytic subunit of PKA in the presence of ATP. In cardiac muscle, β -adrenergic stimulation increases calcium action potential, which strengthens heart muscle contractility. Microinjections of cAMP derivatives, phosphodiesterase (PDE) inhibitors, or the α catalytic subunit of PKA produce similar effects. In neurons, reagents which enhance PKA activity reduce sodium channel currents, which result in a reduction of sodium channel action potential. Therefore, direct phosphorylation of both sodium and calcium channels serve to regulate channel activities and cellular functions; in addition, phosphorylation of channel-associated proteins could also contribute to channel modulation. Furthermore, these phosphorylation events primarily affect channel open probability, resulting in an increase in calcium currents (Cachelin et al., 1983; Reuter et al., 1992) and a decrease in sodium currents (Li et al., 1992). In addition to sodium and calcium channels, regulation of chloride channels by phosphorylation has been recently documented (Cheng et al., 1991; Nishimoto et al., 1991; Tilly et al., 1992).

A variety of potassium channel currents also show sensitivity to phosphorylation events, including the slow-activating Isk potassium channel (Blumenthal and Kaczmarek, 1992; Busch et al., 1992), calcium-activated potassium channels (Chung et al., 1991), and the *Shaker A* voltage-gated potassium channel (Moran et al, 1991). The type *n* potassium channel is likewise subject to phosphorylation-dependent modulation in lymphocytes. Type *n* potassium currents are nearly completely inhibited following stimulation of PKA activity in both B and T lymphocytes. cAMP and forskolin treatment reduces channel currents in B cells (Choquet et al., 1987); and 8-Bromo-cAMP and prostaglandin E₂ (PGE₂) have similar effect in Jurkat cells (Payet and Dupuis, 1992). Additionally, stimulation of the PKC system affects type *n* channel activity in Jurkat cells. Application of TPA nearly completely blocks the type *n* potassium current, with intracellular injection of anti-PKC antibodies abolishing the effect of TPA (Payet and Dupuis, 1992). Moreover, injection of alkaline phosphatase increases type *n* potassium channel currents in Jurkat

cells, suggestive of a basal level of endogenous phosphorylation of the type *n* channel. Similarly, the type *n* channel expressed in *Xenopus* oocytes is also regulated by phosphorylation events, with increased PKC activity serving to dramatically reduce potassium currents (Attali et al., 1992b). These studies together, therefore, indicate that type *n* channel activity is dramatically down-regulated by phosphorylation events directed by both PKA and PKC.

4. Specific aims of the thesis

Aim 1. Molecular characterization of the type *n* potassium channel

The type *n* potassium channel is important to T cell development and function. However, previous characterization of the type *n* channel was limited to the establishment of an electrophysiological and pharmacological profile. Thus, molecular characterization of the type *n* channel would provide additional information regarding the structure and function of this important T lymphocyte channel. This project represents the initial step regarding characterization of the structure of the type *n* potassium channel.

Following T cell activation, type *n* channel density increases about 2-fold in human and 20-fold in mouse. This increase could be due to three distinct biochemical mechanisms, including: 1) increased levels of type *n* channel mRNA, 2) insertion of pre-existing quiescent channels into the membrane, and 3) increased efficacy of functional channels following cellular activation. In this project, type *n* channel mRNA levels were also quantitated at various times following T cell activation, which should provide information regarding the transcriptional activity of the Kv1.3 gene. An increase of type *n* channel mRNA would support the first hypothesis.

Aim 2. Characterization of in vivo and in vitro type *n* channel phosphorylation events

Phosphorylation appears to regulate the properties of type *n* channel currents. However, it is of interest to determine whether the type *n* channel is phosphorylated directly, as in the case of sodium and calcium channels. This project intends to characterize the specific nature of type *n* channel phosphorylation events. First, polyclonal antibodies against different regions unique to Kv1.3 will be generated. Second, these antibodies will be utilized to identify Kv1.3 channel phosphorylation events both in vivo, and in vitro employing purified kinases.

Aim 3. Functional significance of a highly conserved serine residue within the intracellular S4/5 loop of mammalian potassium channels

The S4/5 loop appears to lie in or near the internal mouth of the potassium channel pore, regulating various channel properties such as channel gating and/or ion permeation. The serine residue at position 392 within the S4/5 loop of the *Shaker B* potassium channel is embedded in the consensus sequence recognized by the PKC enzyme. Mutation of this residue reduces the channel conductance by 40%. This consensus sequence is fully conserved in several mammalian potassium channels, including rKv1.2 and hKv1.3. The study presented here seeks to characterize the functional significance of the corresponding serine residue in mammalian potassium channels.

5. Historical aspects of the thesis regarding research performed

Following reports of *Shaker* potassium channel characterization in 1987/88, the laboratories of Drs. Adelman, North and Douglass began a series of collaborative studies

aimed towards the characterization of mammalian voltage-gated potassium channels. Such studies initially resulted in the cloning and expression of the rat Kv1.1 (RBK1) channel (Christie, M.J. et al., 1989), and documentation of the ability of individual potassium channel subunits to form heteropolymeric channels (Christie et al., 1990). At the time I entered the Douglass lab, Jim was in the process of screening a rat genomic DNA library with Kv1.1 cDNA under low stringency hybridization conditions in an attempt to isolate new, additional members of the Kv1 subfamily of potassium channels. One such genomic DNA clone, RGK5 (rKv1.3), had been isolated and restriction mapping analysis revealed that it was indeed different from the Kv1.1 channel. The RGK5 clone was in the process of undergoing nucleotide sequence analysis when I became involved with the project. I thus became familiar with a variety of molecular biological techniques as I performed nucleotide sequence analysis on the RGK5 genomic DNA clone, Southern blot analysis on rat genomic DNA, and Northern blot analysis on various rodent RNAs. I also performed subcloning and *in vitro* transcription reactions in order to generate capped RGK5 RNA for analysis in *Xenopus* oocytes. This work constitutes the Chapter of this thesis entitled, "Characterization and Functional Expression of a Rat Genomic DNA Clone Encoding a Lymphocyte Potassium Channel". The work was published in the **Journal of Immunology** in 1990 (Vol. 144: 4841-4850.), with the following authors contributing to the project: J. Douglass (RGK5 clone isolation, preliminary nucleotide sequence analysis, project development), P. Osborne (channel characterization in *Xenopus* oocytes), Y.-C. Cai (RGK5 sequence analysis, Southern blot analysis, Northern blot analysis, and RGK5 expression cloning procedures), M. Wilkinson (purification of mouse thymus RNA), M. J. Christie (channel characterization in *Xenopus* oocytes), and J. P. Adelman (general project development).

. Following completion of this project, I then began work involving the characterization of human Kv1.3 genomic DNA, and expression of the encoded channel. This work was quite similar to that performed on rat Kv1.3, but included analysis of

hKv1.3 mRNA levels in human T lymphocytes following stimulation with Con A to investigate potential transcriptional changes following T cell activation. This additional work allowed me to gain experience regarding the isolation and manipulation of primary human T lymphocytes under tissue culture conditions. The cumulative work represents the Chapter of this thesis entitled, "Characterization and Functional Expression of Genomic DNA Encoding the Human Lymphocyte Type *n* Potassium Channel". The work was published in the journal **DNA and Cell Biology** in 1992 (Vol. 11: 163-172). The following authors contributed to the project: Y.-C. Cai (all molecular and cellular procedures involving hKv1.3 genomic DNA and mRNA analysis, project development), P. Osborne (channel characterization in *Xenopus* oocytes), R. A. North (minor aspects of project development) D. C. Dooley (isolation of human T lymphocytes), and J. Douglass (project development).

Following completion of the aforementioned project, it was clear that further investigation of hKv1.3 channel activity in T cells would require the ability to study the channel protein itself, with a focus on post-translational modification events which might affect channel activity. Indeed, there were several reports in the literature which suggested that phosphorylation events could affect Kv1.3 channel activity. The major question then became: can the channel itself serve as a substrate for direct phosphorylation events, or are associated proteins the targets of phosphorylation events. Such studies necessitated the ability to directly visualize the Kv1.3 channel protein, and the decision was made to generate a series of polyclonal antibodies against the human, mouse and rat Kv1.3 channel protein. Thus, the results described in the thesis Chapter entitled, "*In vivo* and *in vitro* Phosphorylation of the T Lymphocyte Type *n* (Kv1.3) Potassium Channel" detail the generation and characterization of polyclonal antisera against the mammalian Kv1.3, as well as various experiments regarding Kv1.3 channel phosphorylation. The work described in this chapter has been submitted to the **Journal of Biological Chemistry**, and at the current time this manuscript has been provisionally accepted; some additional

experimentation regarding PKC phosphorylation is required. The following authors contributed to this manuscript: Y.-C. Cai (project development and all experimental studies), and J. Douglass (project development). The work described in this thesis chapter involves the generation of fusion proteins, antibody generation and characterization, immunoprecipitation, surface labeling of membrane proteins, *in vivo* and *in vitro* phosphorylation analysis, and phospho-peptide mapping. Thus, during this phase of my thesis project I gained direct experience with a wide variety of immunological and biochemical techniques.

The final thesis research Chapter is entitled, “Functional Significance of a Highly Conserved Serine Residue within the Intracellular S4/5 Loop of Mammalian Potassium Channels”, and represents studies aimed at determining the functional significance of a serine residue which is located within a consensus PKC phosphorylation site. Following the observation that PKC can directly phosphorylate hKv1.3, coupled with the observation that serine residues represent the major sites for channel phosphorylation in Jurkat cells, it was decided by myself and Jim Douglass that site-specific mutagenesis coupled with functional analysis could be used to determine the significance of specific serine residues which might represent direct phosphorylation sites. The results presented in this chapter represent preliminary studies directed towards such a characterization. Following the generation of additional data, the work will be prepared for submission; we are currently undecided as to what journal we will submit the manuscript. However, the following authors will represent those contributing to this manuscript: Y.-C. Cai (*Shaker B*, Kv1.2 and Kv1.3 mutant generation and characterization, *in vitro* transcription, project development), M. Kavanaugh (channel analysis in *Xenopus* oocytes, project development), and J. Douglass (project development).

I

**CHARACTERIZATION AND FUNCTIONAL EXPRESSION OF A RAT
GENOMIC DNA CLONE ENCODING A LYMPHOCYTE POTASSIUM
CHANNEL**

ABSTRACT

Low stringency hybridization screening of a rat genomic DNA library with a previously described cDNA clone encoding a rat voltage-gated potassium channel has resulted in the characterization of a member of the potassium channel family, RGK5. An uninterrupted nucleotide sequence encodes a protein 525 amino acids in length, revealing that the entire coding region resides on a single exon. RGK5 transcripts are present in both mouse thymus and rat brain, as determined by Northern blot analysis. RNA transcribed in vitro from RGK5 genomic DNA directs the expression of functional potassium currents following injection into *Xenopus* oocytes. The currents are activated by depolarization, being half activated at -14 mV, and inactivate almost completely during depolarizations of 1-2 s. The properties of the currents strongly resemble those of the type *n* potassium channel present on both immature thymocytes and helper T lymphocytes.

INTRODUCTION

Potassium channels are membrane proteins which are selectively permeable to potassium ions (Hille, 1984; Rudy, 1988). Roles for voltage-dependent potassium channels are well established in neurons, and include maintaining a resting potential, action potential repolarization, patterning of spike bursts and limiting synaptic depolarizations. Several types of potassium channels present on neurons are also found on cells of the immune system, most notably thymocytes and T lymphocytes (Cahalan et al., 1987; DeCoursey et al., 1985, 1987). A variety of studies suggest that these channels are necessary for T lymphocyte activation. Specific potassium channel blockers inhibit cellular events associated with T cell activation, including calcium signalling, increased protein synthesis, lymphokine production, and cell proliferation (Cahalan et al., 1987). A role in proliferation or activation is also suggested by the observation that the density of potassium channels in mitogen-stimulated T cells is 10-fold higher than in quiescent splenic or lymph node T cells (Cahalan et al., 1987; DeCoursey et al., 1987). Pharmacological studies suggest that potassium channels are required for target cell lysis by cytotoxic T lymphocytes (Cahalan et al., 1987). Voltage-gated potassium channels are also believed to play a major role in determining the resting potential and volume of T lymphocytes (Cahalan et al., 1987; DeCoursey et al., 1985, 1987). Thus, a specific set of voltage-dependent potassium channels appear to be involved in the maintenance of T lymphocyte function.

Cloning of the *Shaker* locus of *Drosophila melanogaster* has provided the starting point for the molecular characterization of voltage-activated potassium channels (Papazian et al., 1987; Pongs et al., 1988; Tempel et al., 1987; Schwarz et al., 1988). Transcription from the wild type *Shaker* genomic locus results in the production of multiple species of mRNAs, each encoding a potassium channel protein. Distinct *Shaker* mRNAs result from

alternate splicing of precursor mRNA, and the resulting potassium channels share a common core sequence with variant amino and carboxyl termini. Several *Shaker* cDNA clones have been expressed in *Xenopus* oocytes and characterized electrophysiologically (Iverson et al., 1988; Timpe et al., 1988a and b). RNA synthesized *in vitro* from each cDNA clone directs the synthesis of a voltage-dependent potassium channel. Unique kinetics of inactivation are seen for each channel type, indicating that the *Shaker* products may contribute to kinetic diversity in A-channels of the fly, and that sequences in the amino terminal region may be important for inactivation.

Shaker nucleotide sequences have been used as hybridization probes to isolate potassium channel cDNA clones from both mouse (Tempel et al., 1988) and rat (Baumann et al., 1988; Christie et al., 1989; McKinnon, 1989) brain cDNA libraries. Similarly, a rat cDNA clone (RCK1) has been used to isolate related species of potassium channels from a rat brain cDNA library (Stuhmer et al., 1989). Expression cloning has also identified a novel rat brain potassium channel (Frech et al., 1989). Many of these channels have been functionally characterized in *Xenopus* oocytes following injection of *in vitro* transcribed RNA, with each channel exhibiting a unique electrophysiological and pharmacological profile (Christie et al., 1989; Frech et al., 1989; Stuhmer et al., 1988, 1989). In contrast to the *Shaker* gene products, alternate splicing does not appear to be the major basis of diversity among mammalian voltage-gated potassium channels (Stuhmer et al., 1989). Rather, distinct genes appear to encode each unique species of voltage-gated potassium channel in mammals (Chandy et al., 1990; Stuhmer et al., 1989).

Partial nucleotide sequence analysis of a rat genomic DNA clone (λ RGK1) encoding the RBK1 potassium channel (Christie et al., 1989) demonstrated that the entire coding region of RBK1 mRNA is contained on a single exon (Figure 2.1A). It was reasoned that if this genomic architecture was conserved among other members of this gene family, then uninterrupted genomic DNA sequences would encode other species of voltage-gated potassium channels. In the current study, low stringency hybridization screening of

a rat genomic DNA library resulted in the isolation of the gene encoding a potassium channel designated as RGK5. The RGK5 coding region is contained on a single exon, as demonstrated by expression and electrophysiological characterization of the encoded potassium currents in *Xenopus* oocytes. Properties of the expressed current, along with the observation of RGK5 mRNA in thymus, suggest that the cloned channel is the *n* potassium current previously described in both thymocytes and T lymphocytes (Cahalan et al., 1987; DeCoursey et al., 1985, 1987a and b).

MATERIALS AND METHODS

Screening of rat genomic DNA library and nucleotide sequence analysis

A rat λ genomic DNA library (generously provided by Dr. G. Scherer) was constructed by partial Sau3A digestion of adult Sprague Dawley rat liver DNA, followed by cloning into the λ phage vector, EMBL3. 500,000 clones were screened in duplicate with a ^{32}P -labelled cDNA fragment of the rat potassium channel cDNA clone, RBK1 (Christie et al., 1989). The filters were screened at 40% formamide/55°C. Following overnight hybridization, the filters were washed at 1xSSC/55°C and subjected to autoradiography. Duplicate positively hybridizing clones were plaque purified. Phage DNA was prepared and subjected to Southern blot analysis to identify DNA fragments which hybridized to the RBK1 probe. Appropriate restriction fragments were subcloned into M13 mp18 and mp19 vectors for dideoxynucleotide sequence analysis (Sanger et al., 1977). Nucleotide and amino acid sequence analysis was performed using the Intelligenetics and Wisconsin Genetics Computer Group suite of software.

Genomic Southern Blot analysis

10 μg of high molecular weight adult Sprague Dawley rat genomic DNA was digested with EcoRI, HindIII or PstI and electrophoresed on a 1.0% agarose gel. Following transfer to Nytran filter, the blot was hybridized with a random-primed, ^{32}P -labelled 450 bp SacI/HindIII fragment encoding the C terminal 62 amino acids of RGK5, as well as approximately 260 bases of presumed 3' untranslated region. Hybridization at 50% formamide/42°C, was followed by stringent washing at 0.1xSSC/55°C. Following

autoradiography, the size of each hybridizing band was determined by comparison with DNA size markers (1.0 kb DNA size ladder, Bethesda Research Laboratory).

Northern blot analysis

Total cellular RNA from rat brain was prepared by the guanidinium isothiocyanate lysis method (Chirgwin et al., 1979) followed by LiCl precipitation (Cathala et al., 1983). Poly A⁺ mRNA was purified from rat brain by affinity chromatography on oligo(dT)-cellulose. Total thymus RNA was prepared from BALB/c mice as described by Wilkinson (Wilkinson, 1988). For Northern blot analysis, RNA samples were fractionated on a 1.0% agarose/6.25% formaldehyde gel in HEPES electrophoresis buffer. Following capillary transfer to Nytran membrane, the blot was prehybridized (in 50% formamide, 400mM NaPO₄ (pH7.2), 1mM EDTA, 1 mg/ml BSA and 5% SDS) at 62°C. The blot was then incubated with 3x10⁸ cpm of a ³²P-labelled RGK5 cRNA riboprobe representing the 450 bp SacI/HindIII fragment described above. Hybridization was at 62°C for 36 hours. The blot was then washed in 0.05xSSC, 5mM EDTA and 0.5% SDS at 77°C for 10 hours, and exposed to film for 24 hours. The approximate size of RGK5 mRNA(s) was determined by comparison of the resulting autoradiographic signal with RNA size markers (0.24 to 9.49 kb RNA size ladder/Bethesda Research Laboratory).

Expression of RGK5 mRNA in *Xenopus* oocytes

Oocytes (Dumont stage V-VI) were harvested from adult *Xenopus laevis* under anesthesia (0.1% MS-222 Sigma, pH 7) as previously described (Christie et al., 1989). Theca and follicular layers were removed by incubation for 3 h in calcium-free solution containing collagenase A (2 mg/ml; Boehringer Mannheim). Denuded oocytes were maintained in ND-96 solution containing theophylline (0.5 mM), pyruvate (2.5 mM) and gentamycin (50 mg/ml). The composition of ND-96 is (in mM): 96, NaCl; 2, KCl; 1.8, CaCl₂; 1, MgCl₂; 5, HEPES. DNA representing the RGK5 coding sequence, including 35

bp of 5' untranslated region and 270 bp of 3' untranslated region, was introduced into the pGEM3Z transcription vector and the resulting plasmid, pRGK5-EXP, was used to synthesize capped RNA *in vitro* as previously described (Christie et al., 1989). Concentrations of synthesized RNA were estimated spectrophotometrically and confirmed by agarose/formaldehyde gel electrophoresis.

Oocytes were injected within 10 h of harvest with RNA encoding RGK5 (usually 1 ng) in 50 nl sterile water. In preliminary experiments concentration-response relationships were established for each RNA synthesis, eg. 2 days after injection of 0.3, 1, 3, and 10 ng of RNA, currents were 2 ± 1 , 7 ± 1 , 16 ± 1 and 24 ± 3 nA respectively at +40 mV ($n = 5-6$ /group).

Recordings of membrane current were made 1-3 days after injection of RNA as previously described (Christie et al., 1989). Briefly, oocytes were continuously superfused (3 ml/min) with ND-96; the superfusate could be changed within about 1 minute to one which differed only in its content of drug. Oocytes were voltage clamped (Dagan 8500) at various potentials using two microelectrodes (100 - 300 k Ω). Voltage clamp protocols and most analyses were performed using PCLAMP software (Axon Instruments, Burlingame CA). Fitting of activation curves to Boltzmann functions was performed with Kaleidograph software (Synergy Software, Reading, PA.). Fitting of activation time constants to a single exponential was performed with PCLAMP software. These fits are approximations because of contamination of the first 1-3 mS of activation by large capacitive transients.

RESULTS

Isolation and characterization of the rat potassium channel genomic DNA clone, RGK5

A rat genomic DNA library was screened at moderate stringency with a ^{32}P -labelled RBK1 cDNA hybridization probe. Twelve duplicate positively hybridizing clones were isolated and purified via successive rounds of low density screening. One genomic DNA clone, RGK5, was further subjected to Southern analysis and partial nucleotide sequence analysis. Figure 2.1B diagrams the size of the RGK5 genomic DNA insert, pertinent restriction enzyme sites, and strategy which was employed to determine the nucleotide sequence of a 1.9 kb Pst I (partial digest)/ HindIII restriction fragment.

The nucleotide sequence of the aforementioned 1.9 kb genomic DNA fragment which hybridized strongly with the RBK1 cDNA probe is shown in Figure 2.2. Analysis of the sequence reveals the presence of a single, long open reading frame 1575 bases in length, beginning at nucleotide +1. The nucleotide sequence flanking the potential start codon (CCAGACATGA) is similar to the optimal translation initiation sequence described by Kozak (Kozak, 1984). Computer analysis of the predicted 525 amino acid protein reveals six regions of hydrophobicity (boxed areas designated as S1 to S6) which represent putative transmembrane regions of the molecule (Kyte and Doolittle, 1982). Five consensus sequences for N-glycosylation (Asn-X-Ser/Thr) are present (Hubbard and Ivatt, 1981), as well as one potential site for cAMP-dependent phosphorylation (Lys/Arg-Lys/Arg-X(X)-Ser) (Krebs and Beavo, 1979). The predicted amino acid sequence of RGK5 is identical to that predicted from the rat brain cDNA clone, RCK3 (Stuhmer et al.; 1989), except for two amino acids (Phe¹⁰⁶ and Arg¹⁸¹ in RGK5, are Leu¹⁰⁶ and Gly¹⁸¹ in RCK3). Thus, RGK5 presumably represents the genomic counterpart of the RCK3 cDNA clone.

The predicted amino acid sequence of RGK5 is approximately 65% similar to that of RBK1 (Figure 2.3). The sequences encoding transmembrane domains S1 through S6 are highly conserved (greater than 95%) between the two proteins, with amino and carboxyl regions exhibiting the greatest divergence. A more detailed analysis of amino acid homology between RGK5 and previously described rat potassium channels is presented in the discussion section.

A 450 base pair SacI/HindIII fragment (outlined in Figures 2.1B and 2.2) encoding the C-terminal 62 amino acids of the RGK5 channel and approximately 260 nucleotides of presumed 3' untranslated region was radiolabelled by random-priming and used as a hybridization probe to determine the copy number of the RGK5 gene. Figure 2.4 reveals the presence of a single hybridizing fragment in each sample lane following Southern blot analysis of rat genomic DNA, suggesting that the RGK5 gene is present as a single copy in the rat genome. Furthermore, this 450 bp fragment appears to represent sequences unique to the RGK5 gene, and can presumably be used to distinguish the RGK5 gene/mRNA from those encoding other members of the family of voltage-gated potassium channels.

Northern blot analysis was performed to determine the size and limited tissue distribution of RGK5 transcripts (Figure 2.5). The 450 bp SacI/HindIII restriction fragment was subcloned into the transcription vector, pGEM3Z, for the generation of a radiolabelled cRNA probe. As stated previously, this nucleotide sequence is presumably unique to the RGK5 gene, and is not conserved in transcripts representing known members of the rat potassium channel family (Christie et al., 1989; Frech et al., 1989; McKinnon, 1989; Stuhmer et al., 1989). Hybridization signals approximately 9.5 and 7.8 kb in length were observed in total RNA from mouse thymus. The presence of multiple hybridization signals may be due to RNA degradation, or alternate transcriptional or post-transcriptional events. Similarly sized hybridization signals were seen in rat brain poly A⁺ RNA, although the larger transcript is somewhat smaller than that observed in thymus. Species variation may account for this difference. RGK5 mRNA in rat brain is present at much

lower levels than in mouse thymus; with poly A⁺ mRNA from brain compared to total RNA from thymus. No such hybridization signals were observed in poly A⁻ RNA from rat brain. (Additionally, no high molecular weight hybridization signals were detectable in samples of rat heart poly A⁺ mRNA; not shown). A pattern of non-specific hybridization in the 4.5 to 2.0 kb range was observed in all samples, presumably due to the presence of partially complementary sequences in highly abundant species of poly A⁻ RNA.

Functional expression of RGK5 in *Xenopus* oocytes

To determine the functional and pharmacological properties of the RGK5 potassium channel, the 1.9 kb genomic DNA fragment (shown in Figure 2.2) was subcloned into the plasmid expression vector, pGEM3Z, capped RNA synthesized *in vitro* and injected into *Xenopus* oocytes. Voltage-clamp recordings were made 1-3 days after injection of RNA. Depolarizing voltage clamp steps applied from a holding potential of -80 mV produced large outward currents which activated from approximately -35 mV and were maximal at +30 to +40 mV (Fig. 2.6A). The conductance (mean of 5 oocytes, Fig. 6C) was fit by a Boltzmann function ($G/G_{\text{Max}} = 1/(1 + e^{((V_{0.5} - V)/k)})$) with $V_{0.5}$ of -14.1 mV (midpoint) and $k' = 10.3$ mV (slope factor). The time constant of activation (t_n) was 22 ± 2 ms at -10 mV, and 7.8 ± 0.3 ms at +40 mV ($n = 9$).

Measurement of tail current reversal potentials indicated that the currents were carried by potassium ions (Christie et al., 1989). The reversal potential changed by 55 ± 2 mV for a ten-fold change in extracellular potassium concentration (2, 10, 30 and 80 mM; $n = 4-6$ oocytes at each concentration) as compared to the theoretical value of 58 mV per decade calculated from the Nernst equation and assuming an intracellular potassium concentration of 110 mM.

Currents inactivated by 85% during depolarizations sustained for 10 s (Fig. 2.6B). The time constant of inactivation (t_h) was $1,300 \pm 67$ ms at -10 mV and 612 ± 33 ms at +40 mV ($n = 5$). Steady-state inactivation was studied by applying voltage clamp steps (-

60 to +10 mV, 5 mV increments) for 10 s prior to stepping to a test potential of +40 mV. The resulting inactivation-conductance curve fit a Boltzmann function with $V_{0.5} = -33$ mV and $k = -3.7$ mV (Fig. 2.6C). The inactivated current recovered to $50 \pm 2\%$ of peak (+40 mV, $n = 3$) after repolarization to -80 mV for 5 s; recovery was complete in about 90 s.

The inactivation kinetics of the currents were affected by divalent cations. These experiments were performed in extracellular solutions containing 3 mM Mg to prevent changes in the holding current which occurred in the absence of divalent cations. In extracellular solutions containing normal Ca^{++} (2 mM) the currents inactivated by $87 \pm 1\%$ within 10 s with a t_h of 770 ± 59 ms (+40 mV, $n = 4$, Figure 2.6D). Removing external Ca^{++} reduced inactivation to $79 \pm 2.5\%$ and increased t_h to 1063 ± 43 ms (Figure 2.6D). Under these conditions chelation of internal Ca^{++} using BAPTA-AM (20 mM, 4 h) did not further increase t_h . Raising external Ca^{++} to 10 mM increased both the rate ($t_h = 594 \pm 47$ ms) and the amplitude of inactivation ($92 \pm 0.6\%$, Figure 2.6D). Other Group IIA divalent cations also increased the rate and amplitude of inactivation with a potency order $\text{Ca} > \text{Sr} > \text{Ba}$ ($t_h = 780, 798$ and 820 ms respectively at 3 mM, $n = 4$). Increasing Mg to 10 mM did not increase the inactivation rate. Other divalent cations blocked inactivation with a potency order of $\text{Ni} > \text{Co} > \text{Cd} > \text{Mn}$; ($t_h = 4605, 2355, 1266$ and 1344 ms, respectively, at a concentration of 300 mM, except Mn which was 1 mM; $n = 2-3$). Divalent cations also inhibited the peak current with a potency order; Ni (52% of peak in 3 mM Mg) $>$ Cd (63%) $>$ Co (73%) each at 300 mM $>$ Ba (57%) $>$ Mn (84%) $>$ Sr (92%) $>$ Ca (94%) each at 3 mM. These effects were not associated with shifts in activation or steady-state inactivation curves. Co (1 mM) markedly inhibited inactivation (see above), but the activation curve was only shifted 7 mV positive; $V_{0.5}$ shifted from -10.8 to -3.6 mV, while k shifted from 8.1 to 10.6, and the voltage-dependence of steady-state inactivation was unaffected. Increasing Ca^{++} from 2 mM to 10 mM increased the rate of inactivation (Figure 2.6D), but only shifted the activation curve 1 mV positive and did not affect steady-state inactivation.

Currents induced by RGK5 were inhibited by some potassium channel blockers, but not others. The concentrations required to produce 50% inhibition (3-6 determinations at +40 mV) were 11 ± 0.2 mM for tetraethylammonium, and 0.3 ± 0.01 mM for 4-aminopyridine. The currents were inhibited $60 \pm 6\%$ by quinine ($80 \mu\text{M}$, $n=3$) and $49 \pm 2\%$ by verapamil ($30 \mu\text{M}$, $n=3$). α -dendrotoxin (500 nM), β -bungarotoxin (500 nM) and apamin (500 nM) had no effect.

DISCUSSION

RGK5 genomic DNA encodes a voltage-dependent potassium channel

Low stringency hybridization screening of a rat genomic DNA library with a previously characterized rat potassium channel (Christie et al., 1989) has resulted in the isolation and characterization of a member of the family of voltage-dependent potassium channels, RGK5. The nucleotide sequence encoding the RGK5 channel is contained on a single exon, which is different from the genomic arrangement of exons encoding *Drosophila* potassium channels. In the fly, potassium channel transcripts encompass some 130kb of genomic DNA, with approximately 20 introns separating exonic sequences (Schwarz et al., 1988). Multiple species of mRNAs, each encoding a unique potassium channel, are produced as a result of alternate splicing of precursor mRNA. The genomic architecture described in this report suggests that alternate splicing of precursor mRNA might not serve as the major molecular mechanism underlying diversity within this family of mammalian potassium channels. In at least two cases (RBK1/RGK1 and RGK5), the nucleotide sequences encoding rat potassium channels are found on a single exonic domain, precluding any possibility of alternate splicing resulting in the formation of different species of potassium channels from a single genomic locus. A similar genomic architecture has recently been described for three mouse potassium channel genes (Chandy et al., 1990), one of which appears to represent the mouse equivalent of RGK5.

The predicted amino acid sequence of the RGK5 channel is nearly identical (2 amino acid differences) to the predicted amino acid sequence deduced from the rat brain potassium channel cDNA clone, RCK3 (Stuhmer et al., 1989b). Also, nucleotide sequence comparison reveals differences at only six residues between the RGK5 gene and RCK3 cDNA; therefore, the RGK5 genomic clone represents the RCK3 gene.

Figure 2.3 compares the predicted RGK5 sequence with those of previously described rat potassium channels (RBK1: Baumann et al., 1988; Christie et al., 1989; RBK2: McKinnon, 1989; DRK1: Frech et al., 1989). The areas representing hydrophobic transmembrane domains of RGK5 are overlined and designated as S1 to S6. Overall, approximately 25% of the RGK5 coding region is conserved between the four protein sequences (using the Genalign algorithm of Sobel and Martinez, ref. Sobel and Martinez, 1985). This conservation increases to approximately 65% if the DRK1 sequence is removed from the analysis. Both amino and carboxy terminal regions flanking transmembrane domains S1 and S6 contain few fully conserved residues. Thus, it is tempting to speculate that RBK1, RBK2 and RGK5 represent members of a structurally-related subset of potassium channels within the potassium channel family, with DRK1 representing a member of a different structurally-related subset of channels. This classification is consistent with the conservation between rat and *Drosophila* potassium channel sequences. The amino acid sequences of RBK1, RBK2 and RGK5 are 60-70% homologous with the *Shaker* core sequence, but only 35% homologous with *Shab* (Butler et al., 1989). Conversely, DRK1 is only 40% homologous with *Shaker*, but is 70% homologous with *Shab* (Frech et al., 1989).

Conservation of amino acid sequence motifs between these species of potassium channels may indicate specific moieties which are of functional significance. Within the S4 region are 5, fully-conserved, positively charged residues. It is probably this region of voltage-dependent ion channels which responds to changes in membrane potential, regulating ion gating (Noda et al., 1984). A high degree of conservation is maintained from the amino terminal region of S4 through the negatively charged region joining S5 to S6. This latter region, by multimeric subunit association, may be involved in pore formation and ion selectivity. On the basis of the localization of an extracellular toxin binding site (MacKinnon and Miller, 1989), as well as other structural predictions (Guy, 1990), the negatively charged region from S5 to S6 likely forms the extracellular mouth of

the channel. S5, which contains several hydroxyl groups, is therefore likely to be involved in forming the channel pore (Eisenman and Dani, 1987).

Another conserved motif is a series of five leucine residues positioned at intervals of seven amino acids, beginning at the end of the S4 region and extending into the S5 region. Similar leucine zipper motifs are believed to stabilize dimerization of proteins such as C/EBP, Jun, Fos, and CREB, by hydrophobic interactions between closely aligned alpha-helical leucine repeat regions on any two subunits (Mitchell and Tijan, 1989). This motif may also be involved in the interaction of potassium channel subunits, either with other proteins, or in multimeric subunit association (McCormack et al., 1989; Tempel et al., 1987).

Potassium currents are expressed when *in vitro* synthesized RNA encoding RGK5 is injected into *Xenopus* oocytes. Unlike currents expressed by RBK1, RBK2 and DRK1 (Christie et al., 1989; Frech et al., 1989; Stuhmer et al., 1988) these currents inactivate during sustained depolarization. This is a property usually ascribed to "A"- currents (Rudy, 1988). However, the rate of inactivation of RGK5-induced currents is slow (t_h 500 ms versus 50 ms for most A-currents). Divalent cations have little effect on the voltage-dependence of activation and inactivation of RGK5-induced currents, but markedly affect t_h . Ca, Sr and Ba increase the rate of inactivation, while Ni, Cd, Co and Mn markedly slow inactivation. It is possible that Ca, as well as Sr and Ba, binds to a site in the channel which modulates inactivation. Alternatively, direct blockage of the channel by divalent ions may be the inactivation mechanism (Grissmer and Cahalan, 1989). In contrast, divalent cations produce positive shifts in the voltage-dependence activation and inactivation curves of A-currents, with little effect on t_h (Mayer and Sugiyama, 1988). We were unable to test whether divalent cations are absolutely required for inactivation as complete removal of divalents induces large inward currents from endogenous oocyte channels.

RGK5 encodes a channel similar to the T lymphocyte *n* channel

Voltage-gated potassium channels are the most prevalent class of ion channel found on thymocytes and mature T lymphocytes (Cahalan et al., 1987; DeCoursey et al., 1985, 1987). Numerous studies support the notion that voltage-dependent potassium channels are important for T cell activation, mitosis, and cell-mediated killing. Throughout the life cycle of T lymphocytes, the levels of potassium channel expression correlate with the proliferative state; rapidly dividing cells such as mitogen-stimulated splenic T cells contain 10-fold more potassium channels than quiescent, resting splenic T-cells (Cahalan et al., 1987; DeCoursey et al., 1985). ³H-thymidine incorporation by human T lymphocytes following phytohaemagglutinin stimulation is inhibited by classical potassium channel blockers, tetraethylammonium and 4-aminopyridine, at doses found to block potassium channels in voltage-clamped T lymphocytes, suggesting that these channels may play an important role in mitogenesis (DeCoursey et al., 1984). Other properties of T cells associated with activation (including the induction of IL-2 production and a rise in cytoplasmic Ca⁺⁺ levels) are suppressed by these potassium channel blockers (Cahalan, 1987). Similar pharmacological experiments suggest that potassium channels are required by killer T cells during target cell lysis (Cahalan, 1987).

The predominant potassium channel found on both mouse and human thymocytes, T lymphocytes, as well as most T cell lines is the type *n* (for normal) channel (Cahalan, 1987; DeCoursey et al., 1985). The type *n* potassium channel is present at high levels on functionally immature CD4⁻CD8⁻ and CD4⁺CD8⁺ thymocytes, with approximately 100 and 300 channels/cell, respectively (Lewis and Cahalan, 1988). Lower numbers of *n* channels (approximately 10-20 channels/cell) are present on mature CD4⁺CD8⁻ thymocytes destined to become helper T cells (Lewis and Cahalan, 1988). Thus, the average surface density of this major T lymphocyte channel type is developmentally regulated, suggesting that the *n* channel is important for proper T cell development and function.

The presence of relatively high levels of mRNA in the mouse thymus which hybridize with a putative RGK5-specific riboprobe is consistent with the notion that the RGK5 genomic clone encodes a T lymphocyte voltage-gated potassium channel. More importantly, numerous biophysical properties of the RGK5/RCK3 potassium channel suggest that it is the T lymphocyte *n* channel. Table 2.1 serves to compare a variety of biophysical properties of the *n* channel, as characterized in murine thymocytes and human T lymphocytes, with those of the RGK5/RCK3 rat potassium channel, as characterized in *Xenopus* oocytes following injection of in vitro synthesized RNA. Parameters of activation and inactivation are similar for the channels, as well as unit conductance. The channels also exhibit similar profiles regarding the ability of a variety of ion channel blockers to inhibit peak currents. The peak channel currents show 50% inhibition at similar concentrations of TEA and 4-AP. The peptide toxin, α -dendrotoxin, appears to have little effect on the channel current at concentrations up to 500nM, while charybdotoxin exhibits potent inhibitory effects at concentrations as low as 0.2 nM. Interestingly, RGK5 and the mouse thymocyte *n* channel are also effectively blocked by quinine (which also blocks Ca-activated potassium channels), and verapamil (a Ca^{++} channel antagonist). The efficacy of a variety of divalent cations to block both the RGK5 and human *n* channel is also compared in Table 2.1, with similar inhibitory profiles observed. Thus, many of the biophysical properties of the RGK5/RCK3 channel (which serve to distinguish this channel from other cloned mammalian potassium channels) are also observed for both the mouse and human *n* channel.

Some properties, however, are not identical between the in vivo synthesized *n* channel and the in vitro synthesized RGK5/RCK3 channel. For example, the inactivation time constant for RGK5 is approximately 612 mS, while the value for the mouse *n* channel is 107 mS. K_i values for quinine and verapamil also vary by approximately 5-fold between these channels. These variances might be accounted for by differences between oocyte and lymphocyte membranes regarding lipid composition and the presence of membrane bound

proteins, some of which may be associated with the channel (Lester, 1988). Additionally, post-translational modifications may affect specific channel properties, and these modifications may occur in a cell-type specific fashion.

ACKNOWLEDGEMENT

The author thanks James Douglass, Peregrine B. Osborne, Miles Wilkinson, Macdonald J. Christie, and John P. Adelman for their important contributions; Chris Bond and Yanna Wu for expert technical assistance; Vollum Institute Illustrations for help with the artwork; and R. Alan North for support on the project.

II
CHARACTERIZATION AND FUNCTIONAL EXPRESSION OF GENOMIC
DNA ENCODING THE HUMAN LYMPHOCYTE TYPE N POTASSIUM
CHANNEL

Yun-Cai Cai*#, Peregrine B. Osborne*, R. Alan North*, Douglas C. Dooley§, and James
Douglass*¶

Vollum Institute* and the Department of Microbiology and Immunology#
Oregon Health Sciences University
Portland, OR 97201, USA

American Red Cross§
Portland, OR 97208

ABSTRACT

Voltage-gated potassium channels play important functional roles in the development and maintenance of human lymphocyte functions. One such channel, known as the type *n* channel, has been well defined in human T cells and exhibits unique functional properties which serve to distinguish it from other species of potassium channel. We report here the characterization of a human genomic DNA clone, HGK5, encoding a 523 amino acid potassium channel protein on an open reading frame contained on a single exon. RNA transcribed in vitro from HGK5 genomic DNA directs expression of functional voltage-dependent potassium currents in *Xenopus* oocytes. The functional characteristics of the expressed channels are strikingly similar to those of the type *n* channel on human T lymphocytes. This, together with the presence of significant levels of HGK5 mRNA in human T lymphocytes, supports the notion that HGK5 encodes the human type *n* voltage-gated potassium channel. The effects of concanavalin A treatment on HGK5 mRNA levels in cultured human T lymphocytes was also examined. Mitogenic concentrations of concanavalin A induced a time-dependent decrease in HGK5 mRNA levels, suggesting that previously observed increases in potassium current density following concanavalin A treatment of human T lymphocytes are not due to increased transcriptional activity of the type *n* potassium channel gene.

INTRODUCTION

Voltage-sensitive potassium channels are ubiquitous membrane proteins selectively permeable to potassium ions, which open following membrane depolarization (Hille, 1984; Rudy, 1988). Such channels are present on numerous cell types of the mammalian immune system. In both mouse and human T lymphocytes, the major species of potassium channel is the delayed rectifier, type *n* channel (Cahalan et al., 1987). This potassium channel subtype is also present on thymocytes, B lymphocytes, macrophages, and platelets (Lewis and Cahalan, 1988; Sutro et al., 1989; Ypey and Clapham, 1984; Maruyama, 1987). A variety of studies have suggested a functional role of the type *n* channel in the onset of cellular events associated with T cell activation, such as increases in the rate of cell proliferation, and DNA and protein synthesis (Cahalan et al., 1987; DeCoursey et al., 1984; Chandy et al., 1984; Schlichter et al., 1986). Alterations in T cell volume associated with exposure to a hypotonic environment may also involve type *n* potassium channels (Cahalan et al., 1987).

A wide variety of mammalian cDNA and genomic DNA clones have been shown to encode distinct species of voltage-gated potassium channels (Douglass et al., 1990; Christie et al., 1989; Baumann et al., 1988; McKinnon, 1989; Stuhmer et al., 1989; Frech et al., 1989; Yokoyama et al., 1989; Swanson et al., 1990). Many of the potassium channel subtypes have been functionally characterized in *Xenopus* oocytes, with each channel exhibiting unique electrophysiological and pharmacological properties. This has served as a means by which to classify each species of cloned potassium channel. In addition to diversity of primary structure, functional diversity might also arise from association of different subunits to form heteropolymeric channels (Christie et al., 1990; Ruppersberg et al., 1990; Isacoff et al., 1990).

A rat genomic DNA clone, RGK5, has been previously characterized which encodes the rodent type *n* potassium channel (Douglass et al., 1990). In the current study, high stringency screening of a human genomic DNA library with the RGK5 coding region has allowed for the characterization of the human equivalent, HGK5. As seen with RGK5, the HGK5 potassium channel coding region is contained on a single exon. This has allowed for the expression and electrophysiological characterization of the encoded potassium currents in *Xenopus* oocytes. Properties of the expressed current, in addition to the observation of HGK5 mRNA in human T lymphocytes, identify the cloned channel as the human type *n* potassium channel. Although an increase in type *n* potassium currents has been documented in mitogen-stimulated human T lymphocytes, Northern blot analysis of RNA from concanavalin A-treated human T lymphocytes indicates a down-regulation of HGK5 mRNA levels following mitogen treatment.

MATERIALS AND METHODS

Human genomic DNA library screening and nucleotide sequence analysis

A human genomic DNA library was constructed by cloning partial BglII-digested human genomic DNA into the vector, lambda FIX. 600,000 plaques were screened with a [³²P]-labelled DNA probe representing the entire coding region of the RGK5 gene (encoding the rat type *n* potassium channel; Douglass et al., 1990). Hybridization was at 42° C in 50% formamide, followed by washing with 0.2 x SSC, 0.1% SDS, 5 mM EDTA at 42° C. One clone, HGK5, was also hybridization positive following additional screening with a genomic DNA fragment encoding carboxyl coding and 3' non-coding sequences unique to RGK5 (Douglass et al., 1990). HGK5 DNA was further restriction-mapped, and specific DNA fragments were subcloned into M13 DNA for dideoxy sequence analysis (Sanger et al., 1977). Nucleotide and amino acid sequence analysis was performed using the Intelligenetics and Wisconsin Genetics Computer Group suite of software. Both HGK5 nucleotide and amino acid sequences are filed with GenBank under Accession Number M38217, and with EMBL under Accession Number X57342.

Genomic Southern blot analysis

Genomic DNA was purified from human buffy coat cells, digested with restriction endonucleases, separated on a 1% agarose gel, and transferred to nylon filter. The blot was hybridized with a [³²P]-labelled RGK5/HGK5-specific DNA probe (Douglas et al., 1990). Hybridization was performed at 50% formamide/42° C, followed by washing at 0.1 x SSC/55° C. Following autoradiography, the size of each hybridizing band was determined by comparison with DNA size standards.

Expression of HGK5 mRNA in *Xenopus* oocytes

The HGK5 coding region was amplified by PCR for subcloning into an RNA expression vector. The 5' oligo was 5' CGGCGAATTCCGCGAGCTGCCGCCCCGAC 3', while the 3' oligo was 5' CGGCAAGCTTAATGGTCTGGAAATGTAT 3'. The PCR reaction was catalyzed by Taq DNA polymerase on a programmable heat block under conditions of denaturation at 95° C/1 min, annealing at 65° C/1 min, and extension at 72° C/1.5 min. The amplified products were fractionated on a 1% agarose gel, and the expected 1.6 kb band was purified. The DNA was treated with T4 DNA polymerase, digested with EcoRI/HindIII, and directionally subcloned into the transcription vector, pGEM-3Z, resulting in production of the plasmid pHGK5-EXP. The HGK5 expression plasmid was additionally characterized by restriction mapping.

pHGK5-EXP was linearized with HindIII, and transcribed in the presence of m7G(5')ppp(5')G by T7 RNA polymerase. *Xenopus* oocytes were prepared and injected with RNA (Douglass et al., 1990). Recordings of membrane current were made 1-3 days after injection using two electrode voltage clamp methods (Douglass et al., 1990; Christie et al., 1989). Briefly, oocytes were continuously superfused (3 ml/min) with ND-96 at 23-25° C. Oocytes were voltage clamped (Dagan 8500 amplifier) using 100-300 kΩ electrodes. Data acquisition and analysis was performed using PCLAMP software (Axon Instruments) and non-linear curve fitting was carried out using SIGMAPLOT software (Jandel).

The reversal potentials in different external K⁺ concentrations were determined using methods described in (Christie et al., 1989). In 2 and 10 mM K⁺ the reversal of tail currents were observed, and in 80 mM K⁺ the reversal of the current was observed directly. KCl was substituted for NaCl.

Isolation of human T lymphocytes

Leukocytes were obtained from cellular residues generated during plateletapheresis (Dooley et al., 1987). Donors were healthy, and informed consent was obtained. Mononuclear cells (MNC) and granulocytes were separated by centrifugation on Ficoll-diatrizoate. To lyse red blood cells (RBCs) in the granulocyte fraction, the cells were washed three times with 80 mM ammonium oxalate adjusted to pH 6.8 with Sorensen's phosphate buffer, 300 mOsm total. Granulocyte purity was over 96% based on Wright staining. MNC (94%) were rosetted overnight with Sheep erythrocytes (sRBC). E-rosette positive and negative cells were separated on 4 layer Percoll gradients (Dooley et al., 1987). E-rosette positive T cells were collected from the 65%/89% Percoll interface and the sRBC hemolyzed in ammonium oxalate as above. The free T cells were over 86% CD2 positive as determined by flow cytometric analysis.

Northern blot analysis

Total cellular RNA was prepared by the acid guanidine/phenol-chloroform extraction protocol (Chomczynski and Sacchi, 1987). 20 µg of total RNA from human T cells and granulocytes was fractionated on a 1% agarose/6.25% formaldehyde gel and transferred to nylon membrane. The integrity and relative amount of RNA present in each lane was confirmed by staining of the membrane with 0.02% methylene blue. The blot was then incubated with a [³²P]-labelled, HGK5-specific cRNA riboprobe representing the 800 bp HincII/HindIII restriction fragment outlined in Figure 3.1. Hybridization was at 65° C overnight in 50% formamide, followed by washing at 0.05 x SSC at 75° C (Douglass et al., 1990). The resulting autoradiograph was exposed to film for 48 hours. The approximate size of hybridizing species of RNA was determined by comparison of the autoradiographic signals to known RNA size standards.

Concanavalin A treatment of primary human T lymphocytes

Human T lymphocytes were isolated as described above. The cells were cultured in RPMI 1640 supplemented with 10% fetal calf serum. Cell viability was determined by trypan blue exclusion; greater than 90% viability was observed 72 hours after initial plating. Some cells were maintained in the presence of 4 $\mu\text{g/ml}$ or 40 $\mu\text{g/ml}$ concanavalin A (Sigma). Mitogenesis was determined by measuring [^3H]thymidine incorporation. Cells were plated at a density of $2.5 \times 10^6/\text{ml}$. Concanavalin A was then added at the concentrations noted, the cells incubated for 70 hours, followed by addition of 1 μCi [^3H]thymidine for an additional 4 hours. The cells were then harvested, lysed, and [^3H]thymidine incorporation determined (DeCoursey et al., 1984; Chandy et al., 1984). For 5×10^5 cells, 50 cpm was incorporated for non-treated cells, 400 cpm for 4 $\mu\text{g/ml}$ concanavalin A-treated cells, and 2150 cpm for 40 $\mu\text{g/ml}$ concanavalin A-treated cells. Concanavalin A concentration curve analysis also confirmed that the latter concentration is close to that required for maximal [^3H]thymidine incorporation.

To determine the effects of concanavalin A treatment on HGK5 mRNA levels, human T lymphocytes were plated at a density of 3×10^6 cells/ml. Experimental samples were incubated with concanavalin A at 4 $\mu\text{g/ml}$ and 40 $\mu\text{g/ml}$ immediately following plating. At 4, 8, 16, 24, 48, and 72 hours the cells were harvested, and total RNA extracted. Northern blot analysis was performed on 20 μg of total RNA from each sample of T lymphocytes, using [^{32}P]-radiolabelled cRNA or DNA probes to detect HGK5, cyclophilin (Danielson et al., 1988), and interleukin-2 receptor α subunit (Leonard et al., 1984) mRNA. The membrane was also stained with 0.02% methylene blue to detect 28S rRNA. Relative 28S rRNA and HGK5 mRNA autoradiographic intensities were quantitated by laser densitometric scans (LKB Ultrosan, Bromma, Sweden).

RESULTS

Isolation and characterization of the human potassium channel genomic DNA clone, HGK5

A rat genomic DNA clone, RGK5, has been characterized which encodes the rodent type *n* potassium channel (Douglass et al., 1990). A 1.9 kb DNA fragment from the RGK5 gene, including the entire 1575 bp channel coding region, was used as a hybridization probe to screen a human genomic DNA library under high stringency conditions. One hybridization-positive clone, HGK5, was further shown to contain nucleotide sequences homologous to the unique carboxyl coding and 3' untranslated regions of RGK5 mRNA, suggesting that HGK5 was the human equivalent. The HGK5 genomic DNA insert was additionally characterized by restriction mapping (Figure 3.1, upper) and nucleotide sequence analysis (Figure 3.1, lower).

Nucleotide sequence analysis of a 2.8 kb SacI/HindIII restriction fragment revealed the presence of a single open reading frame 1569 nucleotides in length. The deduced amino acid sequence predicts a 523 amino acid protein with structural similarities to other cloned mammalian voltage-gated potassium channels. The predicted amino acid sequence of HGK5 shows 98% similarity to those of the rat RGK5 channel (525 a.a.), and the mouse MK3 channel (528 a.a.). Divergent residues are localized mainly to the amino terminal domain, and the putative extracellular region between transmembrane domains S1 and S2. Within the HGK5 potassium channel are five consensus sequences for N-glycosylation (Hubbard and Ivant, 1981) at positions 57, 227, 469, 486 and 499, as well as one site for potential phosphorylation by cAMP-dependent protein kinase at residue 468 (Krebs and Beavo, 1979). These sites are all conserved between HGK5, RGK5, and MK3.

As noted, the HGK5 coding region is contained on a single exon, similar to the architecture of the corresponding type *n* potassium channel gene in rat (genomic clone, RGK5) and mouse (genomic clone, MK3; Chandy et al., 1990). Genomic Southern blot analysis confirmed that the HGK5 gene exists as a single copy in the human genome (Figure 3.2A).

Functional expression of HGK5 in *Xenopus* oocytes

In order to determine the functional properties of the HGK5 channel, the coding region of the HGK5 gene was amplified by polymerase chain reaction, subcloned into an RNA expression vector, and *in vitro* synthesized, capped RNA injected into *Xenopus* oocytes. Two electrode voltage clamp recordings were made 1-3 days after injection. Depolarizing voltage steps applied from a holding potential of -80 mV produced large outward currents that activated near -40 mV and saturated around +20 mV (Fig. 3.3A). The currents peaked within 30-40 ms and then slowly inactivated with time constants in excess of 700 ms (Fig. 3.3B). High selectivity of the expressed channels for potassium was demonstrated by studying the reversal potentials of tail currents in 2, 10 and 80 mM extracellular potassium. These values were fit by linear regression to the Nernst equation with a slope of 55 ± 0.6 mV (mean \pm sem; $n=3$) per 10-fold change in $[K^+]_{out}$, which is close to the theoretical value of 58 mV per decade assuming a $[K^+]_{in}$ of 110 mM.

The conductance-voltage relation of the HGK5 channel is shown in Fig. 3.3D; normalized chord conductance (mean of 4 oocytes) was fit by a Boltzman function ($G/G_{max} = 1/[1 + e^{(V_{0.5}-V)/k}]$) with $V_{0.5} = -13 \pm 1$ mV (midpoint) and $k' = -8 \pm 0.8$ (slope factor). The channel activated with a time constant (τ) of 24 ± 3 ms at -10 mV, and 7 ± 0.7 ms at +40 mV (both $n=4$, single exponential fits). During 5 s depolarizing voltage steps the HGK5 current inactivated slowly ($\tau = 790 \pm 30$ ms at +40 mV, $n=4$). The decay of the current was well described as a single exponential process and was practically

independent of voltage at potentials positive to -10 mV (Fig. 3.4A). Inactivation of the current was incomplete after 5 s (86% decrease at +40 mV, $n=4$) (Fig. 3.4B), and there was relatively little further inactivation when depolarizing steps were maintained for up to 20 s. The voltage dependence of inactivation was studied by applying voltage clamp steps (-55 to -5 mV, 5 mV increments) for 5 s before stepping to test potential of +40 mV, and the resulting conductances were fit by a Boltzman function with $V_{0.5} = -28$ mV and $k' = 6.1 \pm 0.6$ ($n=4$) (Fig. 3.3D). The time course of recovery from inactivation was studied by holding at -80 mV and varying the interval between pairs of 500 ms test pulses to +40 mV. The ratio of the peak current during the second pulse to that during the first pulse ($I_{k,2} / I_{k,1}$) was moderately well fit by a single exponential with a time constant of 20 ± 1 s ($n=3$) (Fig. 3.4C).

T lymphocyte type *n* potassium channels have an unusual pharmacology in that they are sensitive not only to classical potassium channel blockers (such as tetraethylammonium and 4-aminopyridine), but also to inhibitors of Ca^{++} -sensitive potassium channels (such as quinine) as well as classical Ca^{++} channel blockers (such as diltiazem, nifedipine, and verapamil; Ni^{+} , Cd^{+} , and Co^{+}) (Cahalan et al., 1985, 1987; DeCoursey et al., 1984, 1985; Lewis and Cahalan, 1990; Grissmer and Cahalan, 1989). Inhibition curves for a range of these compounds on expressed HGK5 currents are shown in Figure 3.5. Comparison of the obtained IC_{50} values with those calculated for human type *n* channels (Table 3.1) indicate remarkably similar potencies of blockade. Additionally, certain blockers have been shown to affect T lymphocyte type *n* potassium current kinetics; divalent cations slow inactivation (Cahalan et al., 1985), whereas low concentrations of verapamil speed inactivation (Decoursey et al., 1985). Comparable effects were observed on HGK5 expressed currents. In external ND-96 solution containing 3 mM Mg, the inactivation time constant was 650 ms. In Sr, Ba and Mn (3 mM), the respective inactivation time constants were 710, 840 and 2020 ms; while in Cd

and Co (300 μ M), they were 1200 and 2400 ms. Conversely, in verapamil (3 μ M) the time constant of inactivation was 342 ms.

Expression of HGK5 mRNA in human T lymphocytes

An assignment of the HGK5 gene as that encoding the type *n* potassium channel predicts that HGK5 transcripts should be present in human T lymphocytes. Northern blot analysis using an HGK5-specific cRNA hybridization probe confirmed such a prediction (Figure 3.2B). Total RNA from human granulocytes (comprised mainly of neutrophils, with minor numbers of eosinophils and basophils), on the other hand, contained no detectable levels of HGK5 mRNA. The major species of hybridizing RNA is approximately 9.5 kb in length, similar to that observed for the RGK5 transcript in mouse thymus (Douglass et al., 1990). Two additional hybridizing bands, approximately 4.4 and 2.6 kb in length, are observed. These transcripts are specific to the poly(A) fraction, and may be the result of alternate mRNA splicing, site-specific mRNA degradation, or cross-hybridization with related species of mRNA.

A variety of studies have documented the effects of mitogens on human T lymphocyte potassium channel density (Matteson and Deutsch, 1984; Deutsch et al., 1986, 1991; for review see Deutsch, 1990). Human T lymphocyte potassium currents, with properties of the type *n* channel, are increased nearly 2-fold at 20 hours following stimulation with 50 μ g/ml succinyl concanavalin A (Matteson and Deutsch, 1984). This effect is even more dramatic in murine T lymphocytes (Cahalan et al., 1987; DeCoursey et al., 1985, 1987), where potassium channel density is increased by an order of magnitude following 24 hour treatment with 2 μ g/ml concanavalin A. Here, too, it appears to be type *n* potassium channels that are selectively increased (DeCoursey et al., 1987). It has been speculated that such mitogen-induced increases in potassium current/channel density may

be at least partly due to alterations in the rate of production of nascent type *n* potassium channels.

The following study was performed to determine if concanavalin A- induced alterations in HGK5 mRNA levels were correlative with observed increases in potassium current density. Human T lymphocytes were isolated, and placed in culture for 4 to 72 hours. Experimental samples were incubated with concanavalin A at 4 $\mu\text{g/ml}$ or 40 $\mu\text{g/ml}$ immediately following plating. The latter concentration was within the range required for maximal incorporation of [^3H]thymidine, while the former minimally stimulated [^3H]thymidine incorporation (Fig. 3.6). The cells were then harvested, total RNA extracted, and Northern blot analysis performed to detect HGK5, cyclophilin (Danielson et al., 1988), and interleukin-2 receptor α subunit (Leonard et al., 1984) mRNA (Figure 3.7).

Utilizing 28S rRNA levels for standardization, HGK5 mRNA levels appeared to remain relatively constant between control and concanavalin A-treated cells at the 4, 8, and 16 hour time points. However, HGK5 mRNA levels declined precipitously at 48 and 72 hours in cells treated with a mitogenic concentration of concanavalin A; no apparent alteration in HGK5 mRNA levels was observed in cells treated with 4 $\mu\text{g/ml}$ concanavalin A. Conversely, treatment with 40 $\mu\text{g/ml}$ concanavalin A for 48 and 72 hours did serve to increase cellular levels of cyclophilin and IL-2 receptor (α subunit) mRNAs. The ability of mitogens to increase T lymphocyte IL-2 receptor mRNA levels is well documented (Hatakeyama et al., 1989). Cyclophilin, or peptidyl-prolyl cis-trans isomerase, functions as a cellular protein which helps direct the proper folding of nascent proteins. As mitogen-treatment stimulates the rate of protein synthesis in T lymphocytes, it is not unexpected that cyclophilin mRNA levels would rise in stimulated cells. Increased levels of cyclophilin and IL-2 receptor mRNA were observed only in T cells treated with a mitogenic concentration of concanavalin A.

Stained nylon membranes and autoradiographs were subjected to scanning laser densitometry to semi-quantitate the relative levels of 28S rRNA and HGK5 mRNA. HGK5 mRNA levels were standardized against those for 28S rRNA, and the relative levels of HGK5 mRNA were then compared between stimulated (40 µg/ml Con A) and non-stimulated (non-treated) cells (Figure 3.7, lower). HGK5 mRNA levels began to decline between 16-24 hours in stimulated cells, with maximal reduction observed at 48-72 hours. Thus, conditions which serve to increase human T lymphocyte (type *n*) potassium current density by two-fold, appear to negatively regulate cellular levels of HGK5 mRNA.

DISCUSSION

Previous studies have documented that the rat genomic clone, RGK5, encodes a voltage-gated potassium channel with properties resembling those of the type *n* potassium channel characterized in murine and human T lymphocytes (Douglass et al., 1990). Further evidence for this assignment was provided in a subsequent analysis of the related murine genomic DNA clone, MK3 (Grissmer et al., 1990). We report here the isolation and characterization of the human gene encoding the type *n* potassium channel, HGK5. The presence of HGK5 transcripts in human T lymphocytes, in addition to the qualitative similarity between the functional properties of the HGK5 channel expressed in *Xenopus* oocytes and those of the human T lymphocyte type *n* channel, strongly suggest that the HGK5 genomic DNA clone encodes the human T lymphocyte type *n* potassium channel.

The HGK5 currents expressed in *Xenopus* oocytes display properties that are characteristic of type *n* channels in human T cells, and that distinguish them from other voltage-gated potassium channels (DeCoursey et al., 1984, 1985; Chandy et al., 1984; Cahalan et al., 1985; Lewis and Cahalan, 1990; Grissmer and Cahalan, 1989; Matteson and Deutsch, 1984). They are highly potassium selective, inactivate slowly over hundreds of milliseconds, recover rather slowly from inactivation, and are susceptible to blockade by a unique variety of pharmacological agents and divalent cations (Table 3.1). Although some properties are identical between the HGK5 and human type *n* potassium currents, such as the potency of divalent cations in the reduction of peak current, there are quantitative differences between several of the functional parameters measured. Direct comparisons, however, are complicated by differences in the recording conditions employed. In experiments with human T lymphocytes it has been shown that the properties of type *n* currents change in the period immediately after establishment of the whole cell recording configuration. For example, the midpoint of activation shifts to more

negative potentials, the rate of inactivation becomes faster, and there is a change from incomplete to complete inactivation (Cahalan et al., 1985). To accomodate such alterations, Grissmer et al. (1990) used outside-out oocyte patches and ionic conditions identical to those used when recording from murine T cells, and found that the functional properties of MK3 currents were indistinguishable from murine T cell type *n* currents. However, the data presented in Table 3.1 for human type *n* channels were obtained after a period of equilibration under whole cell conditions (DeCoursey et al., 1984, 1985; Cahalan et al., 1985), potentially accounting for some of the observed differences. Additionally, unique aspects of oocyte and lymphocyte membranes regarding lipid composition and the repertoire of membrane-associated proteins may result in quantitative differences in channel properties. Lastly, it is also possible that during the PCR amplification process used to generate the HGK5-EXP vector, point mutations were generated within the HGK5 coding sequence. Possible amino acid substitutions, if located in key regions determining specific functional properties, could also result in quantitative differences in channel properties.

A number of studies have documented alterations in the density of T lymphocyte potassium channel density following treatment with mitogenic agents (Cahalan et al., 1987; DeCoursey et al., 1985, 1987; Matteson and Deutsch, 1984; Deutsch et al., 1986, 1991; Deutsch, 1990). This mitogen-induced increase in type *n* potassium channel density varies from 2-fold in human T lymphocytes, to 20-fold in murine T lymphocytes. A variety of mechanisms have been proposed which could account for this observation, including the synthesis of new channels, the presence of presynthesized channels which would insert into the membrane as a result of cellular activation, and the presence of nonfunctional channels in quiescent T cell membranes which would then become functional following activation (DeCoursey et al., 1987).

To determine if altered HGK5 mRNA levels are reflective of the increase in type *n* current density, transcript levels were measured in concanavalin A-treated human T lymphocytes. Under conditions which maximally stimulate [³H]thymidine incorporation

and increase cellular levels of cyclophilin and IL-2 receptor mRNA, dramatic decreases in HGK5 mRNA levels were observed. Furthermore, this decrease occurred in a time-dependent fashion, and was only observed when concanavalin A was present at a mitogenic concentration. The identical paradigm was performed with murine T cells, and similar results were observed (Y.-C. Cai, personal observations). Murine T lymphocytes treated with 2 $\mu\text{g/ml}$ Con A (a dose which maximally stimulated [^3H]thymidine incorporation) exhibited no alterations in type *n* channel mRNA levels from 1 to 24 hours after treatment, and mRNA levels began to decline by 48 hours. This identical treatment served to increase murine T lymphocyte type *n* channel density by 10-fold at 24 hours, and by 20-fold at 48 hours (DeCoursey et al., 1987). Thus, these data suggest that an increase in cellular levels of mRNA encoding the type *n* channel does not play a role in mitogen-induced increases in potassium channel density, and that post-transcriptional events underlie this change.

ACKNOWLEDGEMENTS.

The authors thank Dr. J. P. Adelman for synthesis of oligonucleotides for PCR, and (together with Drs. J. T. Williams and A. B. Busch) for constructive comments and support throughout the course of the work; Dr. M. Wilkinson for a cDNA fragment encoding human IL-2 α subunit receptor; Y. Wu for technical support; and Vollum Illustrations for help with figure preparation. The work was supported by Department of Health and Human Services Grants DA04154 (to JD), DA03160, DA03161, DK32979, and MH40416 (to RAN), and Oregon Medical Research Foundation Grant 327-521 (to JD).

III

**In vivo and in vitro Phosphorylation of the T Lymphocyte type n (Kv1.3)
Potassium Channel 1**

Yun-Cai Cai *# and James Douglass *¶

Vollum Institute* and the Department of Microbiology and Immunology#
Oregon Health Sciences University
Portland, OR 97201, USA

¶ To whom correspondence should be sent: Vollum Institute - L474, Oregon Health Sciences University, 3181 SW Sam Jackson Park Road, Portland, Oregon, 97201.

Tel: 503-494-5452

Fax: 503-494-4976

SUMMARY

The major species of voltage-gated potassium channel found on mammalian T lymphocytes is referred to as the type *n* channel. This potassium channel exhibits unique functional properties which distinguish it from other species of potassium channels, including a potential role in the onset of cellular events associated with T cell activation. As a first step in characterizing specific biochemical properties of the type *n* channel, we have generated polyclonal antisera against bacterial fusion proteins containing peptide regions unique to the mouse and human type *n* channel. The type *n* channel can be immunoprecipitated from membranes of T cell lines derived from both mouse (SAK 8 cell line) and human (Jurkat cell line) following either surface labeling with ^{125}I , or metabolic labeling with ^{32}P . The apparent molecular mass of the immunoprecipitated type *n* channel is approximately 65-kDa, significantly greater than that of the 58-kDa in vitro translated product, and suggestive of post-translational modification events. Phosphoamino acid analysis of the metabolically labeled Jurkat type *n* channel reveals phosphorylation of serine residues exclusively, with approximately 3.0 mol of phosphate incorporated per mol of channel subunit. In vitro studies also describe the ability of both PKA and PKC to phosphorylate the Jurkat type *n* channel. The former kinase also appears to phosphorylate a 40-kDa protein which co-immunoprecipitates with the type *n* channel. These data suggest that direct phosphorylation of the T lymphocyte type *n* potassium channel, or its associated 40-kDa subunit, may serve as a means by which channel activity is regulated.

INTRODUCTION

Voltage-sensitive potassium channels are ubiquitous membrane proteins which open following membrane depolarization, resulting in selective flow of potassium ions. A species of voltage-gated potassium channel with unique biophysical and pharmacological properties is present on mammalian T lymphocytes, and is referred to as the type *n* (for normal) potassium channel (for review, see Cahalan et al., 1987; Cahalan and Lewis, 1990; Lewis and Cahalan, 1988 and 1990). A variety of studies have suggested a functional role of the type *n* channel in the onset of cellular events associated with T lymphocyte activation, including increases in the rate of cell proliferation, and DNA and protein synthesis (Cahalan et al., 1987; Chandy et al., 1984; DeCoursey et al., 1984).

Molecular cloning efforts have resulted in the isolation and characterization of both cDNA and genomic DNA encoding the type *n* channel from mouse (Chandy et al., 1990; Grissmer et al., 1990), rat (Douglass et al., 1990), and human (Attali et al., 1992a; Cai et al., 1992). The current nomenclature for cloned mammalian potassium channels assigns the type *n* channel to the designation, Kv1.3 (Chandy et al., 1991). Expression in *Xenopus* oocytes of in vitro synthesized cRNA from the aforementioned cDNA and genomic DNA clones results in the expression of potassium currents whose properties are nearly identical to those of the type *n* potassium current as characterized in T lymphocytes. Furthermore, these studies suggest that the mammalian type *n* channel current results from the formation of a Kv1.3 homotetramer, and is not the result of heteropolymerization of different members of the Kv1 subfamily of potassium channels. Additionally, the presence of mRNA encoding the Kv1.3 channel in both murine and human T lymphocytes, as well as cell lines derived from T cells, confirms the assignment of Kv1.3 as that representing the type *n* channel.

It is well documented that post-translational modification events can affect the functional properties of voltage-gated ion channels (Catterall, 1988). For example, phosphorylation events may serve as a molecular mechanism by which to induce long-term modulation of ion channels (Levitan, 1985). Indeed, this theme has been developed for calcium-activated potassium channels (Chung et al., 1991), the slow-activating Isk potassium channel (Blumenthal and Kaczmarek, 1992; Busch et al., 1992), the *Shaker A* voltage-gated potassium channel (Moran et al., 1991), voltage-sensitive calcium channels (Curtis and Catterall, 1985; De Jongh et al., 1989; Flockerzi et al., 1986; Hymel et al., 1988; Rohrkasten et al., 1988), chloride channels (Cheng, et al., 1991; Nishimoto, et al., 1991; Tilly, et al., 1992), and sodium channels (Li et al., 1992; Rossie et al., 1987; Rossie and Catterall, 1989). More recently, regulation of the type *n* potassium current by protein kinase A (PKA) and protein kinase C (PKC) has been described in both the *Xenopus* oocyte expression system (Attali et al., 1992b) and the human Jurkat T lymphocyte cell line (Payet and Dupuis, 1992). In the *Xenopus* oocyte expression system, activation of PKC serves to produce a long-lasting inhibition of the type *n* current, while elevation of cAMP levels does not affect the current. In Jurkat cells, however, activation of both the PKA and PKC systems results in similar patterns of inactivation of the type *n* potassium current. It is not known, though, if these PKA- and PKC-induced effects are the result of direct phosphorylation of the type *n* channel, or phosphorylation of other cellular proteins which would indirectly alter functional properties of the Kv1.3 channel.

As a first step in the biochemical characterization of the mammalian type *n* potassium channel, we have generated a series of polyclonal antisera directed against regions (both intracellular and extracellular) of the Kv1.3 potassium channel which are unique to this species of potassium channel. Figure 4.1 shows amino acid sequence alignment of murine, rodent, and human Kv1.3 potassium channels. The antisera are able

to immunoprecipitate both in vitro translated Kv1.3, as well as endogenous Kv1.3 located on both murine and human T lymphocyte cell lines. When human Jurkat cells are metabolically labeled with ^{32}P , radiolabeled Kv1.3 can be immunoprecipitated, revealing that the type *n* channel is an endogenous substrate for kinase activity. Phosphoamino acid analysis further shows that serine residues are the primary site(s) for phosphorylation events. In vitro phosphorylation studies also document that both PKA and PKC are capable of directly phosphorylating the type *n* channel. Thus, the reported effects of PKA and PKC on type *n* currents may be the result of direct phosphorylation of the Kv1.3 protein itself.

EXPERIMENTAL PROCEDURES

Materials - Nonidet P-40 (NP40), phosphatidyl serine, diolein, phenylmethylsulfonyl fluoride (PMSF), iodoacetamide, aprotinin, phosphate-free DMEM, lactoperoxidase, phosphoamino acids, isopropyl- β -D-thiogalactoside (IPTG) and protein A Sepharose CL-4B were from Sigma; Microcystin-LR and pre-stained high molecular weight protein standards were from BRL; calf alkaline phosphatase was from Boehringer Mannheim; protein kinase C (rat brain) was from Promega; [^{35}S]L-methionine, [γ - ^{32}P] ATP, $^{32}\text{PO}_4$, and Na^{125}I were from NEN; pMAL-c vector and amylose resin were from New England Biolabs. Purified catalytic subunit of cAMP-dependent protein kinase A from bovine heart was kindly provided by Dr. John Scott (Vollum Institute).

Cell Culture - The Jurkat human leukemic T cell line was obtained from Dr. Michael Davey (Portland VA Research Center), and cultured in RPMI 1640 supplemented with 10% FCS at 37°C, 5% CO_2 . An immature murine T lymphoma clone, SAK8 (a generous gift of Dr. Miles Wilkinson, Oregon Health Sciences University; Wilkinson et al., 1991) was cultured in DMEM with 10% FCS at 37°C, 5% CO_2 .

Preparation of Fusion Proteins and Antisera - Synthetic oligonucleotides (containing Hinc II or Sma I sites at the 5' end, and a Hind III site at the 3' end) were employed in PCR reactions to amplify specific amino acid sequences of the human or mouse Kv1.3 potassium channel. The two PCR-amplified peptides, designated as H1 and H2, are shown in Figure 4.2, and were subcloned into the pMAL-c bacterial fusion protein vector (employing Stu I and Hind III restriction sites). A translational stop codon was included in the 3' PCR oligonucleotides to terminate the translation product. All inserted PCR sequences were characterized by DNA sequence analysis. Fusion proteins MalE-H1

and MalE-H2 were induced with IPTG. MalE-H1 was purified by amylose affinity chromatography. The MalE-H2 bacterial extract was subjected to preparative gel electrophoresis on an 8% SDS-PAGE, and the protein band corresponding to MalE-H2 was prepared into a protein/gel slurry mix by mincing. The aforementioned fusion proteins were injected into rabbits following mixing with complete Freund's adjuvant for the primary injection, and incomplete Freund's adjuvant for subsequent boosts. All injections and bleeds were performed by Hazelton Research Products, Denver, PA.

In Vitro Transcription and Translation - In vitro transcription from the pHGK5 (human Kv1.3) expression plasmid was as described (Cai et al., 1992). In vitro translation employing rabbit reticulocyte lysates was performed according to the instruction supplied by Promega.

Surface iodination - SAK8 cell surface proteins were iodinated by lactoperoxidase-catalyzed reactions (Vitetta et al., 1971). Cells were suspended in PBS at 10^7 cells/ml containing 1 mCi Na^{125}I and 200 μg lactoperoxidase. The reactions were initiated with 25 μl 0.03% H_2O_2 , which was repeated four additional times every 2 minutes. The iodination reactions were terminated with ice-cold PBS supplemented with 0.1% NaN_3 , followed by three additional washes. Cell pellets were resuspended at a density of $0.5 - 1.0 \times 10^7$ cells/ml in lysis buffer containing 0.5% NP40, 0.1M Tris-HCl (pH 7.5), 5 mM EDTA, 0.02% NaN_3 , 1 mM PMSF, 0.2 TIU/ml aprotinin, and 10 mM iodoacetamide. Cells were incubated on ice with occasional shaking for 30 min, and centrifuged at 3,500 rpm to remove debris and nuclear material. The cell extracts were then incubated with preimmune serum and protein A-Sepharose on ice, followed by centrifugation. The precleared extracts were then used in immunoprecipitation reactions with immune serum.

In Vivo Phosphorylation / Metabolic Labeling - Jurkat cells were incubated in phosphate-free DMEM for 30 min. Cells were then labeled with $^{32}\text{PO}_4$ at 1 mCi/ml for 2.5 hr at 37°C. The radiolabeled cells were solubilized (as described above) in lysis buffer supplemented with 50 mM NaF, 100 mM β -glycerophosphate, 15 mM Na-pyrophosphate, and 0.2 μM microcystin-LR. The cell extract was then precleared with preimmune serum/protein A-Sepharose, followed by immunoprecipitation.

Stoichiometry of in vivo Kv1.3 Channel Subunit Phosphorylation in Jurkat Cells - Incorporation of total phosphate into Jurkat Kv1.3 channel subunits during metabolic labeling was estimated from the amount of ^{32}P incorporated per potassium channel, taking into account the specific radioactivity of γ -phosphate of the cellular pool of ATP. The value for the latter variable was assumed to be similar to that for resting T lymphocytes (Patel and Miller, 1991); approximately 3.0×10^{-5} mol of ^{32}P /mol of ATP following a minimum equilibration period of 30 minutes. The number of functional Kv1.3 channels present on Jurkat cells has been previously determined (approximately 400 channels per cell) based on mean Jurkat potassium conductance (DeCoursey et al., 1985) and unit conductance of the hKv1.3 channel (Cahalan et al., 1985; Chandy et al., 1984). The amount of ^{32}P incorporated into Jurkat Kv1.3 protein following a 2.5 hour labeling period was determined by liquid scintillation counting following gel isolation of the metabolically labeled 65-kDa protein from 2.3×10^7 Jurkat cells. The above values were used in calculations to determine that approximately 12.7 mol phosphate is incorporated per functional hKv1.3 channel (ie., approximately 3.0 mol phosphate per mol individual hKv1.3 subunit, assuming that functional voltage-gated potassium channels are the result of a tetrameric configuration; Durell and Guy, 1992; MacKinnon, 1991) at steady state under non-stimulated conditions.

Dephosphorylation - Dephosphorylation of Jurkat protein extracts with calf alkaline phosphatase was performed as described (Driscoll et al., 1990). Solubilized Jurkat cell extracts were adjusted to pH 9.0 with 1 M Tris-HCl (pH 9.5). The phosphatase reactions were initiated by addition of calf alkaline phosphatase to a final concentration of 100 U/ml, followed by incubation at 37°C for 30 min. The reactions were then terminated by addition of 10 mM DTT, followed by further incubation at 4° for 30 min. The pH of the reaction was then shifted to 7.5 with dilute HCl.

In Vitro Phosphorylation - Cell extracts (with or without alkaline phosphatase pre-treatment) were used for in vitro labeling. For PKA labeling, samples were incubated in 6 mM MgCl₂, 6 mM EGTA, 0.2 μM Microcystin-LR, 33 μM [γ-³²P] ATP, and 6 μg/ml catalytic subunit of PKA at 37°C for 30 min. For PKC labeling, samples were incubated in 20 mM Hepes, pH 7.5, 10 mM MgCl₂, 1.6 mM CaCl₂, 10 mM DTT, 20 μg/ml phosphatidyl serine, 0.8 μg/ml diolein, 0.2 μM microcystin-LR, 33 μM [γ-³²P] ATP, and 6 μg/ml PKC at 30°C for 20 min. Reactions were terminated by addition of EDTA to 30 mM final concentration, followed by preclearance with preimmune serum/protein A-Sepharose, and then immunoprecipitation as described below.

Immunoprecipitation and SDS-PAGE - Bacterial acetone powder extracts were prepared from IPTG-induced bacteria containing the plasmid encoding either MalE-βgal (vector alone), MalE-H1, or MalE-H2 fusion proteins (Harlow and Lane, 1988).

Preimmune or immune sera were incubated with 1% acetone powder extracts suspended in cell lysis buffer for 60 min, followed by removal of the acetone powder via centrifugation. This procedure served to absorb (or neutralize) specific antibodies within the sera which are directed against the various fusion proteins, as well as non-specific antibodies which might affect the resulting background. Following preabsorption, sera were then added to cell extracts labeled either in vivo or in vitro. Mixtures were incubated at 4°C for 2 to 18 hr

followed by incubation with protein A-Sepharose for 2 hr. Sepharose beads were isolated by centrifugation, washed with lysis buffer, and resuspended in 2% SDS, 50 mM Tris-HCl (pH 6.8), 0.1% bromophenol blue, 10% glycerol, and 1% 2-mercaptoethanol. Samples were heated at 100°C for 5 min, and applied to SDS-polyacrylamide gels (8% resolving gel / 5% stacking gel). Following electrophoresis, gels were dried and exposed to Kodak XAR film.

Phosphoamino Acid Analysis - Phosphoamino acid analysis was performed as described (Boyle et al., 1991). Briefly, the radiolabeled protein band corresponding to the Jurkat Kv1.3 potassium channel was excised from an SDS-polyacrylamide gel following immunoprecipitation, eluted with NH_4HCO_3 , precipitated with TCA, and hydrolyzed in 6N HCl at 110°C for 1hr. The hydrolysate was dried, and amino acids were separated by thin layer cellulose electrophoresis. Standard phosphoamino acids for phosphoserine, phosphothreonine and phosphotyrosine were added to the hydrolyzed radioactive sample, and their migration determined by ninhydrin staining. Radioactive, in vivo phosphorylated amino acids within Kv1.3 were detected by autoradiography.

RESULTS

Generation of polyclonal antisera against the murine and human Kv1.3 potassium channel

Regions of mouse and human Kv1.3 were chosen for the synthesis of bacterial fusion proteins based upon predicted antigenicity, and uniqueness at the amino acid level when compared to other members of the Kv1 (*Shaker*-related) sub-family of voltage-gated potassium channels (rKv1.1, Baumann et al., 1988; rKv1.2, MacKinnon, 1989; hKv1.4 and hKv1.5, Philipson et al., 1991; hKv1.6, Grupe et al., 1990). Figure 4.2 shows the amino acid sequence of two regions (from human Kv1.3) which met this criteria: region H1, a sequence 45 amino acids in length which represents the entire extracellular domain between transmembrane domains 1 and 2; and region H2, representing the final 46 amino acids of the intracellular carboxy-terminal region of the protein. Amino acid sequence comparison with corresponding regions of other members of the Kv1 sub-family reveals limited homology, suggesting that antibodies generated against these peptides would be unique to the Kv1.3 channel, and not recognize other members of the Kv1 sub-family. DNA sequences encoding human Kv1.3 H1 and H2 regions were amplified by PCR, and ligated into the plasmid pMAL-c to generate fusion proteins designated as MalE-H1 or MalE-H2. The fusion proteins were injected into rabbits and polyclonal antisera generated.

Figure 4.3 exemplifies studies aimed at characterizing the various antisera. In Figure 4.3A, the ability to immunoprecipitate an in vitro translated, ³⁵S-labeled human (h) Kv1.3 protein product is documented. The MalE-H2 antiserum was able to immunoprecipitate the major 58-kDa hKv1.3 in vitro translated product (lane 1). Preabsorption of MalE-H2 antiserum with a bacterial acetone powder extract containing the MalE-H2 fusion protein neutralizes Kv1.3-directed antibodies with the serum, and no

radiolabeled immunoprecipitation product is observed (lane 2). However, preabsorption of MalE-H2 antiserum with a bacterial acetone powder extract containing the MalE- β gal fusion protein results in immunoprecipitation of radiolabeled hKv1.3 (lane 3), implying that antibodies directed against the H2 portion of the fusion protein are responsible for immunoprecipitation of hKv1.3. Identical results were obtained when antiserum against MalE-H1 was tested ². Also, the two antisera were capable of immunoprecipitating in vitro translated rat (r) Kv1.3, but not rKv1.1 or rKv1.2 ². This result implies the specificity of the antisera to the Kv1.3 channel.

In Figure 4.3B the ability of MalE-H2 antiserum to immunoprecipitate an ¹²⁵I surface labeled Kv1.3 channel expressed in SAK8 cells is also documented. SAK8 cells are derived from a spontaneous thymic lymphoma in an AKR mouse. They are CD4⁺/CD8⁺, and thus represent a non-differentiated T lymphoma clone (Wilkinson et al., 1991). Northern blot analysis employing a cRNA probe specific for rKv1.3 mRNA revealed the presence of a 9.5 kb transcript when SAK8 total RNA was analyzed ², thus suggesting that the Kv1.3 channel is expressed on the surface of SAK8 cells. When ¹²⁵I surface labeled proteins were immunoprecipitated with preimmune serum, no radiolabeled immunoprecipitate is observed (lane 1). MalE-H2 antiserum (preabsorbed with MalE- β gal), however, results in the precipitation of a major radiolabeled product with a molecular mass of approximately 65-kDa (lane 2), presumably representing the mKv1.3 protein. This band disappears, as expected, when the MalE-H2 antiserum is preabsorbed with the MalE-H2 fusion protein prior to immunoprecipitation (lane 3), confirming the specificity of the immunoprecipitated product. The apparent molecular mass of Kv1.3 in SAK8 cells is approximately 7-kDa greater than in vitro translated Kv1.3, suggesting that the channel is post-translationally modified.

In vivo phosphorylation of the hKv1.3 channel in human Jurkat cells

One type of post-translational modification event which may have a profound effect on Kv1.3 channel function is phosphorylation. Indeed, it is well documented that modulation of the PKA and PKC systems in the human Jurkat T lymphocyte cell line dramatically alters activity of the type *n* channel current (Payet and Dupuis, 1992). Metabolic labeling studies were thus employed to determine if the type *n* channel is capable of being directly phosphorylated in Jurkat cells (Figure 4.4). Jurkat cells were incubated in phosphate-free DMEM, then labeled with $^{32}\text{PO}_4$ for 2.5 hr. Cell extracts were then subjected to immunoprecipitation with antiserum against the MalE-H1 fusion protein. Preimmune serum immunoprecipitated several proteins with molecular mass greater than 100-kDa (lane 1). MalE-H1 antiserum (preabsorbed with MalE- β gal), however, resulted in the immunoprecipitation of a major phosphorylated protein with a molecular mass of approximately 65-kDa (lane 2), presumably representing hKv1.3. The identity of this protein as Kv1.3 was confirmed, since preabsorption of MalE-H1 antiserum with MalE-H1 fusion protein prevented immunoprecipitation of only this phosphorylated protein (lane 3). Thus, Kv1.3 appears to be a substrate for endogenous kinase activity in the Jurkat cell line.

The stoichiometry of phosphorylation was also calculated as described in Materials and Methods. Under steady state basal conditions, approximately 3.0 mol of phosphate were incorporated per mol of 65-kDa hKv1.3 channel subunit. Thus, in Jurkat cells the type *n* channel is apparently phosphorylated to a significant extent, reducing the possibility of non-specific endogenous phosphorylation.

As a prelude study towards the identification of Kv1.3 residues which serve as the sites for Jurkat phosphorylation events, phosphoamino acid analysis was performed on the 65-kDa immunoprecipitated product (Figure 4.5). Serine residues appear to be the major (if not only) species of amino acid phosphorylated on the Kv1.3 channel expressed in

Jurkat cells; no evidence was observed supportive of phosphorylation of threonine or tyrosine residues.

The effects of various second messengers on in vivo hKv1.3 phosphorylation were also examined in an attempt to determine if modulation of specific kinase systems altered the degree of endogenous channel phosphorylation. To examine the PKA system, cells were treated with 8-Br-cAMP (1mM or 50 mM), 8-Br-cAMP and IBMX (at 1 mM and 50 μ M, respectively), or forskolin (200 μ M) for the final 30 minutes during the 2.5 hr labeling period. Following quantitative immunoprecipitation, no observable differences were detected regarding the level of 65-kDa hKv1.3 phosphorylation ². To examine the PKC system, cells were treated with TPA (0.1, 1.0 and 10.0 μ g/ml) under the same time constraints. The lowest levels of TPA produced no observable effects, however treatment of Jurkat cells with 10.0 μ g/ml TPA resulted in an approximate 2-fold increase in the level of radiolabeled immunoprecipitated 65-kDa hKv1.3 ². These results suggest that the endogenous Jurkat PKC system may be at least partially responsible for in vivo phosphorylation of the type *n* channel. In vitro phosphorylation studies described below support this notion.

In vitro phosphorylation of Jurkat Kv1.3 by protein kinase A and protein kinase C

Two serine/threonine kinases whose activity has been associated with regulation of the type *n* potassium current in Jurkat cells are protein kinase A and protein kinase C (Attali et al., 1992; Payet and Dupuis, 1992). In vitro phosphorylation studies were thus performed to determine if Jurkat Kv1.3 could serve as a substrate for PKA and PKC phosphorylation.

Figure 4.6 shows the results of such studies examining PKA phosphorylation events. As a control, the Jurkat cell extract was tested for endogenous kinase activity in PKA buffer conditions (lane 1). Following immunoprecipitation with MalE-H1 antiserum, a faint 65-kDa radiolabeled band was observed, indicating the presence of a small level of endogenous kinase activity in the extract capable of phosphorylating Kv1.3. When PKA was added to the assay (lane 3), a major 65-kDa phosphoprotein was immunoprecipitated by the MalE-H1 antiserum, indicating that Kv1.3 can be significantly phosphorylated by PKA. The identification of the 65-kDa phosphoprotein as Kv1.3 was confirmed by antiserum preabsorption reactions; MalE-H1 preabsorption (lane 4) neutralizes H1-directed antibodies from the antiserum and the 65-kDa signal is no longer observed, while MalE- β gal (lane 3) or MalE-H2 (lane 5) preabsorption has no effect on immunoprecipitation of the 65-kDa protein. Also, preimmune serum cannot immunoprecipitate the phosphorylated form of Kv1.3 (lane 2). Thus, Kv1.3 present in Jurkat cellular extracts can serve as an excellent substrate for phosphorylation by PKA.

Jurkat cell extracts were also treated with calf alkaline phosphatase prior to PKA treatment to determine the relative degree of endogenous phosphorylation of Kv1.3 (Figure 4.6, lanes 6-9). As a control for endogenous kinase activity, Jurkat extracts were incubated with PKA buffer alone followed by immunoprecipitation with MalE-H1 antiserum (lane 6). Several high molecular weight bands were observed, none of which corresponds to 65-kDa radiolabeled Kv1.3. When extracts were incubated with PKA, MalE-H1 antiserum once again immunoprecipitated radiolabeled 65-kDa Kv1.3 (lane 8), however the background was significantly higher. The relative intensity of the Kv1.3 signal, though, was not significantly increased as a result of phosphatase pretreatment, suggesting that Jurkat Kv1.3 is not heavily phosphorylated *in vivo* by endogenous PKA or related kinases which may recognize similar phosphorylation sites. This suggestion is also based on the assumption that alkaline phosphatase would be capable of interacting with any

phosphorylated form(s) of Kv1.3. As before, the specificity of the 65-kDa phosphoprotein as Kv1.3 was confirmed by antiserum preabsorption reactions; MalE-H1 preabsorption (lane 9) neutralizes H1-directed antibodies from the antiserum and the 65-kDa signal is no longer observed. Additionally, preimmune serum could not immunoprecipitate the phosphorylated form of Kv1.3 (lane 7).

Examination of the profile of PKA-radiolabeled immunoprecipitated products also revealed the presence of an approximately 40-kDa protein which appears to co-precipitate with the 65-kDa Kv1.3. The 40-kDa protein was only observed in MalE-H1 antiserum immunoprecipitates (lane 8), and was not observed when the antiserum was preabsorbed with MalE-H1 (lane 9), or when preimmune serum was used (lane 7). The approximate molecular mass, and profile of appearance of this protein is similar to that previously described for a cellular protein associated with other mammalian voltage-gated potassium channels (Parcej and Dolly, 1989; Rehm and Lazdunski, 1988; Rehm et al., 1989; Scott et al., 1990; Trimmer, 1991). The results presented here suggest that this channel-associated product is also associated with the Jurkat Kv1.3 channel, and can serve as a substrate for phosphorylation by PKA.

Other studies were aimed at determining whether PKC is capable of phosphorylating Jurkat Kv1.3. In experiments not shown, non-alkaline phosphatase treated Jurkat extracts were incubated under appropriate PKC conditions, in the presence and absence of exogenous PKC. Following immunoprecipitation, a specific 65-kDa radiolabeled product was observed, however its presence was not dependent on the addition of exogenous PKC. These results imply the presence of significant levels of endogenous PKC (or PKC-like) activity in Jurkat extracts which is capable of phosphorylating hKv1.3 in vitro. For the study shown in Figure 4.7, Jurkat cell extracts were pre-treated with calf alkaline phosphatase prior to addition of PKC. Lanes 1 and 2 are

reproduced from Figure 4.6 (lanes 8/9; PKA treatment), and serve to show the precise location of immunoprecipitated phosphorylated 65-kDa Kv1.3 following gel electrophoresis. As a control for endogenous Jurkat PKC activity (both PKC α and β isoforms are present in Jurkat cells ; Lucas et al., 1990), extracts were incubated with PKC buffer alone followed by immunoprecipitation with MalE-H1 antiserum (lane 3). Several high molecular weight phosphoproteins were immunoprecipitated with MalE-H1 antiserum, and a faint diffuse signal was also observed in the 65-kDa region. However, when PKC was added to the extract, MalE-H1 antiserum was able to immunoprecipitate higher levels of radiolabeled 65-kDa Kv1.3 (lane 5). The relative intensity of the Kv1.3 signal, though, was significantly less following PKC treatment than that observed following PKA treatment. Lastly, the specificity of the 65-kDa phosphoprotein as Kv1.3 was once again confirmed by an antiserum preabsorption reaction; MalE-H1 preabsorption (lane 6) resulted in the specific disappearance of the 65-kDa signal. Additionally, preimmune serum could not immunoprecipitate phosphorylated 65-kDa Kv1.3 (lane 4). These data suggest that PKC, similar to PKA, is capable of phosphorylating Jurkat Kv1.3. Unlike PKA, however, it appears that PKC is unable to phosphorylate the 40-kDa protein presumably associated with Kv1.3.

DISCUSSION

The Kv1.3 voltage-gated potassium channel was originally characterized as a cDNA clone isolated from a rat cortex cDNA library (Stuhmer et al., 1989). Northern blot analysis of total RNA isolated from dissected rat brain regions indicated that Kv1.3 mRNA was present at vanishingly small levels in neural tissue when compared to levels of Kv1.1, Kv1.2 and Kv1.4 mRNA (Beckh and Pongs, 1990). Additional electrophysiological and pharmacological characterization in *Xenopus* oocytes of potassium currents resulting from injection of *in vitro* synthesized Kv1.3 RNA revealed several properties unique to the channel; there was inactivation following depolarizing voltage commands, the channel was sensitive to blockers of both Ca^{++} -activated potassium channels (quinine) and calcium channels (verapamil), and divalent cations served to dramatically reduce potassium conductance (Douglass et al., 1990; Grissmer et al., 1990). This unique compilation of properties had never been previously observed for neuronal potassium currents, but had been well characterized in mammalian T lymphocytes (Cahalan et al., 1987; Cahalan and Lewis, 1990; DeCoursey et al., 1985; Lewis and Cahalan, 1990). The lymphocyte potassium channel exhibiting these specific properties was termed the "type *n*" channel, and demonstration of high levels of Kv1.3 mRNA in mammalian T lymphocytes subsequently confirmed the identity of Kv1.3 as that of the type *n* lymphocyte potassium channel.

A wide variety of studies have documented alterations in the density of Kv1.3 currents in mammalian T lymphocytes following activation by mitogenic agents (Cahalan et al., 1987; DeCoursey et al., 1985, 1987; Deutsch, 1990; Deutsch et al., 1986, 1991; Matteson and Deutsch, 1984). This mitogen-induced increase in Kv1.3 current density varies from 2-fold in human T lymphocytes, to 20-fold in murine T lymphocytes,

suggesting that this potassium channel may play a role in mitogenesis. Moreover, the increase in current density is probably not the result of stimulated transcription of the Kv1.3 gene, as the levels of mRNA encoding the type *n* potassium channel appear to be down-regulated in both murine and human T lymphocytes following treatment with mitogens (Attali et al., 1992a; Cai et al., 1992). One possible mechanism by which Kv1.3 currents may be functionally regulated is through post-translational modification of the channel protein. Recent studies have suggested that this may indeed be the case, as manipulation of intracellular PKA and PKC systems in cells expressing Kv1.3 dramatically alter type *n* channel currents. Employing the *Xenopus* oocyte expression system, Attali and co-workers (1992b) have presented data suggesting that second messengers generated by phospholipase C activation may be important modulators of Kv1.3 channel activity. This observation has also been extended to the Jurkat Kv1.3 channel (Payet and Dupuis, 1992). In these cells, not only does modulation of the PKC system appear to affect channel activity, but modulation of the PKA system as well. In both reports, activation of kinase systems served to inhibit type *n* currents. Moreover, agents which antagonized kinase activities prevented kinase-induced effects on type *n* currents. Additionally, when Jurkat cells were exposed to alkaline phosphatase via the patch pipet, a dramatic increase in type *n* current amplitude was observed (Payet and Dupuis, 1992). As a result of these observations, both groups speculated that direct phosphorylation/de-phosphorylation of the Kv1.3 channel underlies these PKA- and PKC-dependent events.

As a first step in the biochemical characterization of the Kv1.3 channel, a series of polyclonal antisera were generated against unique regions of both the mouse and human channel. The antisera work well for immunoprecipitation of the Kv1.3 channel, and do not appear to recognize other members of the Kv1 subfamily of potassium channels².

Following polyacrylamide gel electrophoresis, immunoprecipitated *in vitro* translated hKv1.3 exhibited an apparent molecular mass of approximately 58-kDa, as expected for the

unmodified channel. However, ^{125}I surface labeled Kv1.3 from the SAK8 murine lymphoma cell line appeared to have an apparent molecular mass of approximately 65-kDa. We were unable to demonstrate that N-linked glycosylation events serve as the molecular basis for this apparent size difference ². Treatment of SAK8 cell membranes with N-glycosidase F failed to produce a downward shift in apparent molecular mass. This observation is in contrast to that reported for bovine Kv1.2, where N-glycosidase treatment of the affinity-purified channel (from bovine brain) resulted in an apparent molecular mass shift from 78-kDa to 65-kDa (Scott et al., 1990). Still, though, the resulting 65-kDa form was significantly larger than the predicted 57-kDa form which would represent a completely unmodified Kv1.2 channel. Thus, a wide variety of post-translational modification events such as O-linked glycosylation may occur on mammalian Kv1 potassium channels.

Metabolic labeling of the human Jurkat cell line, followed by immunoprecipitation, clearly demonstrated that the Kv1.3 channel is directly phosphorylated in vivo. Moreover, phosphoamino acid analysis of the radiolabeled protein showed that serine residues are the major, if not only, sites for kinase activity in the Jurkat cell line. Furthermore, the stoichiometry of phosphorylation under steady state basal conditions suggests approximately 3.0 mol of phosphate incorporated per mol of Kv1.3 channel subunit. Thus, in Jurkat cells the type *n* channel is apparently phosphorylated at serine residues to a significant extent. Two candidate serine/threonine kinase systems which are present in this cell line are PKA (Bastin et al., 1990) and PKC (Lucas et al., 1990). Addition of various pharmacological agents to Jurkat cell cultures which are known to increase cellular levels of PKA activity, failed to produce an increase in the level of in vivo phosphorylation of 65-kDa Kv1.3. However, treatment of Jurkat cells with relatively high levels of the phorbol ester, TPA, produced an approximately 2-fold increase in the level of phosphorylated 65-kDa Kv1.3 as determined by quantitative immunoprecipitation. Thus, the endogenous

Jurkat PKC system appears to be at least partially responsible for in vivo phosphorylation of the type *n* channel.

In vitro phosphorylation studies with purified PKA showed that Jurkat Kv1.3 serves as an excellent substrate for phosphorylation. Inspection of the primary amino acid sequence of hKv1.3 suggests several potential sites for PKA phosphorylation (Kemp and Pearson, 1990; Kennelly and Krebs, 1991). One such site is located within the carboxy-terminal intracellular domain; Arg - Lys - Ala - Arg - Ser⁴⁶⁸ - Asn. The intensity of PKA-radiolabeled Kv1.3 was unaffected by alkaline phosphatase pre-treatment of Jurkat cell extracts, suggesting that the channel is not heavily phosphorylated by PKA in vivo in this cell line. As noted earlier, this suggestion is based on the assumption that alkaline phosphatase is capable of interacting with phosphorylated forms of Kv1.3. Alkaline phosphatase pre-treatment did, however, result in co-precipitation of a radiolabeled protein approximately 40-kDa in size. Interestingly, immunological evidence for the association of a 38-kDa protein with both rat and bovine brain potassium channels has been previously documented (Rehm et al., 1989; Trimmer, 1991), and we speculate here that the PKA-phosphorylated 40-kDa protein which co-precipitates with Kv1.3 may be related to that described above. If so, PKA phosphorylation events associated with this 40-kDa protein may represent another mechanism by which Kv1.3 channel activity could be modulated. This concept has indeed been documented for the 54-kDa β subunit which is associated with the 212-kDa $\alpha 1$ subunit of the skeletal muscle calcium channel (De Jongh et al., 1989).

Although not as dramatic as the results observed employing PKA, in vitro phosphorylation studies also suggest that PKC is capable of directly phosphorylating Kv1.3. These studies, though, were hampered by the presence of significant levels of PKC (or PKC-like activity) in Jurkat extracts. In non-alkaline phosphatase treated Jurkat

extracts, in vitro phosphorylation of 65-kDa Kv1.3 under PKC buffer conditions was not dependent on the addition of exogenous PKC². Only with alkaline phosphatase treated Jurkat extracts did exogenous PKC stimulate phosphorylation of hKv1.3. These results further support the notion that PKC, or an enzyme with PKC-like activity, plays a prominent role regarding in vivo phosphorylation of the type *n* channel in Jurkat cells. Inspection of the human Kv1.3 sequence identifies the motif, Lys - Ala - Ser³⁴² - Met - Arg, located in the intracellular loop between S4/S5 transmembrane domains. This site conforms to that of a PKC recognition site (Kemp and Pearson, 1990; Kennelly and Krebs, 1991), and is also conserved among human, rat and mouse Kv1.3. Additionally, this sequence is conserved in the *Drosophila Shaker* potassium channel, and mutagenesis of the corresponding serine residue to either alanine or cysteine results in the reduction of single channel conductance values by almost 50% (Isacoff et al., 1991). Thus, this serine residue may also play an important role in modulating Kv1.3 functional activity, perhaps via a PKC-dependent mechanism.

The results presented here suggest a variety of areas for future investigation. Perhaps the most straightforward line of investigation will be the characterization of the specific serine residues which serve as Kv1.3 phosphorylation sites. The use of phosphopeptide mapping protocols has successfully served to determine the specific residues phosphorylated in the CFTR chloride channel (Cheng et al., 1991), the skeletal muscle calcium channel (Rohrkasten et al., 1988), and the rat brain sodium channel (Rossie et al., 1987, 1989). Similar methods of characterization should result in the identification of specific serine residues in Kv1.3 which serve as phosphorylation sites. The functional significance of phosphorylation at these sites must also be determined. Such structure - function correlations have been previously documented for the CFTR chloride channel (Cheng et al., 1991).

The significance of Kv1.3 phosphorylation as related to lymphocyte functions is also a topic for future investigation. A diverse array of cytokine and neurohormone receptors are present on T lymphocytes, involving several distinct signal transduction systems (Plaut, 1987; Miyajima et al., 1992). In general, receptors activating adenylate cyclase inhibit lymphocyte function, while those activating phospholipase C stimulate lymphocyte function. Modulation of lymphocyte PKA and PKC, as well as phosphatase, activities following cell surface receptor activation may thus regulate Kv1.3 channel function through direct phosphorylation and dephosphorylation events. It remains to be determined, however, if such events play a significant role in the cellular events associated with T lymphocyte activation.

ACKNOWLEDGEMENTS

The authors thank Drs. Paul Shapiro for assistance with the phosphoamino acid analysis and critical reading of the manuscript, John Scott for the gift of purified PKA, Miles Wilkinson for the gift of the SAK8 cell line, and Michael Davey for the gift of the Jurkat cell line.

Footnotes

1 The work was supported by Department of Health and Human Services Grant DA04154 to JD.

2 Yun-Cai Cai, unpublished experiments and observations.

3 The abbreviations used are: 8-Br-cAMP, 8-brommoadenosine 3'cyclic monophosphate; IBMX, isobutylmethylxanthine; TPA, phorbol 12-myristate 13-acetate.

IV

**FUNCTIONAL SIGNIFICANCE OF A HIGHLY CONSERVED SERINE
RESIDUE WITHIN THE INTRACELLULAR S4/5 LOOP OF MAMMALIAN
POTASSIUM CHANNELS**

Yun-Cai Cai *#, Michael Kavanaugh *, and James Douglass *

Vollum Institute* and the Department of Microbiology and Immunology#
Oregon Health Sciences University
Portland, OR 97201, USA

Manuscript in preparation; 1993.

ABSTRACT

The intracellular S4/5 loop is involved in determining gating and/or ion permeation properties of voltage-gated potassium channels. Substitution of ³⁹²Ser within this region with an alanine residue reduces the single channel conductance of the *Drosophila Shaker B* potassium channel by 40% (Isacoff et al., 1991). The present results demonstrated that substitution of the corresponding serine residue with alanine totally abolishes ionic conductance for at least two mammalian potassium channels (hKv1.3 and rKv1.2). However, gating currents similar to the hKv1.3 ³⁴²Ser channel (wild type) were observed for the hKv1.3 ³⁴²Ala mutant. The ³⁴²Ala channel subunit also retains the ability to heteropolymerize with functional subunits to form a conducting channel, as determined by RNA co-injection experiments. Thus, mutation of the highly conserved serine residue within the intracellular S4/5 loop affects the ionic conductance of both *Drosophila* and mammalian potassium channels, without significantly disrupting gating charge movement or subunit assembly.

INTRODUCTION

Voltage-gated potassium channels are membrane proteins which open in response to membrane depolarization. Mutational analysis of these channels has provided significant information regarding specific amino acid residues involved in controlling channel properties such as voltage-dependent activation, ion selectivity, inactivation, and tetrameric complex formation (reviewed by Durell and Guy, 1992; Jan and Jan, 1992; Stuhmer, 1991). Both the S4 transmembrane region and the intracellular S4/5 loop are involved in mediating potassium channel activation, since mutations within these two regions affect voltage-dependence of activation (Isacoff et al., 1991; Liman et al., 1991; Logothetis et al., 1992; McCormack et al., 1991; Papazian et al., 1991; Stuhmer et al., 1989). The SS1 and SS2 regions between the transmembrane domains S5 and S6 form the majority of the channel pore region (MacKinnon and Yellen, 1990; Yellen et al., 1991; Yool and Schwarz, 1991); in addition, mutational analysis also indicates that the intracellular S4/5 loop lies in or near the internal mouth of the channel pore (Isacoff et al., 1991). Furthermore, the primary amino acid sequence of the S4/5 loop is highly conserved among voltage-gated potassium channels. Thus, the S4/5 loop appears to be critical for voltage-dependent activation and/or potassium ion flow rate of voltage-gated potassium channels.

The ³⁹²Ser within the S4/5 loop of the *Shaker B* potassium channel has been subjected to mutational analysis described previously by Isacoff et al. (1991). Substitution of ³⁹²Ser with either alanine or cysteine residues reduces the single channel conductance by approximately 40 %.

The primary amino acid sequence of the S4/5 loop is almost identical between *ShB* and rKv1.3/hKv1.3 potassium channels (Fig. 5.1). In order to study potential functional roles of the corresponding serine residue in mammalian potassium channels, similar mutants were generated for hKv1.3 and rKv1.2. The presented results reveal that such a

mutation totally abolishes potassium currents following expression in *Xenopus* oocytes, a much more dramatic result when compared to the counterpart mutation in *Drosophila ShB*.

EXPERIMENTAL PROCEDURES

Site-directed mutagenesis -- The hKv1.3 (HGK5) coding sequence (Cai et al., 1992) was subcloned into the EcoRI/HindIII sites within the vector, pSELECT⁻ (a generous gift from Dr. John Adelman). The ³⁴²Ser within the hKv1.3 S4/5 loop was subjected to site-directed mutagenesis according to the protocol provided by Promega. For reverse mutation (³⁴²Ala -> ³⁴²Ser), the construct was re-subcloned into pSELECT⁻, followed by back-mutagenesis. All mutations were identified by dideoxy DNA sequence analysis. A 0.6 kb PstI/HindIII fragment containing the ³⁴²Ala mutation was further subcloned into M13 vectors for additional sequence verification, with both strands fully sequenced. All 0.6 kb PstI/HindIII fragments with mutations at position 342 were then subcloned into the 3.7 kb PstI/HindIII cut vector of pHGK5-EXP (Cai et al., 1992), for expression in *Xenopus* oocytes.

A rat Kv1.2 expression clone, containing the RBK2 coding region subcloned into the vector pSELECT⁻, was also generously provided by Dr. John Adelman. Similar to hKv1.3, the ³²⁴Ser was mutated to either alanine or aspartate residues. Mutations were identified by dideoxy DNA sequence analysis. These constructs were then directly used for expression analysis in *Xenopus* oocytes.

A list of mutations involving the conserved serine residue located within the S4/5 loop is shown in Fig. 5.1. Each expression construct was thus named after the residue mutated, and this nomenclature is used throughout the text. One additional mutation involved conversion of hKv1.3 ³⁹⁹His to ³⁹⁹Tyr. Generation and analysis of this mutant was identical to that described above.

Expression of hKv1.3 and rKv1.2 mRNAs in *Xenopus* oocytes -- Each expression vector was linearized with HindIII, transcribed *in vitro*, and resulting mRNA was injected into *Xenopus* oocytes as described (Cai et al., 1992). Two electrode

voltage-clamp analysis was performed 3 days after injection, as described (Kavanaugh et al., 1991).

Recording of gating currents in *Xenopus* oocytes -- Recordings were made using a cut-open oocyte vaseline gap configuration (Taglialatela et al., 1992). The external solution contained 0.14 M Na methanesulfonate, 1.8 mM Ca^{++} , 2 mM K^{+} , 1 mM Mg^{++} , and the internal solution contained 0.14 M K methanesulfonate, 1 mM Mg^{++} . Recordings were made using a Dagan CA-1 clamp amplifier with an Axon Instrument Axolab-1 A/D interface. Data were sampled at 20 kHz, and low pass filtered at 5 kHz. The oocyte membrane was held at -90 mV and voltage steps were applied in 10 mV increments. Linear capacitive currents were subtracted using a p/4 protocol (sub-pulse holding potential = -120 mV).

Co-expression of hKv1.3 mutants in *Xenopus* oocytes -- For co-injection experiments, concentrations of hKv1.3 ³⁴²Ala and ³⁹⁹Tyr expression DNA vectors were quantitated by spectrometry and equal amounts of DNA mixed together, followed by linearization, in vitro transcription, and mRNA injection into *Xenopus* oocytes (Cai et al., 1992). The external TEA inhibition analysis was performed as described previously (Kavanaugh et al., 1991). Data were fit to a logistic function of the form: $\%I = 100[\text{TEA}]^n/([\text{TEA}]^n + K_d^n)$.

RESULTS

Expression of hKv1.3 and rKv1.2 mutants in *Xenopus* oocytes -- The hKv1.3 ³⁴²Ala channel was subjected to functional analysis in *Xenopus* oocytes. The in vitro transcribed ³⁴²Ser (wide type) and ³⁴²Ala (mutant) mRNAs were injected individually into oocytes, followed by two-electrode recording. Depolarization of the oocyte membrane elicits large outward potassium currents in ³⁴²Ser as described previously (Cai et al., 1992); however, no ionic currents were recorded from the oocytes injected with ³⁴²Ala mRNA (Fig. 5.2). Full DNA sequence analysis of a 0.6 kb PstI/HindIII fragment containing residue 342 indicated that no additional mutation existed in the coding region of ³⁴²Ala. Furthermore, the reverse mutation of ³⁴²Ala->³⁴²Ser resulted in the recovery of ionic currents identical to those observed for ³⁴²Ser (Fig. 5.2). Thus, mutation of hKv1.3 ³⁴²Ser to ³⁴²Ala results in loss of potassium currents in response to membrane depolarization.

Similar mutational analysis was conducted with the rKv1.2 potassium channel. rKv1.2 ³²⁴Ser elicits strong outward potassium currents as previously described (Kavanaugh et al., 1991; Stuhmer et al., 1989) (data not shown). However, no ionic currents were recorded from the oocytes injected with rKv1.2 ³²⁴Ala mRNA (data not shown), as in the case of hKv1.3 ³⁴²Ala. Therefore, mutation of this highly conserved serine residue within the intracellular S4/5 loop completely eliminates voltage-dependent potassium currents for the hKv1.3 and rKv1.2 mammalian voltage-gated potassium channels.

Both hKv1.3 ³⁴²Ser and rKv1.2 ³²⁴Ser are located within a putative protein kinase C recognition sequence (K-A-S-M-R), as is the corresponding ³⁹²Ser of *Shaker B*. This observation has suggested that phosphorylation of this particular serine residue may play a crucial role in channel function. The overall structure of an aspartate residue is

similar to that of a phosphoserine residue, thus allowing for an opportunity to determine the effects of a potential negative charge at this position on channel activity. The hKv1.3 ³⁴²Ser was thus mutated to ³⁴²Asp, and mRNA from this expression vector injected into *Xenopus* oocytes. As for the ³⁴²Ala channel, the ³⁴²Asp channel did not produce any voltage-dependent ionic currents (data not shown). A similar result was likewise observed for rKv1.2 ³²⁴Asp (data not shown). These results are thus indicative of either a substantial difference of structure between an aspartate residue and a phosphoserine residue, or just a simple requirement of a serine residue at this position.

An alanine residue has a side chain structure which is reasonably similar to that of a serine residue; however, we can not rule out the possibility of significant conformational disruption resulting from the ³⁴²Ala substitution within the S4/5 loop. The studies described below were thus aimed at determining the ability of hKv1.3 ³⁴²Ala to form either homo- or heter-tetrameric complexes by measuring gating currents of homotetramers, and TEA sensitivity of heterotetramers.

Gating currents of hKv1.3 ³⁴²Ser and ³⁴²Ala -- Gating currents represent charge movement associated with channel conformational transitions in response to membrane depolarization, which are intrinsic to voltage-gated potassium channels (Durell and Guy, 1992). As shown in Fig. 5.3A, a gating charge movement is evident at -70 mV, while ionic current activates near -40 mV in oocytes injected with wide-type hKv1.3 ³⁴²Ser. ³⁴²Ala exhibited transient currents resembling those of ³⁴²Ser with no ionic current recorded (Fig. 5.3B). As expected, control oocyte membrane exhibited no detectable non-linear capacitive current (Fig. 5.3C). These results indicate that the ³⁴²Ala potassium channel is expressed to a significant level on the oocyte membrane. The existence of gating currents in ³⁴²Ala further suggests that the alanine substitution does not prevent voltage-dependent conformational transitions of the channel, but does block at least one transition prior to channel opening.

Coexpression of hKv1.3 ³⁴²Ala and ³⁹⁹Tyr -- A functional potassium channel is currently thought to represent a protein complex in which four individual channel subunits associate. Thus, the ability to form a tetrameric structure is required for channel function. Such a property was analyzed for the hKv1.3 ³⁴²Ala potassium channel.

Previous studies have shown that the ⁴⁰¹His residue in rKv1.3 (RGK5) is a primary determinant of sensitivity to the potassium channel blocker, TEA. The wild type rKv1.3 has a K_d of 11 mM (Kavanaugh et al., 1991). Substitution of ⁴⁰¹His with a tyrosine residue increases TEA sensitivity approximately 20-fold (K_d = 0.5 mM). The corresponding residue in hKv1.3 is ³⁹⁹His. The substitution of ³⁹⁹His with ³⁹⁹Tyr thus should convert the hKv1.3 potassium channel from low to high TEA sensitivity. Here, the hKv1.3 ³⁹⁹His was mutated to ³⁹⁹Tyr, and the mRNA of ³⁹⁹Tyr injected into oocytes. The resulting ³⁹⁹Tyr channel exhibited a TEA K_d of 1.1 mM, compared to a K_d of 20 mM for the ³⁹⁹His channel (Fig. 5.4). These results conform with those of the rKv1.3 ⁴⁰¹His and ⁴⁰¹Tyr channels as described previously (Kavanaugh et al., 1991).

The ability of the ³⁴²Ala subunit to form polymeric structures was studied by co-expression of the hKv1.3 ³⁴²Ala and ³⁹⁹Tyr channels in *Xenopus* oocytes followed by an evaluation of sensitivity of resulting currents to various concentrations of TEA. Equal amounts of ³⁴²Ala and ³⁹⁹Tyr plasmid DNAs were mixed, linearized with HindIII, transcribed in vitro, and the resulting mRNAs then injected into *Xenopus* oocytes. The whole cell currents were recorded in the presence of different concentrations of TEA. As shown in Fig. 5.4, the concentration curve of inhibition for coinjected mRNAs was shifted significantly to the right of that observed for ³⁹⁹Tyr. Because multiple subunits contribute to the TEA binding site (Kavanaugh et al., 1992), this result thus suggests that the low-affinity ³⁴²Ala subunit must be able to associate with the high-affinity ³⁹⁹Tyr subunit, resulting in the formation of a heteropolymeric channel population with intermediate sensitivity to TEA.

DISCUSSION

The S4/5 loop has been proposed to lie near or at the mouth of the channel pore of voltage-gated potassium channels (Isacoff et al., 1991). Furthermore, a functional potassium channel has been shown to result from the association of four individual potassium channel subunits (Liman et al., 1992; MacKinnon, 1991). Thus, four S4/5 loops appear to surround the internal mouth of a potassium channel complex. In addition, the S4/5 loop also appears to participate in potassium channel gating (McCormack, 1991).

The significance of *Shaker B* ³⁹²Ser has been studied previously (Isacoff et al., 1991). The conservative mutation of *Shaker B* ³⁹²Ser to ³⁹²Ala or ³⁹²Cys reduces channel conductance by 40%, as well as the time constant associated with onset of channel inactivation. The corresponding serine residue was mutated to alanine in the mammalian channels, rKv1.2 and hKv1.3. However, instead of merely reducing resulting potassium conductance, a more dramatic effect was observed, with complete disappearance of ionic currents. Thus, mutation of this specific serine residue affects potassium conductance to dramatically different extents when comparing *Drosophila ShB* to mammalian rKv1.2 and hKv1.3. The molecular basis underlying these divergent effects is unknown.

Analysis of hKv1.3 ³⁴²Ala gating currents, coupled with studies of co-expression of hKv1.3 ³⁴²Ala and ³⁹⁹Tyr, indicates that mutation of ³⁴²Ser does not have profound effects on channel properties such as voltage-dependent charge movement, and the capability to form a polymeric structure. Therefore, the resulting disappearance of potassium currents is presumably due to the effect of the serine mutation on the mechanics of channel opening.

The pore of a functional hKv1.3 voltage-gated potassium channel appears to be exposed to four ³⁴²Ser residues at the internal mouth, with each ³⁴²Ser contributed by an individual channel subunit. The ³⁴²Ala, when substituted for ³⁴²Ser, may simply result

in a block of the channel permeation pathway. However, since the S4/5 loop has also been suggested to be involved in potassium channel gating (McCormack et al., 1991), ^{342}Ala could also result in a mechanical uncoupling of potassium channel gating, making the channel pore unable to open following gating charge movement. Further analysis of the ^{342}Ala mutant should allow us to distinguish between these two different mechanisms, as well as provide additional evidence for the role the S4/5 loop may play in potassium channel function.

hKv1.3 ^{342}Ala did not result in the elimination of ionic currents when incorporated into a hetero-polymeric channel with ^{399}Tyr , indicating that a potassium channel tetramer with a mixture of ^{342}Ser and ^{342}Ala is still functional. Further studies employing linked tetramers with ^{342}Ser and ^{342}Ala located on various individual subunits should provide information regarding the number of ^{342}Ser residues required for channel function.

The ^{342}Ser is located within the PKC consensus sequence of K-x-S-x-R, where x can be any residue. The phosphorylation of ^{342}Ser by an endogenous kinase in *Xenopus* oocytes would presumably add negative charges to the region near the internal mouth. In an attempt to mimic this situation, hKv1.3 ^{342}Ser and rKv1.2 ^{324}Ser were also mutated to ^{342}Asp and ^{324}Asp , respectively. However, such a substitution still does not produce ionic currents from these two channels following membrane depolarization. Therefore, it still remains to be determined whether the effects of such a mutation are the result of removal of a serine residue, or a phosphoserine residue.

ACKNOWLEDGEMENT

The author thanks Michael Kavanaugh for his contributions regarding *Xenopus* oocyte analysis; and Armando Lagrutta, Raymond Hurst, and Yanna Wu for their expert technical assistance.

SUMMARY AND DISCUSSION

1. Molecular characterization of the type *n* potassium channel

The rat RGK5 clone was first isolated from a rat genomic DNA library, and later employed as a hybridization probe for the isolation of the corresponding human HGK5 clone from a human genomic DNA library. The RGK5 and HGK5 clones encode 525 and 523 amino acid polypeptides, respectively. Both genes exist as a single copy in the rat and human genome. Fig. 4.1 shows a sequence comparison between RGK5, HGK5, and the corresponding mouse clone, MK3 (Chandy et al., 1990). The homology is over 97% between each species. This specific type of potassium channel has been subsequently classified as Kv1.3. It shares over 70% sequence homology with other members of the Kv1 family. In both rat and human, the nucleotide sequence encoding Kv1.3 is contained on a single exon, as in the case of the Kv1.1 and Kv1.2 channels. This genomic DNA arrangement is different from that of the genomic arrangement of the *Shaker* gene (also in the Kv1 family) in *Drosophila*, in which the protein coding region is separated into approximately 20 exons (Schwarz et al., 1988). Alternative splicing events in the *Drosophila Shaker* gene is responsible for the generation of multiple potassium channels; while multiple genes encode distinct members of the Kv1 family of potassium channels in mammals.

Several features shared among other voltage-gated potassium channels are found in rat and human Kv1.3. These include the presence of six transmembrane regions; a voltage-sensor motif in the S4 regions; and a pore region between S5 and S6.

RGK5 and HGK5 clones (Kv1.3) encode functional voltage-gated potassium channels

The coding regions from both genomic clones were subcloned into expression vectors, transcribed in vitro, and resulting RNA injected into *Xenopus* oocytes for channel expression. Outward currents were elicited with membrane depolarization as measured by dual-electrode recording. The voltage-current plots indicated that these currents were voltage-dependent. The reversal potentials of tail currents were also measured, and the exponential change was close to the theoretical value for the potassium equilibrium potential. Thus, the channel currents were the result of movement of potassium ions. As a result, the rat RGK5 and human HGK5 clones were shown to encode functional voltage-gated potassium channels.

The RGK5 and HGK5 clones (Kv1.3) encode the lymphocyte type *n* potassium channel

Many characterized properties of these two channels as measured following expression in *Xenopus* oocytes serve to develop a unique electrophysiological and pharmacological profile for the Kv1.3 channel. When these properties are compared with those of the type *n* potassium channel as characterized in both mouse and human T lymphocytes, numerous properties are shared (Table 2.1 and 3.1). Both Kv1.3 and the type *n* channel inactivate over a period of hundreds of milliseconds and have a unitary conductance of approximately 10 pS. They both exhibit similar IC₅₀ to a variety of channel blockers, including those specific for voltage-gated potassium channels (such as TEA and 4-AP), for calcium-activated potassium channels (such as CTX and quinine), and for voltage-gated calcium channels (such as verapamil). These two currents are also inhibited by a variety of divalent cations at similar potencies. These similarities indicate that Kv1.3 encodes the type *n* potassium channel. The existence of Kv1.3 mRNA in T cells supports this notion. Additionally, the mouse Kv1.3 was assigned to the murine type *n* potassium channel based on similar analysis (Grissmer et al., 1990). Together, these studies indicate that Kv1.3 encodes the lymphocyte type *n* potassium channel.

Down-regulation of Kv1.3 mRNA following T cell activation

The type *n* potassium channel plays important roles in T cell development and activation as indicated by the correlation between apparent channel density and cell proliferation. It has been observed that the number of active type *n* channels increases following mitogen activation of both human and murine T lymphocytes (DeCoursey et al., 1987; Matteson and Deutsch, 1984; Sutro et al., 1989). Several mechanisms have thus been proposed to account for this increase, including newly-synthesized channels, insertion of pre-existing channels into the membrane, and activation of non-functional channels on the lipid bilayer. Here, quantitation of Kv1.3 mRNA was used as a way to determine whether newly-synthesized channels are responsible for the increase of observed channel density.

Purified human T lymphocytes were stimulated with ConA, and an effective concentration curve was established by measuring [³H]thymidine incorporation (Fig. 3.6). Both mitogenic and non-mitogenic concentrations of ConA were applied, followed by mRNA analysis via Northern blot hybridization. Over periods of treatment ranging from 1 to 72 hours, cellular levels of Kv1.3 mRNA were unaltered if treated with a the non-mitogenic concentration of ConA. However, Kv1.3 mRNA levels decreased dramatically following stimulation with a mitogenic concentration of ConA. The resulting decrease initiates at 16 hr and peaks at 48 - 72 hr. Under similar conditions, a 2-fold increase of potassium current density is observed at 20 hr following ConA stimulation (Matteson and Deutsh, 1984). A similar down-regulation of Kv1.3 mRNA was also observed following stimulation of human T cells with the mitogens PMA and A23187 (Attali et al., 1992). A similar paradigm was employed with murine T lymphocytes stimulated with ConA. The ConA concentration required for optimal stimulation was again determined by [³H]thymidine incorporation. When murine T cells were stimulated with a mitogenic

concentration of ConA, Kv1.3 mRNA levels did not alter significantly during the first 24 hr following activation; however they began to decline by 48 hr (personal observations). Under similar conditions, a 20-fold increase of potassium channel density has been reported at 24 - 48 hr (DeCoursey et al., 1987; Sutro et al., 1989). These data suggest that it is unlikely that newly-synthesized channels are responsible for the increase of observed channel density following cellular activation by mitogens. We speculate here that posttranslational events may well serve as the biochemical basis for this observation.

Also, in a separate study, the channel blocker, CTX, was used to determine the cell surface expression of the type *n* channel (Deutsch et al., 1991). In this report, the number of type *n* channels appeared to increase 2- to 3-fold at 72 hr following stimulation of human T cells with anti-CD3 plus IL-2. This result suggests that new channel proteins were inserted into the membrane. Combined with our results, it is also possible that insertion of pre-existing quiescent channels into the membrane following stimulation could be the mechanism responsible for the increase of type *n* channel density following activation. However, parallel measurements of channel currents, number of CTX binding sites, and Kv1.3 mRNA levels in a single stimulatory paradigm will be required to address this question unambiguously.

2. Phosphorylation of the type *n* channel in T lymphocytes

Phosphorylation is a common cellular event which regulates various ion channel activities. The type *n* channel is also subjected to phosphorylation-dependent regulation by both PKC and PKA systems. In Jurkat cells, both PKC and PKA systems reduced whole cell currents of the type *n* channel (Payet and Dupuis, 1992). Reagents antagonizing these kinases abolish their inhibitory effects. Moreover, dephosphorylation with alkaline phosphatase enhances channel activity, indicating basal phosphorylation of the type *n* channel by endogenous kinases in Jurkat cells. Similar inhibition of Kv1.3 channel activity

by the PKC system has been observed for type *n* currents expressed in *Xenopus* oocytes (Attali et al., 1992).

In order to characterize biochemically the type *n* channel, including possible phosphorylation events, several polyclonal antisera were developed against different regions of the type *n* channel. A 65-kDa protein was specifically immunoprecipitated with these antisera from both murine and human T cell lines. The size of 65-kDa is significantly larger than that of 58-kDa, which is observed following in vitro translation of Kv1.3 mRNA, indicating posttranslational modification of the type *n* channel in vivo. Specific Kv1.3 phosphorylation events were then analyzed in the Jurkat cell line. First, Jurkat cells were metabolically labeled with ^{32}P , and the 65-kDa protein was revealed as a phosphoprotein by immunoprecipitation, indicating that the 65-kDa Kv1.3 protein is phosphorylated by endogenous kinases. Thus, direct phosphorylation of the type *n* channel in T lymphocytes could account for the observation that basal channel activity is enhanced following dephosphorylation with alkaline phosphatase (Payet and Dupuis, 1992). The phosphorylation sites for endogenous kinases were also identified as serine residues by phosphoamino acid analysis.

The 65-kDa Kv1.3 protein is also capable of being phosphorylated in vitro by purified PKA and PKC. However, phosphorylation by PKC requires pre-dephosphorylation with alkaline phosphatase, which suggests that PKC sites are phosphorylated by endogenous kinases in Jurkat cells. In contrast, PKA sites were not heavily phosphorylated in Jurkat cells, as pre-treatment with alkaline phosphatase did not significantly alter the intensity of phosphorylated 65-kDa protein. Furthermore, a 40-kDa phosphoprotein was identified to be associated with the 65-kDa Kv1.3 protein by co-immunoprecipitation. Channel-associated polypeptides have been characterized for a variety of channels, including sodium, calcium, and potassium channels (Catterall, 1987; Rehm et al., 1989; Trimmer, 1991). However, phosphorylation events have only been defined for the 54-kDa β subunit which is associated with the 212-kDa $\alpha 1$ subunit of the

skeletal muscle calcium channel. (De Jongh et al., 1989). Phosphorylation of channel-associated polypeptides, thus, represents another mechanism by which channel activities could be regulated. Modification of the 40-kDa subunit could also offer a partial explanation for differences regarding kinase-dependent modulation of type *n* channel activity observed between T lymphocytes and Kv1.3-expressing *Xenopus* oocytes (Attali et al., 1992; Payet and Dupuis, 1992).

Phosphorylational modulation of the type *n* channel could play an important role in T cell functions. First, as we know, apparent type *n* channel activity is regulated during T cell development and activation. Control of phosphorylation could serve as an effective means for lymphocytes to regulate type *n* channel activity. Second, lymphocyte functions are modulated by a variety of cytokines and neurohormones. Occupancies of respective receptors by these ligands activate different signal transduction pathways. Alteration of kinase and phosphatase activities could in turn modulate the type *n* channel activity.

3. Functional significance of a highly conserved serine residue within the intracellular S4/5 loop of mammalian potassium channels

Voltage-gated potassium channels are defined by a wide variety of intrinsic properties, such as voltage-dependence of activation, a potassium-selective permeation pore, inactivation, and the ability to form a polymeric structure. The S4/5 loop lies between transmembrane domains S4 (which contains the voltage sensor motif) and S5, and is located within the cytoplasm. The primary sequence of this region is highly conserved among subfamilies of the voltage-gated (Kv) potassium channel superfamily. Within the mammalian Kv1 subfamily, only two amino acid substitutions are present within the sequence representing the S4/5 loop (Fig. 6.1). Mutational analysis suggests that the S4/5 loop is involved in voltage-dependence of activation, inactivation, and potassium permeability in voltage-gated potassium channels.

A PKC consensus recognition sequence (R/K-x-S-x-R/K) is found within the S4/5 loop, and is conserved among most voltage-gated potassium channels of the Kv family. Phosphorylational modification of the serine residue located within the S4/5 loop could serve as a means by which to regulate channel gating and potassium permeation. Biochemical evidence of direct phosphorylation of potassium channels, and C kinase-dependent modulation of channel activity support this notion.

The ³⁹²Ser of the *Drosophila Shaker B* potassium channel, located within the PKC consensus sequence, has been subjected to mutational analysis as previously described (Isacoff et al., 1991). Such a mutation reduced potassium channel conductance by 40%, and altered the inactivation constant. Two mammalian potassium channels (rKv1.2 and hKv1.3), sharing identical amino acids within the S4/5 loop with the *ShB* channel, except for a single substitution, were subjected to similar serine residue mutagenesis and functional analysis in *Xenopus* oocytes. The alanine substitution produced similar but more dramatic effects upon both mammalian potassium channels, with complete elimination of voltage-dependent potassium currents. However, the molecular mechanism underlying such a dramatic difference is unclear.

Two intrinsic channel properties were further analyzed for the hKv1.3 ³⁴²Ala potassium channel. The gating currents were identical between the ³⁴²Ala and ³⁴²Ser channels, indicating a similar gating charge movement during depolarization; the ³⁴²Ala subunit was also able to form functional heteropolymeric channels with the ³⁹⁹Tyr subunit. Thus, the alanine substitution appears not to affect channel properties involved with gating and polymerization, but dramatically affects channel conductance.

The ³⁴²Ala residues in homopolymeric potassium channels result in the elimination of potassium currents; however, a mixture of ³⁴²Ala and ³⁴²Ser subunits results in the formation of functional hetero-polymeric potassium channels. Further analysis of linked ³⁴²Ser/³⁴²Ala channels would clarify the number of ³⁴²Ser subunits required for the

generation of conducting channels, and further define the role of ³⁴²Ser in channel function.

Preliminary studies have also been carried out with regard to phosphorylation of the hKv1.3 ³⁴²Ser residue and potential effects on channel properties. However, substitution of ³⁴²Ser with an aspartate residue, which is structurally similar to a phosphoserine residue, also resulted in loss of potassium permeation. Therefore, no conclusion at this point in time can be made which would distinguish between the requirement for a serine residue, or a phosphoserine residue at position 342 for maintenance of channel function.

REFERENCES

- Aldrich, R.W. (1989) Mutating and gating. *Nature* 339:578-579.
- Armstrong, C.M., and Bezanilla, F. (1977) Inactivation of the sodium channel. II. Gating current experiments. *J. Gen. Physiol.* 70:567-590.
- Atkinson, N.S., Robertson, G.A., and Ganetzky, B. (1991) A component of calcium-activated potassium channels encoded by the *Drosophila* slo locus. *Science* 253:551-555.
- Attali, B., Romey, G., Honore, E., Schmid-Alliana, A., Mattei, M.-G., Lesage, F., Ricard, P., Barhanin, J., and Lazdunski, M. (1992a) Cloning, functional expression, and regulation of two K⁺ channels in human T lymphocytes. *J. Biol. Chem.* 267:8650-8657.
- Attali, B., Honore, E., Lesage, F., Lazdunski, M., and Barhanin, J. (1992b) Regulation of a major cloned voltage-gated K⁺ channel from human T lymphocytes. *FEBS Lett.* 303:229-232.
- Auld, V.J., Goldin, A.L., Krafte, D.S., Caterall, W.A., Lester, H.A., Davidson, N., and Dunn, R.J. (1990) A neutral amino acid change in segment IIS4 dramatically alters gating properties of the voltage-dependent sodium channel. *Proc. Natl. Acad. Sci. USA* 87:323-327.
- Bastin, B., Payet, M.D., and Dupuis, G. (1990) Effects of modulators of adenylyl cyclase on interleukin-2 production, cytosolic Ca²⁺ elevation, and K⁺ channel activity in Jurkat T cells. *Cell. Immunol.* 128:385-399.
- Baumann, A., Grupe, A., Ackermann, A., and Pongs, O. (1988) Structure of the voltage-dependent potassium channels is highly conserved from *Drosophila* to vertebrate central nervous systems. *EMBO J.* 7:2457-2463.
- Beckh, S., and Pongs, O. (1990) Members of the RCK potassium channel family are differentially expressed in the rat nervous system. *EMBO J.* 9:777-782.
- Berridge, M.J., and Irvine, R.F. (1989) Inositol phosphates and cell signaling. *Nature* 341:197-204.
- Blumenthal, E.M., and Kaczmarek, L.K. (1992) Modulation by cAMP of a slowly activating potassium channel expressed in *Xenopus* oocytes. *J. Neurosci.* 12:290-296.
- Boyle, W.J., Geer, P.V.D., and Hunter, T. (1991) Phosphopeptide mapping and phosphoamino acid analysis by two-dimensional separation on thin-layer cellulose plates. *Methods Enzymol.* 201:110-149.
- Bregestovski, P., Redkozubov, A., and Alexeev, A. (1986) Elevation of intracellular calcium reduces voltage-dependent potassium conductance in human T cells. *Nature* 319:776-778.

Busch, A.E., Varnum, M.D., North, R.A., and Adelman, J.P. (1992) An amino acid mutation in a potassium channel that prevents inhibition by protein kinase C. *Science* 255:1705-1707.

Butler, A., Wei, A., Baker, K., and Salkoff, L. (1989) A family of putative potassium channel genes in *Drosophila*. *Science* 243:943.

Cachelin, A.B., De Peyer, J.E., Kokubun, S., and Reuter, H. (1983) Ca²⁺ channel modulation by 8-bromocyclic AMP in cultured heart cells. *Nature* 304:462-464.

Cahalan, M.D., Chandy, K.G., DeCoursey, T.E., and Gupta, S. (1985) A voltage-gated potassium channel in human T lymphocytes. *J. Physiol.* 358:197-237.

Cahalan, M.D., Chandy, K.G., DeCoursey, T.E., Gupta, S., Lewis, R.S., and Sutro, J.B. (1987) Ion channels in T cells. In *Mechanisms of Lymphocyte Activation and Immune Regulation* (Gupta, S., Paul, W.E., and Fauci, A.S., eds.) pp.85-101, Plenum, New York.

Cahalan, M.D., and Lewis, R.S. (1990) Functional roles of ion channels in lymphocytes. *Sem. Immunol.* 2:107-117.

Cai, Y.-C., Osborne, P.B., North, R.A., Dooley, D.C., and Douglass, J. (1992) Characterization and functional expression of genomic DNA encoding the human lymphocyte type *n* potassium channel. *DNA Cell. Biol.* 11:163-172.

Cathala, G., J.-T. Savouret, B. Mendez, B. L. West, M. Karin, J. A. Martial, and J. D. Baxter. (1983) A method for the isolation of intact, translationally active ribonucleic acid. *DNA* 2:329.

Catterall, W.A. (1988) Structure and function of voltage-sensitive ion channels. *Science* 242: 50-61.

Chandy, K.G., DeCoursey, T.E., Cahalan, M.D., McLaughlin, C., and Gupta, S. (1984) Voltage-gated potassium channels are required for human T lymphocyte activation. *J. Exp. Med.* 160:369-385.

Chandy, K.G., DeCoursey, T.E., Fischbach, M., Talal, N., Cahalan, M.D., and Gupta, S. (1986) Altered K⁺ channel expression in abnormal T lymphocytes from mice with the *lpr* gene mutation. *Science* 233:1197-1200.

Chandy, K.G., Williams, C.B., Spencer, R.H., Aguilar, B.A., Ghanshani, S., Tempel, B.L., and Gutman, G.A. (1990) A family of three mouse potassium channel genes with intronless coding regions. *Science* 247:973-975.

Chandy, K.G., Douglass, J., Gutman, G.A., Jan, L., Joho, R., Kaczmarek, L., McKinnon, D., North, R.A., Numa, S., Philipson, L., Ribera, A.B., Rudy, B., Salkoff, L., Swanson, R.A., Steiner, D., Tanouye, M., and Tempel, B.L. (1991) Simplified gene nomenclature. *Nature* 352:26.

Cheng, S.H., Rich, D.P., Marshall, J., Gregory, R.J., Welsh, M.J., and Smith, A.E. (1991) Phosphorylation of the R domain by cAMP-dependent protein kinase regulates the CFTR chloride channel. *Cell* 66:1027-1036.

- Chirgwin, J.W., Przybyla, A.E. MacDonald, R.J. and Rutter, W.J. (1979) Isolation of biologically active ribonucleic acid from sources enriched in ribonuclease. *Biochem.* 18:5294.
- Chomczynski, P., and Sacchi, N. (1987) Single-step method of RNA isolation by acid guanidinium thiocyanate-phenol-chloroform extraction. *Analytical Biochem.* 162:56-161.
- Choquet, D., Sarthou, P., Primi, D., Cazenave, P.-A., and Korn, H. (1987) Cyclic AMP-modulated potassium channel in murine B cells and their precursors. *Science* 235:1211-1214.
- Christie, M.J., Adelman, J.P., Douglass, J., and North, R.A. (1989) Expression of a cloned rat brain potassium channel in *Xenopus* oocytes. *Science* 244:221-224.
- Christie, M.J., North, R.A., Osborne, P.B., Douglass, J., and Adelman, J.P. (1990) Heteropolymeric potassium channels expressed in *Xenopus* oocytes from cloned subunits. *Neuron* 2:405-411.
- Chung, S., Reinhart, P.H., Martin, B.L., Brautigan, D., and Levitan, I.B. (1991) Protein kinase activity closely associated with a reconstituted calcium-activated potassium channel. *Science* 253:560-562.
- Curtis, B.M., and Catterall, W.A. (1985) Phosphorylation of the calcium antagonist receptor of the voltage-sensitive calcium channel by cAMP-dependent protein kinase. *Proc. Natl. Acad. Sci. USA* 82:2528-2532.
- Danielson, P.E., Forss-Peter, S., Brow, M.A., Calavetta, L., Douglass, J., Milner, R.J., and Sutcliffe, J.G. (1988) p1B15: a cDNA clone of the rat mRNA encoding cyclophilin. *DNA* 7:261-267.
- DeCoursey, T.E., Chandy, K.G., Gupta, S., and Cahalan, M.D. (1984) Voltage-gated K⁺ channels in human T lymphocytes: a role in mitogenesis? *Nature* 307:465-468.
- DeCoursey, T.E., Chandy, K.G., Gupta, S., and Cahalan, M.D. (1985) Voltage-dependent ion channels in T-lymphocytes. *J. Neuroimmunol.* 10:71-95.
- DeCoursey, T.E., Chandy, K.G., Gupta, S., and Cahalan, M.D. (1987a) Two types of potassium channels in murine T lymphocytes. *J. Gen. Physiol.* 89:379.
- DeCoursey, T.E., Chandy, K.G., Gupta, S., and Cahalan, M.D. (1987b) Mitogen induction of ion channels in murine T lymphocytes. *J. Gen. Physiol.* 89:405-420.
- De Jongh, K.S., Merrick, D.K., and Catterall, W.A. (1989) Subunits of purified calcium channels: a 212-kDa form of $\alpha 1$ and partial amino acid sequence of a phosphorylation site of an independent β subunit. *Proc. Natl. Acad. Sci. USA* 86:8585-8589.
- Deutsch, C., Krause, D., and Lee, S.C. (1986) Voltage-gated potassium conductance in human T lymphocytes stimulated with phorbol ester. *J. Physiol. (London)* 372:405-423.
- Deutsch, C. (1990) K⁺ channels and mitogenesis. In *Potassium Channels: Basic Functions and Therapeutic Aspects*. T.J. Colatsky, ed. (Wiley-Liss, New York) pp.251-271.

- Deutsch, C., Price, M., Lee, S., King, V.F., and Garcia, M.L. (1991) Characterization of high affinity binding sites for charybdotoxin in human T lymphocytes. *J. Biol. Chem.* 266:3668-3674.
- Dooley, D.C., Law, P., and Alsop, P. (1987) A new density gradient for the separation of large quantities of rosette positive and rosette negative cells. *Exp. Hematol.* 15:296-303.
- Douglass, J., Osborne, P.B., Cai, Y.-C., Wilkinson, M., Christie, M.J., and Adelman, J.P. (1990) Characterization and functional expression of a rat genomic DNA clone encoding a lymphocyte potassium channel. *J. Immunol.* 144:4841-4850.
- Driscoll, W.J., Lee, Y.C., and Strott, C.A. (1990) Regulation of adrenocortical pregnenolone-binding protein activity by phosphorylation/dephosphorylation. *J. Biol. Chem.* 265:12306-12311.
- Durell, S.R., and Guy, H.R. (1992) Atomic scale structure and functional models of voltage-gated potassium channels. *Biophys. J.* 62:238-250.
- Eisenman, G., and Dani, J. A. (1987) An introduction to molecular architecture and permeability of ion channels. *Annu. Rev. Biophys. Chem.* 16:205.
- Ellis, S.B., Williams, M.E., Ways, N.R., Brenner, R., Sharp, A.H., Leung, A.T., Campbell, K.P., McKenna, E., Koch, W.J., Hui, A., Schwartz, A., and Harpold, M.M. (1988) Sequence and expression of mRNAs encoding the α_1 and α_2 subunits of a DHP-sensitive calcium channel. *Science* 241:1661.
- Flockerzi, V., Oeken, H., Hofmann, F., Pelzer, D., Cavalie, A., and Trautwein, W. (1986) Purified dihydropyridine-binding site from skeletal muscle t-tubules is a functional calcium channel. *Nature* 323:66-68.
- Frech, G.C., VanDongen, A.M.J., Schuster, G., Brown, A.M., and Joho, R.H. (1989) A novel potassium channel with delayed rectifier properties isolated from rat brain by expression cloning. *Nature* 340:642-645.
- Fukushima, Y., Hagiwara, S., and Henkart, M. (1984) Potassium current in clonal cytotoxic T lymphocytes from the mouse. *J. Physiol.* 351:645-656.
- Gisselmann, G., Sewing, S., Madsen, B.W., Mallart, A., Angaut-Petit, D., Muller-Holtkamp, F., Ferrus, A., and Pongs, O. (1989) The interference of truncated with normal potassium channel subunits leads to abnormal behaviour in transgenic *Drosophila melanogaster*. *EMBO J.* 9:2359-2364.
- Grissmer, S., and Cahalan, M. (1989a) Ionomycin activates a potassium-selective conductance in human T lymphocytes. *Biophys. J.* 55:245a (Abstr.).
- Grissmer, S., and Cahalan, M.D. (1989b) Divalent ion trapping inside potassium channels of human T lymphocytes. *J. Gen. Physiol.* 93:609-630.
- Grissmer, S., Dethlefs, B., Wasmuth, J.J., Goldin, A.L., Gutman, G.A., Cahalan, M.D., and Chandy, K.G. (1990) Expression and chromosomal localization of a lymphocyte K^+ channel gene. *Proc. Natl. Acad. Sci. USA* 87:9411-9415.

Grupe, A., Schroter, K.H., Ruppertsberg, J.P., Stocker, M., Drewes, T., Beckh, S., and Pongs, O. (1990) Cloning and expression of a human voltage-gated potassium channel. A novel member of the RCK potassium channel family. *EMBO J.* 9:1749-1756.

Guy, H.R. (1990) Models of voltage- and transmitter-activated channels based on their amino acid sequences. In monovalent cations in biological systems. Pasternak, C.A., editor. CRC Press, Boca Raton, FL. 31-58.

Guy, H.R., and Conti, F. (1990) Pursuing the structure and function of voltage-gated channels. *Trends Neurosci.* 13:201-206.

Harlow, E., and Lane, D. (1988) *Antibodies: a Laboratory Manual* pp. 633, Cold Spring Harbor.

Hatakeyama, M., Tsudo, M., Minamoto, S., Kono, T., Doi, T., Miyata, T., Miyasaka, M., and Taniguchi, T. (1989) Interleukin-2 receptor β chain gene: generation of three receptor forms by cloned human α and β chain cDNA's. *Science* 244:551-556.

Heinemann, S.H., Terlau, H., Stuhmer, W., Imoto, K., and Numa, S. (1992) Calcium channel characteristics conferred on the sodium channel by single mutations. *Nature* 356:441-443.

Hille, B. (1984). *Ionic Channels in Excitable Membranes* (Sinauer Associates, Inc., Sunderland, MA).

Hoshi, T., Zagotta, W.N., and Aldrich, R.W. (1990) Biophysical and molecular mechanisms of *Shaker* potassium channel inactivation. *Science* 250:533-538.

Hoshi, T., Zagotta, W.N., and Aldrich, R.W. (1991) Two types of inactivation in *Shaker* K^+ channels: effects of alterations in the carboxy-terminal region. *Neuron* 7:547-556.

Hubbard, S.C., and Ivatt, R.J. (1981) Synthesis and processing of asparagine-linked oligosaccharides. *Ann. Rev. Biochem.* 50:555-583.

Hymel, L., Striessnig, J., Glossmann, H., and Schindler, H. (1988) Purified skeletal muscle 1,4-dihydropyridine receptor forms phosphorylation-dependent oligomeric calcium channels in planar bilayers. *Proc. Natl. Acad. Sci. USA* 85:4290-4294.

Isacoff, E.Y., Jan, Y.N., and Jan, L.Y. (1990) Evidence for the formation of heteropolymeric potassium channels in *Xenopus* oocytes. *Nature* 345:530-534.

Isacoff, E.Y., Jan, Y.N., and Jan, L.Y. (1991) Identification of a putative receptor for the cytoplasmic inactivation gate in the *Shaker* K^+ channel. *Nature* 353:86-90.

Iverson, L.E., Tanouye, M.A., Lester, H.A., Davidson, N., and Rudy, B. (1988) A-type potassium channels expressed from *Shaker* locus cDNA. *Proc. Natl. Acad. Sci. USA* 85:5723.

Jan, L.Y., and Jan, Y.N. (1989) Voltage-sensitive ion channels. *Cell* 56:13-25.

Jan, L.Y., and Jan, Y.N. (1992) Structural elements involved in specific K^+ channel functions. *Annu. Rev. Physiol.* 54:537-555.

- Kavanaugh, M., Varnum, M.D., Osborne, P.B., Christie, M.J., Busch, A.E., Adelman, J.P., and North, R.A. (1991) Interaction between tetraethylammonium and amino acid residues in the pore of cloned voltage-dependent potassium channels. *J. Biol. Biochem.* 266:7583-7587.
- Kavanaugh, M.P., Hurst, R.S., Yakel, J., Varnum, M.D., Adelman, J.P., and North, R.A. (1992) Multiple subunits of a voltage-dependent potassium channel contribute to the binding site for tetraethylammonium. *Neuron* 8:493-497.
- Kemp, B.E., and Pearson, R.B. (1990) Protein kinase recognition sequence motifs. *Trends Biol. Sci.* 15:342-346.
- Kennelly, P.J., and Krebs, E.G. (1991) Consensus sequences as substrate specificity determinants for protein kinases and protein phosphatases. *J. Biol. Chem.* 266:15555-15558.
- Kirsch, G.E., Drewe, J.A., Hartmann, H.A., Taglialatela, M., Biasi, M.D., Brown, A.M., and Joho, R.H. (1992) Differences between the deep pores of K^+ channels determined by an interacting pair of nonpolar amino acids. *Neuron* 8:499-505.
- Kozak, M. (1984) Compilation and analysis of sequences upstream from the translation start site in eukaryotic mRNAs. *Nucl. Acids Res.* 12:857.
- Krebs, E.G., and Beavo, J.A. (1979) Phosphorylation-dephosphorylation of enzymes. *Ann. Rev. Biochem.* 48:923-959.
- Kuno, M., Goronzy, J., Weyand, G.M., and Gardner, P. (1986) Single channel and whole-cell recordings of mitogen-regulated inward currents in human cloned helper T lymphocytes. *Nature* 323:269-273.
- Kuno, M., and Gardner, P. (1987) Ion channels activated by inositol 1,4,5-triphosphate in plasma membrane of human T lymphocyte. *Nature* 326:301-304.
- Kyte, J., and Doolittle, R.F. (1982) A simple method for displaying the hydropathic character of a protein. *J. Mol. Biol.* 157:105.
- Lee, S.C., Sabath, D.E., Deutsch, C., and Prystowsky, M.B. (1986) Increased voltage-gated potassium conductance during interleukin 2-stimulated proliferation of a mouse helper T lymphocyte clone. *J. Cell Biol.* 102:1200-8.
- Leonard, W.J., Depper, J.M., Crabtree, G.R., Rudikoff, S., Pumphrey, J., Robb, R.J., Kronke, M., Svetlik, P.B., Pfeffer, N.J., Waldmann, T.A., and Greene, W.C. (1984) Molecular cloning and expression of cDNAs for the human interleukin-2 receptor. *Nature* 311:626-631.
- Lester, H. A. (1988) Heterologous expression of excitability proteins: route to more specific drugs? *Science* 241:1057.
- Levitan, I.B. (1985) Phosphorylation of ion channels. *J. Membrane Biol.* 87:177-190.
- Lewis, R.S., and Cahalan, M.D. (1988a) The plasticity of ion channels: parallels between the nervous and immune system. *Trends Neurosci.* 11:214-218.

- Lewis, R.S., and Cahalan, M.D. (1988b) Subset-specific expression of potassium channels in developing murine T lymphocytes. *Science* 239:771-775.
- Lewis, R.S., and Cahalan, M.D. (1989) Mitogen-induced oscillations of cytosolic Ca^{++} and transmembrane Ca^{++} current in human leukemic T cells. *Cell Regul.* 1:99-112.
- Lewis, R.S., and Cahalan, M.D. (1990) Ion channels and signal transduction in lymphocytes. *Ann. Rev. Physiol.* 52:415-430.
- Li, M., West, J.W., Lai, Y., Scheuer, T., and Catterall, W.A. (1992) Functional modulation of brain sodium channels by cAMP-dependent phosphorylation. *Neuron* 8:1151-1159.
- Liman, E.R., Hess, P., Weaver, F., and Koren, G. (1991) Voltage-sensing residues in the S4 region of a mammalian K^+ channel. *Nature* 353:752-756.
- Liman, E.R., Tytgat, J., and Hess, P. (1992) Subunit stoichiometry of a mammalian K^+ channel determined by construction of multimeric cDNAs. *Neuron* 9:861-871.
- Logothetis, D.E., Movahedi, S., Satler, C., Lindpaintner, K., and Nadal-Ginard, B. (1992) Incremental reductions of positive charge within the S4 region of a voltage-gated K^+ channel result in corresponding decreases in gating charge. *Neuron* 8:531-540.
- Lopez, G.A., Jan, Y.N., and Jan, L.Y. (1991) Hydrophobic substitution mutations in the S4 sequence alter voltage-dependent gating in *Shaker* K^+ channels. *Neuron* 7:327-336.
- Lucas, S., Marais, R., Graves, J.D., Alexander, D., Parker, P., and Cantrell, D.A. (1990) Heterogeneity of protein kinase C expression and regulation in T lymphocytes. *FEBS Lett.* 260:53-56.
- Luneau, C.J., Williams, J.B., Marshall, J., Levitan, E.S., Oliva, C., et al. (1991) Alternative splicing contributes to K^+ channel diversity in the mammalian central nervous system. *Proc. Natl. Acad. Sci. USA* 88:3932-3936.
- McCormack, K., Campanelli, J.T., Ramaswami, M., Mathew, M. A. Tanouye, M.A., Iverson, L.I., and Rudy, B. (1989) Leucine-zipper motif update. *Nature* 340:103.
- McCormack, K., Vega-Saenz de Miera, E.C., and Rudy, B. (1990a) Molecular cloning of a member of a third class of *Shaker* family K^+ channel genes in mammals. *Proc. Natl. Acad. Sci. USA* 87:5227-5231.
- McCormack, K., Lin, J.W., Iverson, L.E., Rudy, B. (1990b) *Shaker* K^+ channel subunits form heteromultimeric channels with novel functional properties. *Biochem. Biophys. Res. Commun.* 171:1361-1371.
- McCormack, K., Tanouye, M.A., Iverson, L.E., Lin, J.-W., Ramaswami, M., McCormack, T., Campanelli, J.T., Mathew, M., and Rudy, B. (1991) A role for hydrophobic residues in the voltage-dependent gating of *Shaker* K^+ channels. *Proc. Natl. Acad. Sci. USA* 88:2931-2935.
- McKinnon, D. (1989) Isolation of a cDNA clone coding for a putative second potassium channel indicates the existence of a gene family. *J. Biol. Chem.* 264:8230-8236.

- MacDonald, H.R., and Nabholz, M. (1986) T cell activation. *Annu. Rev. Cell Biol.* 2:231-253.
- MacKinnon, R., and Miller, C. (1989) Mutant potassium channels with altered binding of charybdotoxin, a pore-blocking peptide inhibitor. *Science* 245:1382.
- MacKinnon, R., and Yellen, G. (1990) Mutations affecting TEA blockade and ion permeation in voltage-activated K⁺ channel. *Science* 250:276-279.
- MacKinnon, R. (1991) Determination of the subunit stoichiometry of a voltage-activated potassium channel. *Nature* 350:232-235.
- Maruyama, Y. (1987) A patch-clamp study of mammalian platelets and their voltage-gated potassium current. *J. Physiol.* 391:467-485.
- Matteson, D.R., and Deutsch, C. (1984) K⁺ channels in T lymphocytes: a patch clamp study using monoclonal antibody adhesion. *Nature* 307:468-471.
- Mayer, M.L., and Sugiyama, K. (1988) A modulatory action of divalent cations on transient outward currents in cultured rat sensory neurons. *J. Physiol.* 396:417.
- Mitchell, P.J., and Tjian, R. (1989) Transcriptional regulation in mammalian cells by sequence-specific DNA binding proteins. *Science* 245:371.
- Miyajima, A., Kitamura, T., Harada, N., Yokota, T., and Arai, K.-I. (1992) Cytokine receptors and signal transduction. *Annu. Rev. Immunol.* 10:295-331.
- Moran, O., Dascal, N., and Lotan, I. (1991) Modulation of a *Shaker* potassium A-channel by protein kinase C activation. *FEBS Lett.* 279:256-260.
- Moss, S.J., Doherty, C.A., and Huganir, R.L. (1992) Identification of the cAMP-dependent protein kinase and protein kinase C phosphorylation sites within the major intracellular domains of the $\beta 1$, $\beta 2S$, and $\beta 2L$ subunits of the α -aminobutyric acid type A receptor. *J. Biol. Chem.* 267:14470-14476.
- Murai, T., Kakizuka, A., Takumi, T., Ohkubo, H., and Nakanishi, S. (1989) Molecular cloning and sequence analysis of human genomic DNA encoding a novel membrane protein which exhibits a slowly activating potassium channel activity. *Biochem. Biophys. Res. Commun.* 161:176-181.
- Nishimoto, I., Wagner, J.A., Schulman, H., and Gardner, P. (1991) Regulation of Cl⁻ channels by multifunctional CaM kinase. *Neuron* 6:547-555.
- Noda, M., Shimizu, S., Tanabe, T., Takai, T., Kayano, T., Ikeda, T., Takahashi, H., Nakayama, H., Kanaoka, Y., Minamino, N., Kangawa, K., Matsuo, H., Raftery, M.A., Hirose, T., Inayama, S., Hayashida, H., Miyata, T., and Numa, S. (1984) Primary structure of *Electrophorus electricus* sodium channel deduced from cDNA sequence. *Nature* 312:121.
- Noda, M., Suzuki, J., Numa, S., and Stuhmer, W. (1989) A single point mutation confers tetrodotoxin and saxitoxin insensitivity on the sodium channel II. *FEBS Lett.* 259:213-216.

- Oettgen, H.C., Terhorst, C., Cantley, L.C., and Rosoff, P.M. (1985) Stimulation of the T3-T cell receptor complex induces a membrane potential-sensitive calcium influx. *Cell* 40:583-590.
- Pak, M., Covarrubias, M., Ratcliffe, A., and Salkoff, L. (1991a) A mouse brain homolog of the *Drosophila Shab* K⁺ channel with conserved delayed-rectifier properties. *J. Neurosci.* 11:869-880.
- Pak, M., Baker, K., Covarrubias, M., Butler, A., Ratcliffe, A., and Salkoff, L., (1991b) mShal, a new subfamily of a type K⁺ channel cloned from mammalian brain. *Proc. Natl. Acad. Sci. USA* 88:4386-4390.
- Papazian, D.M., Schwarz, T.L., Timpe, L.C., Jan, Y.N., and Jan, L.Y. (1987) Cloning of genomic and complementary DNA from *Shaker*, a putative potassium channel gene from *Drosophila*. *Science* 237:749.
- Papazian, D.M., Timpe, L.C., Jan, Y.N., and Jan, L.Y. (1991) Alteration of voltage-dependence of *Shaker* potassium channel by mutations in the S4 sequence. *Nature* 349:305-10
- Parcej, D.N. and Dolly, J.O. (1989) Dendrotoxin acceptor from bovine synaptic plasma membranes. *Biochem. J.* 257:899-903.
- Patel, H.R., and Miller, R.A. (1991) Analysis of protein phosphorylation patterns reveals unanticipated complexity in T lymphocyte activation pathways. *J. Immunol.* 146:3332-3339.
- Payet, M.D., and Dupuis, G. (1992) Dual regulation of the *n* type K⁺ channel in Jurkat T lymphocytes by protein kinases A and C. *J. Biol. Chem.* 267:18270-18273.
- Philipson, L.H., Hice, R.E., Schaefer, K., LaMendola, J., Bell, G.I., Nelson, D.J., and Steiner, D.F. (1991) Sequence and functional expression in *Xenopus* oocytes of a human insulinoma and islet potassium channel. *Proc. Natl. Acad. Sci. USA* 88:53-57.
- Plaut, M. (1987) Lymphocyte hormone receptors. *Annu. Rev. Immunol.* 5:621-669.
- Poenie, M., Tsien, R.Y., and Schmitt-Verhulst, A.-M. (1987) Sequential activation and lethal hit measured by [Ca]²⁺ in individual cytolytic T cells and targets. *EMBO J.* 6:2223-2232.
- Pongs, O., Kecskemethy, N., Muller, R., Krah-Jentgens, I., Baumann, A., Kiltz, H.H., Canal, I., Llamazares, S., and Fesus, F. (1988) *Shaker* encodes a family of putative potassium channel proteins in the nervous system of *Drosophila*. *EMBO J.* 7:1087.
- Rehm, H., and Lazdunski, M. (1988) Purification and subunit structure of a putative K⁺ channel protein identified by its binding properties for dendrotoxin I. *Proc. Natl. Acad. Sci. USA* 85:4919-4923.
- Rehm, H., Newitt, R.A., and Tempel, B.L. (1989) Immunological evidence for a relationship between the dendrotoxin-binding protein and the mammalian homologue of the *Drosophila Shaker* K⁺ channel. *FEBS Lett.* 249:224-228.

- Reuter, H., Stevens, C.F., Tsien, R.W., and Yellen, G. (1982) Properties of single calcium channels in cardiac cell culture. *Nature* 297:501-504.
- Ribera, A. B. (1990) A potassium channel gene is expressed at neural induction. *Neuron* 5:691-701.
- Rohrkasten, A., Meyer, H.E., Nastainczyk, W., Sieber, M., and Hofmann, F. (1988) cAMP-dependent protein kinase rapidly phosphorylates serine-6 of the skeletal muscle receptor for calcium channel blockers. *J. Biol. Chem.* 263:15325-15329.
- Ross, C.A., Meldolesi, J., Milner, T.A., Satoh, T., Supattapone, S., and Snyder, S.H. (1989) Inositol 1,4,5-trisphosphate receptor localized to endoplasmic reticulum in cerebellar Purkinje neuron. *Nature* 339:468-470.
- Rossie, S., Gordon, D., and Catterall, W.A. (1987) Identification of an intracellular domain of the sodium channel having multiple cAMP-dependent phosphorylation sites. *J. Biol. Chem.* 262:17530-17535.
- Rossie, S., and Catterall, W.A. (1987) Cyclic AMP-dependent phosphorylation of voltage-sensitive sodium channels in primary cultures of rat brain neurons. *J. Biol. Chem.* 262:12735-12744.
- Rossie, S., and Catterall, W.A. (1989) Phosphorylation of the α subunit of rat brain sodium channels by cAMP-dependent protein kinase at a new site containing Ser686 and Ser687. *J. Biol. Chem.* 264:14220-14224.
- Rudy, B. (1988) Diversity and ubiquity of K^+ channels. *Neurosci.* 25:729-749.
- Ruppersberg, J.P., Schroter, K.H., Sakmann, B., Stocker, M., Sewing, S., and Pongs, O. (1990). Heteromultimeric channels formed by rat brain potassium-channel proteins. *Nature* 345:535-537.
- Russell, J.H., and Dobos, C.B. (1983) Accelerated $^{86}Rb^+$ (K^+) release from the cytotoxic T lymphocyte is a physiologic event associated with delivery of the lethal hit. *J. Immunol.* 131:1138-1141.
- Sabath, E.E., Monos, D.S., Lee, S.C., Deutsch, C., and Prystowsky, M.B. (1986) Cloned T-cell proliferation and synthesis of specific proteins are inhibited by quinine. *Proc. Natl. Acad. Sci. USA* 83:4739-43.
- Sanger, F., Nicklen, S., and Coulson, A.R. (1977) DNA sequencing with chain termination inhibitors. *Proc. Natl. Acad. Sci. USA.* 74:5463-5467.
- Sands, S.B., Lewis, R.S., and Cahalan, M.D.. (1988) Charybdotoxin blocks voltage-gated K^+ channels in T lymphocytes. *J. Gen. Physiol.* 93:1061-74.
- Sarkadi, B., Mack, E., and Rothstein, A. (1984) Ionic events during the volume response of human peripheral blood lymphocytes to hypotonic media. *J. Gen. Physiol.* 84:497-512.
- Schell, S.R., Nelson, D.J., Fozzard, H.A., and Fitch, F.W. (1987) The inhibitory effects of K^+ channel-blocking agents on T lymphocyte proliferation and lymphokine production are "nonspecific". *J. Immunol.* 139:3224-30.

- Schlichter, L., Sidell, N., and Hagiwara, S. (1986) Potassium channels mediate killing by human natural killer cells. *Proc. Natl. Acad. Sci. USA* 83:451-455.
- Schwarz, T.L., Tempel, B.L., Papazian, D.M., Jan, N.Y., and Jan, L.Y. (1988) Multiple potassium-channel components are produced by alternative splicing at the *Shaker* locus in *Drosophila*. *Nature* 331:137.
- Scott, V.E.S., Parcej, D.N., Keen, J.N., Findlay, J.B.C., and Dolly, J.O. (1990) a-Dendrotoxin acceptor from bovine brain is a K⁺ channel protein. *J. Biol. Chem.* 265:20094-20097.
- Segel, G.B., Simon, W., and Lichtman, M.A. (1979) Regulation of sodium and potassium transport in phytohemagglutinin-stimulated human blood lymphocytes. *J. Clin. Invest.* 64:834-841.
- Sharma, B. (1988) Inhibition of the generation of cytotoxic lymphocytes by potassium ion channel blockers. *Immunol.* 65:101-105.
- Sobel, E., and Martinez, H.M. (1985) A multiple sequence alignment program. *Nuc. Acids Res.* 14:363.
- Stocker, M., Stuhmer, W., Wittka, R., Wang, X., Muller, R., Ferrus, A., and Pongs, O. (1990) Alternative *Shaker* transcripts express either rapidly inactivating or noninactivating K⁺ channels. *Proc. Natl. Acad. Sci. USA* 87:8903-8907.
- Stuhmer, W., Stocker, M., Sakmann, B., Seeburg, P., Baumann, A., Grupe, A., and Pongs, O. (1988) Potassium channels expressed from rat brain cDNA have delayed rectifier properties. *FEBS Letters* 242:199.
- Stuhmer, W., Conti, F., Suzuki, H., Wang, X., Noda, M., Yahagi, N., Kubo, H., and Numa, S. (1989a) Structural parts involved in activation and inactivation of the sodium channel. *Nature* 339:597-603.
- Stuhmer, W., Ruppersberg, J.P., Schroter, K.H., Sakmann, B., Stocker, M., Giese, K.P., Perschke, A., Baumann, A., and Pongs, O. (1989b) Molecular basis of functional diversity of voltage-gated potassium channels in mammalian brain. *EMBO J.* 8:3235-3244.
- Sutro, J.B., Vayuvegula, B.S., Gupta, S., and Cahalan, M.D. (1988) Up-regulation of voltage-sensitive K⁺ channels in mitogen-stimulated B lymphocytes. *Biophys. J.* 53:460a (Abstr.).
- Sutro, J.B., Vayuvegula, B.S., Gupta, S., and Cahalan, M.D. (1989) Voltage-sensitive ion channels in human B lymphocytes. In *Mechanisms of Lymphocyte Activation and Immune Regulation*. S. Gupta, W.E. Paul, and A.S. Fauci, eds. (Plenum Press, New York) pp.113-127.
- Swanson, R., Marshall, J., Smith, J.S., Williams, J.B., Boyle, M.B., Folander, K., Luneau, C.J., Antanavage, J., Oliva, C., Buhrow, S.A., Bennett, C., Stein, R.B., and Kaczmarek, L.K. (1990) Cloning and expression of cDNA and genomic clones encoding three delayed rectifier potassium channels in rat brain. *Neuron* 4:929-939.

- Taglialatela, M., Toro, L., and Stefani, E. (1992) Novel voltage clamp to record small, fast currents from ion channels expressed in *Xenopus* oocytes. *Biophys. J.* 61:78-82.
- Takumi, T., Ohkubo, H., and Nakanishi, S. (1988) Cloning of a membrane protein that induces a slow voltage-gated potassium current. *Science* 242:1042-1045.
- Tanouye, M.A., Ferrus, A., and Fujita, S.C. (1981) Abnormal action potentials associated with the *Shaker* complex locus of *Drosophila*. *Proc. Natl. Acad. Sci. USA* 78:6548-6552.
- Tempel, B.L., Papazian, D.M., Schwarz, T.L., Jan, Y.N., and Jan, L.Y. (1987) Sequence of a probable potassium channel component encoded at *Shaker* locus of *Drosophila*. *Science* 237:770.
- Tempel, B. L., Jan, Y. N., and Jan, L.Y. (1988) Cloning of a probable potassium channel gene from mouse brain. *Nature* 332:837.
- Tilly, B.C., Winter, M.C., Ostedgaard, L.S., O'Riordan, C., Smith, A.E., and Welsh, M.J. (1992) Cyclic AMP-dependent protein kinase activation of cystic fibrosis transmembrane conductance regulator chloride channels in planar lipid bilayers. *J. Biol. Chem.* 267:9470-9473.
- Timpe, L.C., Schwarz, T.L., Tempel, B.L., Papazian, D.M., Jan, Y.N., and Jan, L.Y. (1988a) Expression of functional potassium channels from *Shaker* cDNA in *Xenopus* oocytes. *Nature* 331:143.
- Timpe, L.C., Jan, Y.N., and Jan, L.Y. (1988b) Four cDNA clones from *Shaker* locus of *Drosophila* induce kinetically distinct A-type potassium currents in *Xenopus* oocytes. *Neuron* 1:659.
- Trimmer, K. (1991) Immunological identification and characterization of a delayed rectifier K⁺ channel polypeptide in rat brain. *Proc. Natl. Acad. Sci. USA* 88:10764-10768.
- Vassilev, P., Scheuer, T., and Catterall, W.A. (1989) Inhibition of inactivation of single sodium channels by a site-directed antibody. *Proc. Natl. Acad. Sci. USA* 86:8147-8151.
- Vitetta, E.S., Baur, S., and Uhr, J.W. (1971) Cell surface immunoglobulin. II. Isolation and characterization of immunoglobulin from mouse splenic lymphocytes. *J. Exp. Med.* 134:242-264.
- Warmke, J., Drysdale, R., and Ganetzky, B. (1991) A distinct potassium channel polypeptide encoded by the *Drosophila* eag locus. *Science* 252:1560-1562.
- Wei, A., Covarrubias, M., Butler, A., Baker, K., Pak, M., and Salkoff, L. (1990) K⁺ current diversity is produced by an extended gene family conserved in *Drosophila* and mouse. *Science* 248:599-603.
- Weiss, M.J., Imboden, J., Shoback, D., and Stobo, J. (1984) Role of T3 surface molecules in human T-cell activation: T3-dependent activation results in an increase in cytoplasmic free calcium. *Proc. Natl. Acad. Sci. USA* 81:4269-4273.

- Weiss, A., and Imboden, J.B. (1987) Cell surface molecules and early events involved in human T lymphocyte activation. *Adv. Immunol.* 41:1-38.
- Wilkinson, M. (1988) A rapid and convenient method for isolation of nuclear, cytoplasmic and total cellular RNA. *Nuc. Acids Res.* 16:10934.
- Wilkinson, M.F., Doskow, J., Borstel, R.V., Fong, A.M., and MacLeod, C.L. (1991) The expression of several T cell-specific and novel genes is repressed by trans-acting factors in immature T lymphoma clones. *J. Exp. Med.* 174:269-280.
- Yellen, G., Jurman, M.E., Abramson, T., and MacKinnon, R. (1991) Mutations affecting internal TEA blockade identify the probable pore-forming region of a K⁺ channel. *Science* 251:939-942.
- Yokoyama, S., Imoto, K., Kawamura, T., Higashida, H., Iwabe, N., Miyata, T., and Numa, S. (1989) Potassium channels from NG108-15 neuroblastoma-glioma hybrid cells: primary structure and functional expression from cDNAs. *FEBS Lett.* 259:37-42.
- Yool, A.J., and Schwarz, T.L. (1991) Alteration of ionic selectivity of a K⁺ channel by mutation of the H5 region. *Nature* 349:700-704.
- Ypey, D.L., and Clapham, D.E. (1984) Development of a delayed outward-rectifying K⁺ conductance in cultured mouse peritoneal macrophages. *Proc. Natl. Acad. Sci. USA* 81:3083-3087.
- Zagotta, W.N., Hoshi, T., and Aldrich, R.W. (1990) Restoration of inactivation in mutants of *Shaker* potassium channels by a peptide derived from *ShB*. *Science* 250:568-571.

FIGURE 1.1

The proposed topological structure of voltage-gated potassium channels

S1 to S6 represent transmembrane domains. SS1 and SS2 represent short segments 1 and 2, both of which span the lipid bilayer, and constitute the major structural elements of the channel pore.

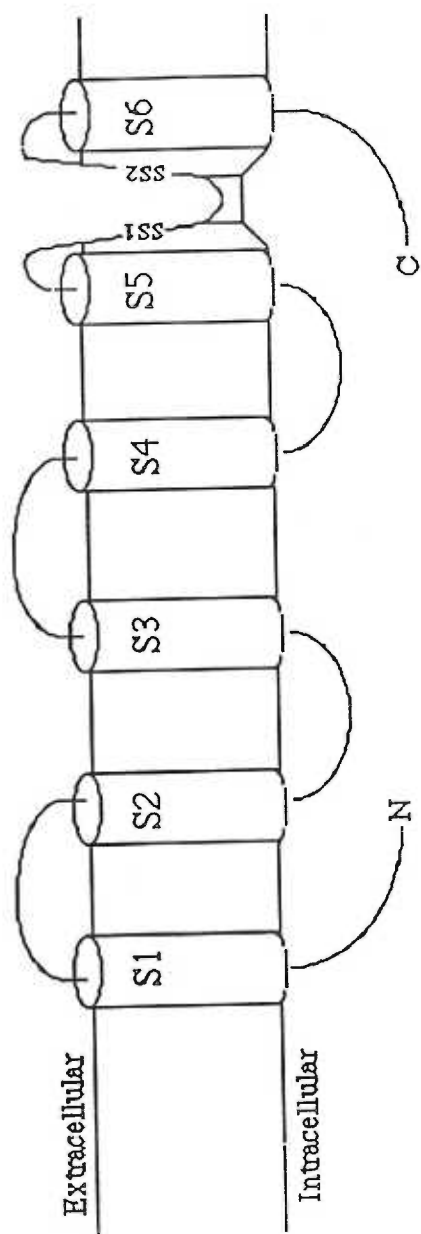


FIGURE 2.1

Diagram of rat genomic DNA clones RGK1 and RGK5 encoding voltage-dependent potassium channels

2.1A diagrams the RGK1 genomic clone; 2.1B diagrams the RGK5 genomic clone. Pertinent restriction enzyme sites are noted (R, EcoRI; P, PstI; H, HindIII; S, SacI; C, ClaI). Boxed areas represent protein coding regions, with translation start and stop sites noted. Putative transmembrane domains are shaded. Arrows denote regions of DNA which were subjected to nucleotide sequence analysis. A 450 bp SacI/HindIII fragment represents a putative RGK5-specific probe.

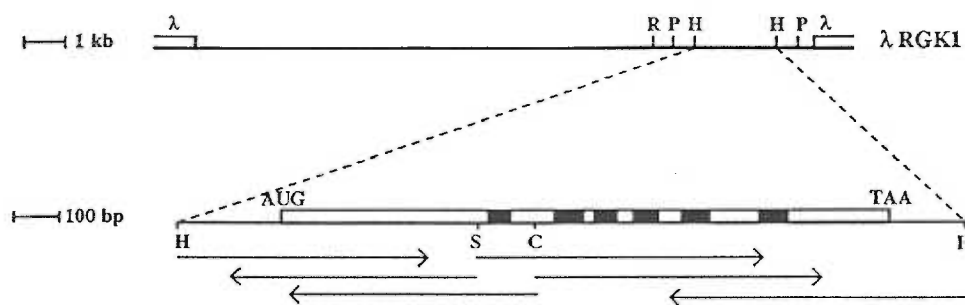
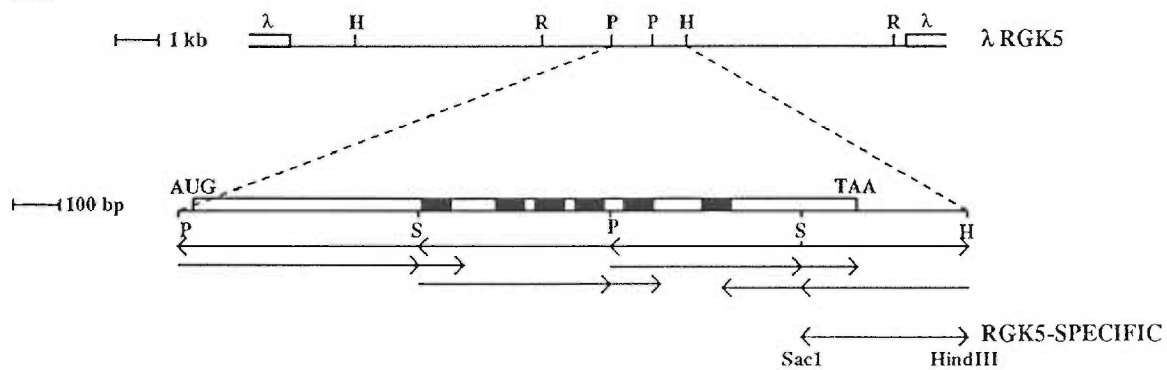
A**B**

FIGURE 2.2

Nucleotide and predicted translation product sequence of RGK5 genomic DNA

Hydrophobic, potential transmembrane domains S1 to S6 are contained within the shaded, boxed areas. Asterisks represent potential sites for N-linked glycosylation. The solid bar represents a possible A kinase phosphorylation site. Arrows denote boundaries of the *SacI*/*HindIII* fragment used as a putative RGK5-specific hybridization probe.

5'—CTGCAGAGCCAGGCTACGCGAGCTGCCGCCAGAC—1

ATG ACC GTG GTG CCC GGG GAC CAC CTG CTG GAG CCA GAA GCG GCG GGA GGC GGC GGC GGC GAC CCG CCT CAG GGA GGC TGT GTC AGT GGC 90
Met Thr Val Val Pro Gly Asp His Leu Leu Glu Pro Glu Ala Ala Gly Gly Gly Gly Gly Asp Pro Pro Gln Gly Gly Cys Val Ser Gly 30

GGC GGC TGC GAC CGC TAC GAA CCG CTG CCG CCC GCG CTG CCC GCG GCG GGC GAG CAG GAT TGC TGC GGC GAG CGC GTG GTC ATC AAC ATC 180
Gly Gly Cys Asp Arg Tyr Glu Pro Leu Pro Pro Ala Leu Pro Ala Ala Gly Glu Gln Asp Cys Cys Gly Glu Arg Val Val Ile Asn Ile 60

TCC GGG CTG CCG TTC GAG ACA CAG CTC AAG ACC CTC TGC CAG TTC CCT GAG ACG CTG CTA GGC GAC CCC AAG CCG CGC ATG CGA TAC TTC 270
Ser Gly Leu Arg Phe Glu Thr Gln Leu Lys Thr Leu Cys Gln Phe Pro Glu Thr Leu Leu Gly Asp Pro Lys Arg Arg Met Arg Tyr Phe 90

GAC CCG CTC CGC AAT GAG TAC TTC TTC GAC CGC AAC AGA CCC AGC TTC GAC GCC ATC CTC TAC TAC TAC CAG TCC GGC GGC CGC ATC CGC 360
Asp Pro Leu Arg Asn Glu Tyr Phe Phe Asp Arg Asn Arg Pro Ser Phe Asp Ala Ile Leu Tyr Tyr Tyr Gln Ser Gly Gly Arg Ile Arg 120

CGG CCG GTC AAC GTG CCC ATC GAC ATC TTC TCC GAG GAG ATC CGC TTC TAC CAA CTG GGT GAG GAG GCT ATG GAG AAG TTC CGT GAG GAC 450
Arg Pro Val Asn Val Pro Ile Asp Ile Phe Ser Glu Glu Ile Arg Phe Tyr Gln Leu Gly Glu Glu Ala Met Glu Lys Phe Arg Glu Asp 150

GAG GGC TTC CTG CCG GAG GAG GAG CGA CCC CTG CCC GCG CGT GAC TTC CAG CGC CAG GTG TGG CTG CTC TTC GAA TAC CCC GAG AGC TCG 540
Glu Gly Phe Leu Arg Glu Glu Glu Arg Pro Leu Pro Arg Arg Asp Phe Gln Arg Gln Val Trp Leu Leu Phe Glu Tyr Pro Glu Ser Ser 180

CGG CCG GCC CGG GGC ATT GCC ATC GTG TCA GTG CTG GTC ATT CTC ATC TCC ATT GTC ATC TTC TCC TTC GAG ACA CTA CCC GAG TTT CGC 630
Arg Pro Ala Arg Gly Ile Ala Ile Val Ser Val Leu Val Ile Leu Ile Ser Ile Val Ile Phe Cys Leu Glu Thr Leu Pro Glu Phe Arg 210

S1

GAC GAG AAG GAC TAT CCC GCC TCT CCG TCG CAG GAC GTG TTT GAG GCT GCC AAC AAC AGC ACG TCG GGC GCC TCC TCT GGA GCC TCC AGC 720
Asp Glu Lys Asp Tyr Pro Ala Ser Pro Ser Gln Asp Val Phe Glu Ala Ala Asn Asn Ser Thr Ser Gly Ala Ser Ser Gly Ala Ser Ser 240

TTC TCG GAC CCC TTC TTC GTA GTG GAG ACC CTC TGC ATC ATC TGG TTC TCC TTT GAG CTG CTG GTG CGA TTC TTT GCT TCG CCC AGT AAA 810
Phe Ser Asp Pro Phe Phe Val Val Glu Thr Leu Cys Ile Ile Trp Phe Ser Phe Glu Leu Leu Val Arg Phe Phe Ala Cys Pro Ser Lys 270

S2

GCC ACC TTC TCC AGA AAT ATC ATG AAC CTG ATA GAC ATT GTA GCC ATC ATC CCT TAT TTT ATT ACT CTG GGC ACT GAG CTG GCT GAG CGA 900
Ala Thr Phe Ser Arg Asn Ile Met Asn Leu Ile Asp Ile Val Ala Ile Ile Pro Tyr Phe Ile Thr Leu Gly Thr Glu Leu Ala Glu Arg 300

S3

CAG GGT AAT GGG CAG CAG GCT ATG TCA CTG GCC ATC CTG AGG GTC ATC CGC CTA GTA AGG GTC TTC CGC ATC TTC AAG CTC TCC CGC CAT 990
Gln Gly Asn Gly Gln Gln Ala Met Ser Leu Ala Ile Leu Arg Val Ile Arg Leu Val Arg Val Phe Arg Ile Phe Lys Leu Ser Arg His 330

S4

TCT AAG GGG CTG CAG ATC CTG GGA CAG ACA CTG AAG GCT TCC ATG CGA GAG CTG GGG CTG CTC ATT TTC TTC CTT TTC ATT GGG GTC ATC 1080
Ser Lys Gly Leu Gln Ile Leu Gly Gln Thr Leu Lys Ala Ser Met Arg Glu Leu Gly Leu Leu Ile Phe Phe Leu Phe Ile Gly Val Ile 360

S5

TTT TTC TCC AGT GCA GTC TAC TTT GCT GAG GCA GAC GAC CCT TCT TCG GGT TTT AAC AGT ATC CCG GAT GCC TTC TGG TGG GCC GTG GTA 1170
Leu Phe Ser Ser Ala Val Tyr Phe Ala Glu Ala Asp Asp Pro Ser Ser Gly Phe Asn Ser Ile Pro Asp Ala Phe Trp Trp Ala Val Val 390

ACC ATG ACA ACT GTC GGT TAT GGT GAT ATG CAC CCA GTG ACC ATA GGA GGC AAG ATT GTC GGC TCT CTT TGT GCC ATC GCA GGT GTC TTG 1260
Thr Met Thr Thr Val Gly Tyr Gly Asp Met His Pro Val Thr Ile Gly Gly Lys Ile Val Gly Ser Leu Cys Ala Ile Ala Gly Val Leu 420

S6

ACC ATT GCA TTG CCG GTT GGT GTC ATT GTT TTC AAC TTC AAT TAC TTC TAC CAC CGG GAG ACA GAA GGG GAA GAG CAA GCC CAG TAC ATG 1350
Thr Ile Ala Leu Pro Val Pro Val Ile Val Ser Asn Phe Asn Tyr Phe Tyr His Arg Glu Thr Glu Gly Glu Glu Gln Ala Gln Tyr Met 450

CAC GTG GGA AGC TGC CAG CAC CTC TCC TCT TCA GCA GAG GAG CTC CGA AAA GCC CGG AGT AAC TCC ACT CTG AGT AAG TCG GAG TAT ATG 1440
His Val Gly Ser Cys Gln His Leu Ser Ser Ser Ala Glu Glu Leu Arg Lys Ala Arg Ser Asn Ser Thr Leu Ser Lys Ser Glu Tyr Met 480

GTG ATC GAA GAG GGG GGT ATG AAC CAC AGC GCC TTC CCC CAG ACC CCC TTC AAA ACG GGC AAC TCC ACT GCC ACT TGC ACC ACC AAC AAT 1530
Val Ile Glu Glu Gly Gly Met Asn His Ser Ala Phe Pro Gln Thr Pro Phe Lys Thr Gly Asn Ser Thr Ala Thr Cys Thr Thr Asn Asn 510

AAT CCC AAC TCC TGT GTC AAC ATC AAA AAG ATA TTC ACT GAT GTC TAA TAGATGATACGATTGCCATTCTGTGCCAGTATTGTGTGGAACATGCCCCCTTGG 1633
Asn Pro Asn Ser Cys Val Asn Ile Lys Lys Ile Phe Thr Asp Val stop

TCGTGTATGCCCTTGATTATACATTCCAGACCATTCATCAAGGAAAGTACATGAAGAAGTGAAAGACACACTTCATTCTCCCTCTCCCTATTGCTTCATACTGAAACAGGTGCCT 1752

GGTTTTCAGTGGGCTCATTCTCTCAGCTCTTTTCTCTCCCTCTCTCTCCCTGTTTCTTAATTTTGTGAACAACAACTTACATTAAGCTT—3'

FIGURE 2.3

Amino acid sequence alignment of the cloned rat potassium channels RGK5, RBK1, RBK2 and DRK1

The Intelligenetics 'Genalign' algorithm was employed for sequence comparison analysis. Boxed amino acids represent fully conserved moieties between the four species of potassium channels. Overlined regions, S1 to S6, represent putative transmembrane domains of the channels. Fully conserved, positively charged residues (R/K, denoted by a + symbol) within the S4 region are noted, as well as a series of evenly spaced leucine residues (L, denoted with a closed circle) in the S4/S5 spacer region which conform to a leucine zipper motif.

RGK5 1 MT VVPGDHLLEPEAAGGGGDPFQGGCVSGGGCDRYEPLPPALPAAGEQDCCGERVWINISGLRFETQ
 RBK1 1 MTV MSG ENADEASAAPGHPQDGSYPRQADHDDHECC ERVVINISGLRFETQ
 RBK2 1 MTV ATGDP VDEAAALPGHPQD TYDPEADHECC ERVVINISGLRFETQ
 DRK1 1 MT KHGSRSTSSLPPEP MEIVRSKACSRRLNVGGLAHEVLWRTLRLPRT

RGK5 69 LKTLQFPETLLGDPKKRMRYFDPLRNEYFFDRNRPSFDAILYYQSGGLRRFPVNVPLDIFS EEIR
 RBK1 52 LKTLAQFPNTLLGNPKRMRYFDPLRNEYFFDRNRPSFDAILYYQSGGLRRFPVNVPLDMFS EEIK
 RBK2 48 LKTLAQFPETLLGDPKKRMRYFDPLRNEYFFDRNRPSFDAILYYQSGGLRRFPVNVPLDIFS EEIR
 DRK1 52 RLGLKLRDCT HDSLLQVCDYSLDNEYFFDRHPGAEISIL NFYRTGLHMMEECALSESQELDY

S1

RGK5 136 FYQLGEEAMEKFREDEGFLRE EERPLPRRDFQRQVWLLFEYPPSSRFARGIAIVSVLVLLISIVI
 RBK1 119 FYELGEEAMEKFREDEGFIKE EERPLPEKEYQRQVWLLFEYPPSSGPARVIAIVSVMLVLLISIVI
 RBK2 115 FYELGEEAMEKFREDEGYIKE EERPLPENEFQRQVWLLFEYPPSSGPARIIAIVSVMLVLLISIVS
 DRK1 118 WGIDEIYLESCCQARYHQKKEQMNNEE LKREAETLREREGEEDFNTCCAERKKLWDLLEKDP

S2

RGK5 201 FCLETLPFRDEKDYSPASQDVFEAANNSTSGASSGASSFS PFFVVTCLIIWFSFELLVREFA
 RBK1 184 FCLETLP ELKDDKDFGTIHRIDNTTVIYTSNIFTD PFFIVETCLIIWFSFELLVREFA
 RBK2 180 FCLETLPFRDE NEDMHGGVTFHTYSNST IGYQSTSTFD PFFIVETCLIIWFSFELLVREFA
 DRK1 180 NSSVAAKILAIISIMFIVLSTAILSLNLTPELQSLDEFGQSTNPQLASVEAVCLAWETMEYLLRELS

S3

S4

RGK5 267 CPSKATFSRNIMLIDIVAIIEY FITLGTSLAE RQNGQQAMSLAILRVIRLVRFRIKLSRH
 RBK1 243 CPSKTDFKNIMLIDIVAIIEY FITLGTSLAE QEGNQKGEQATSLAILRVIRLVRFRIKLSRH
 RBK2 244 CPSKAGFTNIMLIDIVAIIEY FITLGTSLAEKPEDAQGGQQAMSLAILRVIRLVRFRIKLSRH
 DRK1 248 SPKEWKEFKGPLAAILDLIAIEYVVTIFLTE SNKSVLQFQNVRRVQIFRIMRILRLKLARH
 + + + +

S5

RGK5 331 SKGLQILGQTLKASMRGLGLLFFIFIGVILFSSAVYFAHADDPSSGNSIPDAFWWAVVMTTVGYG
 RBK1 309 SKGLQILGQTLKASMRGLGLLFFIFIGVILFSSAVYFAHAEAESEHSSIPDAFWWAVVMTTVGYG
 RBK2 311 SKGLQILGQTLKASMRGLGLLFFIFIGVILFSSAVYFAHADERDSQFSPIDPAFWWAVVMTTVGYG
 DRK1 311 STGLQSLGFTLRSYNELGLLILFLAMGIMIFSSIVFAEKREDDTKFKSPASFWWATITMTTVGY
 • • • •

S6

RGK5 399 DMHEVTIGGKIVGSLCAIAGVLTIALPVPVIVSNFNIFY HRE
 RBK1 377 DMHEVTIGGKIVGSLCAIAGVLTIALPVPVIVSNFNIFY HRE
 RBK2 379 DMHEVTIGGKIVGSLCAIAGVLTIALPVPVIVSNFNIFY HRE
 DRK1 378 DIYEKTLGKIVGSLCAIAGVLTIALPVPVIVSNFNIFY KEQKRQGAIKRREALERAKRNGSIVSMN

RGK5 441 TEGE EQAQ YMHVGSQHLSSS AEELRKARS
 RBK1 419 TEGE EQAQLLVSSPN LASDSDL RRS
 RBK2 421 TEGE EQAQ YLQVTSCKPISSPDL KKSRS
 DRK1 446 MKDAFARS IEMDIVVEKNESIAKKDKVQDNHLSPNKWKWKRALSETSSSKSFETKEQGSPEKARS

RGK5 471 NSTLSKSEYMVIEE GCMNHSAPFQTPFKTGNST
 RBK1 446 SSTISKSEYMEIEEDM NNSIAHYRQANIRT
 RBK2 450 ASTISKSDYMEICE G VNNSNEDFREENLKT
 DRK1 514 SS SPQHLNVQQLIEDMYSKMAKTQSQPILNTKEMAPQSKPPEELEMSSMPSVPVAPLPARTEGVIDMRS

RGK5 504 ATCT
 RBK1 476 GNCTATD
 RBK2 480 ANCT
 DRK1 581 MSSIDSFISCATDFEATRFHSHPLASLSSKAGSSSTAPEVWGRGALGASGGRLTETNPETSRSGFF

DRK1 649 VESPRSSMKTNNPLKLRALKVNFVEGDPTFLPLSLGLYHDPLRNRGGAAAAGLECASLLDKFVLSP

DRK1 717 ESSIYTTASARTPPRSPEKHTAIAFNFEAGVHHYIDTDDEGQLLYSVDSSPPKSLHGSTSPKFSTG

RGK5 508 TNNPNNSCV NIKK IFTDV
 RBK1 483 QNCV NKSCL LTDV
 RBK2 484 LANTNYV NITK MLTDV
 DRK1 785 ARTEKNHFESSPLPTSPKFLRPNVYSSEGLTGKGPQAQEKLENHIPPVHMLPGGGGAHGSTRDQSI

FIGURE 2.4**Genomic Southern blot analysis**

Rat genomic DNA was digested with EcoRI, HindIII and PstI and separated by size on a 1.0% agarose gel. Following transfer to Nytran filter, the blot has hybridized under stringent conditions with a radiolabelled RGK5 SacI/HindIII restriction fragment described earlier. The sizes of the hybridizing genomic DNA fragments were determined by comparison to co-electrophoresed DNA size markers.

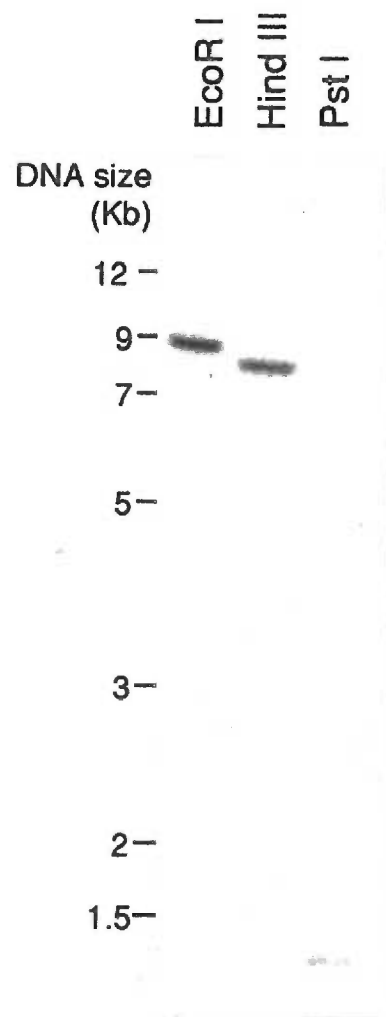


FIGURE 2.5**Northern blot analysis of RGK5 transcripts**

The 450 bp SacI/HindIII fragment, representing nucleotides 1390-1850 (as shown in Figures 2.1B and 2.2), was subcloned into pGEM3Z for the generation of a ^{32}P -labelled cRNA probe. RNA was isolated, and Northern analysis performed as described in Materials and Methods. Samples represent: 1), 10 μg total RNA from mouse thymus; 2), 10 μg poly A⁺ mRNA from total rat brain, and; 3), 10 μg poly A⁻ RNA from total rat brain. The location of co-electrophoresed RNA size standards is noted.

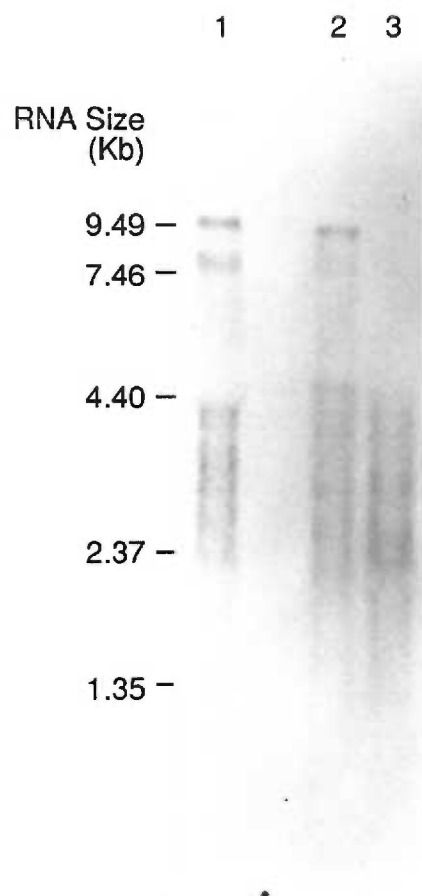


FIGURE 2.6

Expression of potassium currents in *Xenopus* oocytes 2 days after injection of RNA (1ng) encoding RGK5

A & B), Currents evoked by depolarizing commands from a holding potential of -70 mV to the test potentials shown (leak current was subtracted). In A), the depolarization was of 50 ms duration; in B), it was 4 s long. C), Peak conductance (filled circles, mean of 5 oocytes \pm SEM) was determined from depolarizations similar to those shown in A. Conductance was normalized to the chord conductance at 40 mV assuming $E_K = -102$ mV. Steady state inactivation was determined in the same cells (open circles) at 40 mV using 10 s prepulses to the potentials shown. D), Modulation of inactivation by extracellular calcium. Currents were evoked by depolarization to 40 mV for 4s. Elevating extracellular calcium (concentrations shown) increased the rate of inactivation.

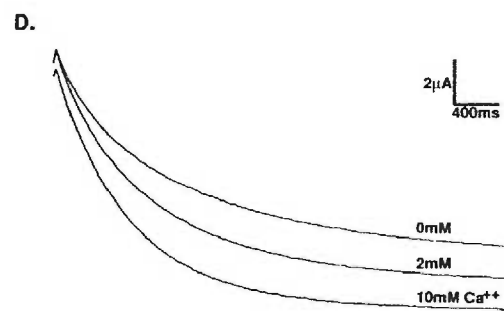
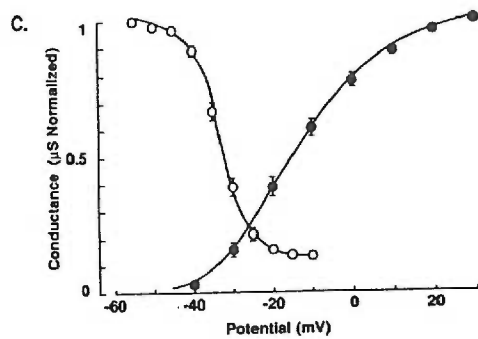
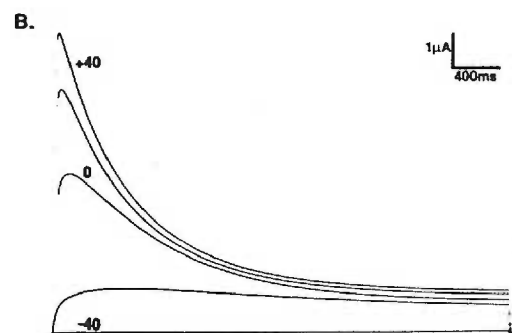
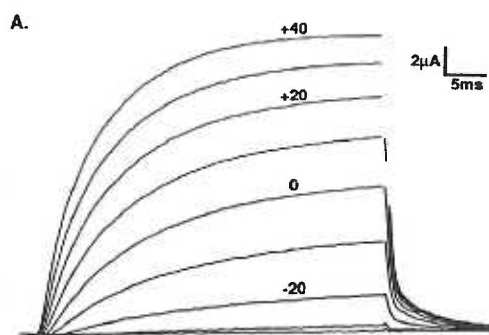


TABLE 2.1

Comparison of biophysical properties of RGK5, RCK3 and mammalian T lymphocyte *n* potassium channels ^a

a RGK5 currents were characterized as described in the text. RCK3 currents were characterized following injection of *in vitro* synthesized RNA into *Xenopus* oocytes as described (Stuhmer et al., 1989). Mouse and human T lymphocyte *n* currents were characterized in isolated thymic or splenic T cells as described (Cahalan et al., 1987; DeCoursey et al., 1985, 1987a; Grissmer and Cahalan, 1989; Lester, 1988; Sands et al., 1988).

b Estimated from Boltzmann function as described in the text.

c Single-channel chord conductance.

d Test potential in mV where conductance increase is one-half of its maximum value.

e Slope of normalized voltage-conductance relation. The value corresponds to the change in test potential needed to generate an e-fold change in current.

f Prepulse membrane potential at which the current response to a step to 0 mV test potential is one-half of the maximal value.

g Slope of steady state inactivation curve. The value corresponds to the change in prepulse membrane potential needed to cause an e-fold reduction in the size of the response to a 0 mV test pulse.

h Time constant of inactivation at +40 mV.

i Values refer to concentrations at which 50% inhibition of peak current is observed.

j Single dose measurements. RGK5 currents were inhibited 60% by 80 mM quinine, with 49% inhibition seen at 30 mM verapamil.

	Activation ^b		Inactivation ^b			Unit Conductance ^c (pS)
	Midpoint (mV) ^d	Slope (mV) ^e	Midpoint (mV) ^f	Slope (mV) ^g	τ inactivation @ +40 mV (mS) ^h	
RGK5	-14.1	-10.3	-33.0	3.7	612	
RCK3	-25.2	-6.6	-44.7	16.0		10
n Channel (mouse)	-36.0	-7.3	-68.0	8.3	107	12
				IC ₅₀ [of K _i for block of peak I] ⁱ		
	TEA (mM)	4-AP (mM)	α -DTX (nM)	CTX (nM)	Guinine (μ M)	Verapamil (μ M)
RGK5	11	0.3	>500		~80 ^j	~30 ^j
RCK3	50	1.5	>600	1		
n Channel (mouse)	8-16	0.2		0.2	14	6
			Reduction of K ⁺ Conductance by Divalent Cations			
	Most potent	Cd > Co > Ba	Ba > Cd > Mn	> Sr	Ca > Sr	Least potent Mg > Mg
RGK5		Cd > Co > Ba	Ba > Cd > Mn	> Sr	Ca > Sr	
n Channel (human)		Cd > Co > Ba	Ba > Cd > Mn	> Sr	Ca > Sr	

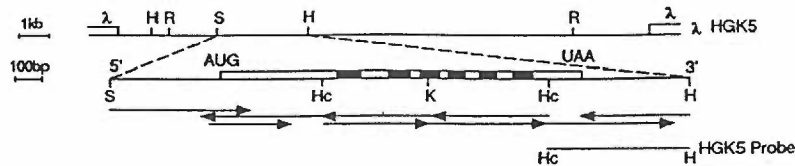
FIGURE 3.1

(upper) Diagram of the human genomic DNA clone, HGK5

The boxed area indicates open reading frame with translation start (AUG) and stop (UAA) codons noted. Shaded areas represent putative hydrophobic transmembrane domains. Arrows denote restriction fragments subjected to nucleotide sequence analysis. Pertinent restriction enzyme sites are noted: H, HindIII; Hc, HincII; K, KpnI; R, EcoRI; S, SacI.

(lower) Nucleotide and deduced amino acid sequence of HGK5

Hydrophobic, potential transmembrane domains S1 through S6 are shaded and boxed. Overlined solid bar denotes possible protein kinase A phosphorylation site, while asterisks note sites for potential N-linked glycosylation. "+" symbols represent conserved, positively charged residues (R/K), which have been suggested to form a potential voltage sensor. Arrows indicate boundaries of the HincII/HindIII fragment used as an HGK5-specific hybridization probe for Northern blot analysis.



-18
5'---CGCGAGCTGCCGCCGAC---3'

ATG ACC GTG GTG CCC GGG GAC CAC CTG CTG GAG CCG GAG GTG GCC GAT GGT GGA GGG GCC CCG CCT CAA GGC GGC TGT GGC GGC GGC GGC 90
Met Thr Val Val Pro Gly Asp His Leu Leu Glu Pro Glu Val Ala Asp Gly Gly Gly Ala Pro Pro Gln Gly Gly Cys Gly Gly Gly Gly 30

TGC GAC CGC TAC GAG CCG CTG CCG CCC TCA CTG CCG GCC GCG GCG GAG CAG GAC TGC TGC GGG GAG CGC GTG GTC ATC AAC ATC TCC GGG 180
Cys Asp Arg Tyr Glu Pro Leu Pro Pro Ser Leu Pro Ala Ala Gly Glu Gln Asp Cys Cys Gly Glu Arg Val Val Ile Asn Ile Ser Gly 60

CTG CGC TTC GAG ACG CAG CTG AAG ACC CTT TGC CAG TTC CCC GAG ACG CTG CTG GGC GAC CCC AAG CCG CGC ATG AGG TAC TTC GAC CCG 270
Leu Arg Phe Glu Thr Gln Leu Lys Thr Leu Cys Gln Phe Pro Glu Thr Leu Leu Gly Asp Pro Lys Arg Arg Met Arg Tyr Phe Asp Pro 90

CTC CGC AAC GAG TAC TTC TTC GAC CGC AAC CCG CCC AGC TTC GAC GCC ATC CTC TAC TAC TAT CAG TCC GGG GGC CGC ATC CGC CGG CCG 360
Leu Arg Asn Glu Tyr Phe Phe Asp Arg Asn Arg Pro Ser Phe Asp Ala Ile Leu Tyr Tyr Gln Ser Gly Arg Ile Arg Arg Pro 120

GTC AAC GTG CCC ATC GAC ATT TTC TCC GAG GAG ATC CGC TTC TAC CAG CTG GGC GAG GAG GCC ATG GAG AAG TTC CGC GAG GAC GAG GGC 450
Val Asn Val Pro Ile Asp Ile Phe Ser Glu Glu Ile Arg Phe Tyr Gln Leu Gly Glu Glu Ala Met Glu Lys Phe Arg Glu Asp Glu Gly 150

TTC CTG CCG GAG GAG GAG CCG CCC TTG CCC CGC CGC GAC TTC CAG CGC CAG GTG TGG CTG CTC TTC GAG TAC CCC GAG AGC TCC GGG CCG 540
Phe Leu Arg Glu Glu Glu Arg Pro Leu Pro Arg Arg Asp Phe Glu Arg Gln Val Trp Leu Leu Phe Glu Tyr Pro Glu Ser Ser Gly Pro 180

GCC CGG GGC ATC CCC ATC CTG TCC CTG CTG GTC ATC CTG ATC TCC ATT GTC ATC TTC TGC CTG GAG 630
Ala Arg Gly Ile Ala Ile Val Ser Val Leu Val Ile Leu Ile Ser Ile Val Ile Phe Cys Leu Glu Thr Leu Pro Glu Phe Arg Asp Glu 210

S1

AAG GAC TAC CCG GCC TCG ACG TCG GAC TCA TTC GAA GCA GCC GGC AAC AGC ACG TCG GGG TCC CGC GCA GGA GCC TCC AGC TTC TCC 720
Lys Asp Tyr Pro Ala Ser Thr Ser Gln Asp Ser Phe Glu Ala Ala Gly Asn Ser Thr Ser Gly Ser Arg Ala Gly Ala Ser Ser Phe Ser 240

GAT CCC TTC TTC GTG GTG GAG ACG CTG TGC ATC ATC TGG TTC TCC TTC GAA CTG CTG GGG TTC TTC GCT TGT 810
Asp Pro Phe Phe Val Val Glu Thr Leu Cys Ile Ile Trp Phe Ser Phe Glu Leu Leu Val Arg Phe Phe Ala Cys Pro Ser Lys Ala Thr 270

S2

TTC TCG CGA AAC ATC ATG AAC CTG ATC GAC ATT GTG GCC ATC ATT CTT TAT TTT ATC ACT CTG GGT ACC GAG 900
Phe Ser Arg Asn Ile Met Asn Leu Ile Asp Ile Val Ala Ile Ile Pro Tyr Phe Ile Thr Leu Gly Thr Glu Leu Ala Glu Arg Gln Gly 300

S3

AAT GGA CAG CAG GCC ATG TCT CTG GCC ATC CTG AGG GTC ATC CGC CTG GTA AGG GTC TTC CGC ATC TTC AAG 990
Asn Gly Gln Gln Ala Met Ser Leu Ala Ile Leu Arg Val Ile Arg Leu Val Arg Val Phe Arg Ile Phe Lys Leu Ser Arg His Ser Lys 330

S4

GGG CTG CAG ATC CTC GGG CAA ACG CTG AAG GCG TCC ATG CCG GAG CTG GGA TTG CTC ATC TTC TTC CTC TTT ATT GGG GTC ATC CTT TTC 1080
Gly Leu Gln Ile Leu Gly Gln Thr Leu Lys Ala Ser Met Arg Glu Leu Gly Leu Leu Ile Phe Phe Leu Phe Ile Gly Val Ile Leu Phe 360

S5

TCC AGC CGC GTC TAC TTT GGC GAG GCA GAC GAC CCC ACT TCA GGT TTC AGC AGC ATC CCG GAT GCC TTC TGG TGG GCA GTG GTA ACC ATG 1170
Ser Ser Ala Val Tyr Phe Ala Glu Ala Asp Asp Pro Thr Ser Gly Phe Ser Ser Ile Pro Asp Ala Phe Trp Trp Ala Val Val Thr Met 390

ACA ACA CTG GGT TAC GGC GAT ATG CAC CCA GTG ACC ATA GGG GGC AAG ATT GTG GGA TCT CTC TGT GCC ATC GCC GGT GTC TTG ACC ATC 1260
Thr Thr Val Gly Tyr Gly Asp Met His Pro Val Thr Ile Gly Gly Lys Ile Val Gly Ser Leu Cys Ala Ile Ala Gly Val Leu Thr Ile 420

S6

GCA TTG CCA GTT CCC GTG ATT GTT TCC AAC TTC AAT TAC TTC TAC CAC CCG GAG ACA GAA GGG GAA GAG CAA TCC CAG TAC ATG CAC GTG 1350
Ala Leu Pro Val Pro Val Ile Val Ser Asn Phe Asn Tyr Phe Tyr His Arg Glu Thr Glu Glu Glu Gln Ser Gln Tyr Met His Val 450

GGA AGT TGC CAG CAC CTC TCC TCT TCA GCC GAG GAG CTC CGA AAA GCA AGG AGT AAC TCG ACT CTG AGT AAG TCG GAG TAT ATG GTG ATC 1440
Gly Ser Cys Gln His Leu Ser Ser Ser Ala Glu Glu Leu Arg Lys Ala Arg Ser Asn Ser Thr Leu Ser Lys Ser Glu Tyr Met Val Ile 480

GAA GAG GGG GGT ATG AAC CAT AGC GCT TTC CCC CAG ACC CCT TTC AAA ACG GGC AAT TCC ACT GCC ACC TGC ACC ACG AAC AAT AAT CCC 1530
Glu Glu Gly Gly Met Asn His Ser Ala Phe Pro Gln Thr Pro Phe Lys Thr Gly Asn Ser Thr Ala Thr Cys Thr Thr Asn Asn Asn Pro 510

AAC TCT TGT GTC AAC ATC AAA AAG ATA TTC ACC GAT GTT TAATATGTGATCAAGTGACATGCTGTGCTCAGTATTGTGTGGAACGTGCCCTTGGTCTGCCTAT 1636
Asn Ser Cys Val Asn Ile Lys Lys Ile Phe Thr Asp Val 523

GCCCTTGTATTATACATTCCAGACCATTCATCAAGGAAAGGACCTGAAGAAGTGGAAAGCACACTTCATTCTCCCTCTCCCTGTGCTTCATCTGAAACAGGTGCCTGTTTGAAG 1755
TGGGCTGCATTCTCTCAGCTCTCTTTTCCCTCTTACCTCTCTCTCTGAACATTGTAACACACAGACTTACGTTAACTTCATTCTAGTACACGCCCTATTTAAAAAGAGCAGTAC 1874
ATCCTGGGAGAAATGAACATAAAGAACAGTTAGAGTAACTGTTAACTCAGAAATTTAAAGGACAGTTGTTTCTTCTTCAAGCACATCAATTCGTAGTAAATGATGCTTGGTGTGAT 1993
GGACCTTCAACGTTATTTATTTGAATATGTTTCCGCTGCTACCTGTAGATATCTGGATGAAGAGTCTAACTAGATAAATGACITGTAAACCCACCATGAGTTATTTGGTGTGAT 2112
CTTAAATCTTATTTGAATCCCTTTCCCGGAATTTAAGTGTCTCTACAACTTGAATAAAGGAAATGCCAAGATGCTGATCTGACTAATTAGTTAATCTTCCGGCTTGTG 2231
AAGCATTTCTAAAGCATTAGACTAACAGATTCTGTGAAGTTTACAGGACATATGCCAGCCCCAACAACTATCAAAAGTCTAGAACAGATGTTTTCAGTGTGCTGAGAGAAACAAAA 2350

S7

ATTTCTAATGCATCTGAGAGATAAGCTT-----3'

2379

FIGURE 3.2**(A) Genomic Southern blot analysis**

20 μ g of human genomic DNA was digested with EcoRI, HindIII, or PstI, as noted. The sizes of the hybridizing genomic DNA fragments were determined by comparison to co-electrophoresed size standards.

(B) Northern blot analysis of HGK5 transcripts

Samples represent: 1) 20 μ g total RNA from human granulocytes; 2) 20 μ g total RNA from human T lymphocytes. The location of co-electrophoresed RNA size markers is noted.

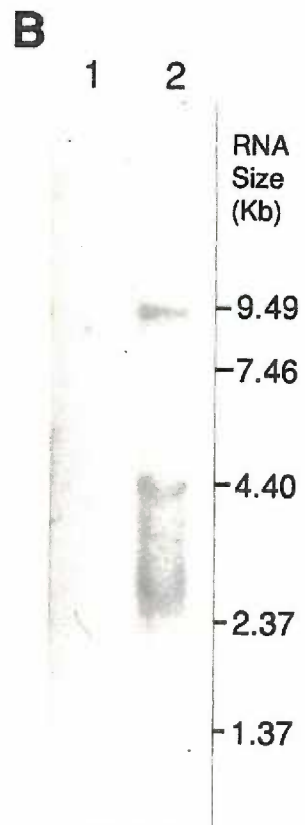
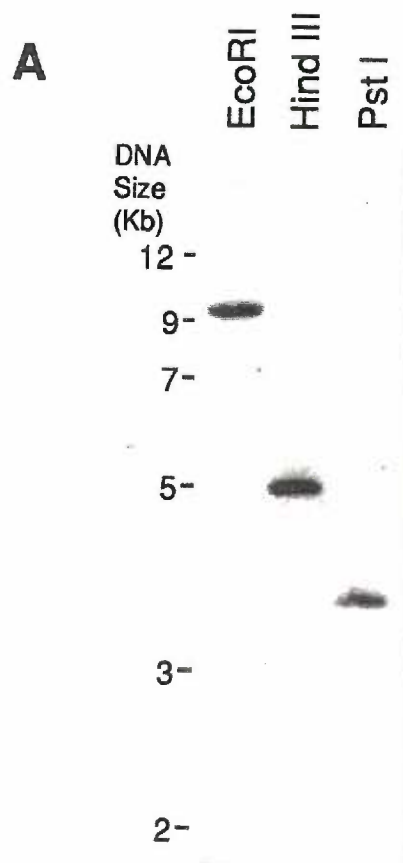


FIGURE 3.3

Expression of potassium currents in *Xenopus* oocytes after injection of RNA encoding HGK5

(A) and (B) show currents evoked by depolarizing voltage steps from a holding potential of -80 mV to the test potentials indicated. In (A), the leak current was subtracted and the step was 50 ms long, while in (B) the step was 5 s long. In (C) paired-pulses were used to determine the voltage-dependence of channel inactivation (shown in D). From a holding potential of -80 mV, 5 s prepulses incremented 5 mV from -50 to -5 mV were followed by 5 s test pulses to +40 mV. Paired pulses were separated by intervals sufficiently long to allow complete recovery from inactivation. In (D) the peak chord conductance-voltage relationship (open circles) and the voltage dependence of inactivation (closed circles) are illustrated. The data points represent means and standard errors ($n = 3-5$) and was fit to a Boltzman function (see text) The values of the fitted parameters are given in Table 3.1.

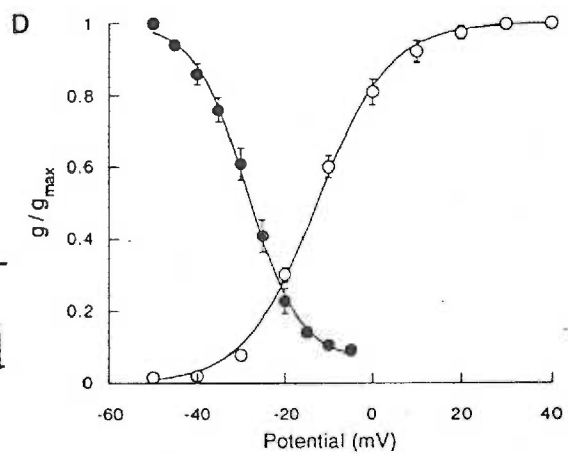
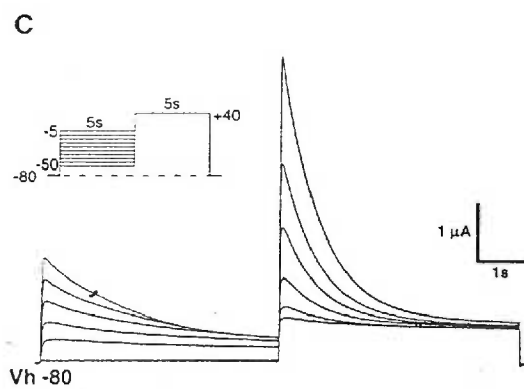
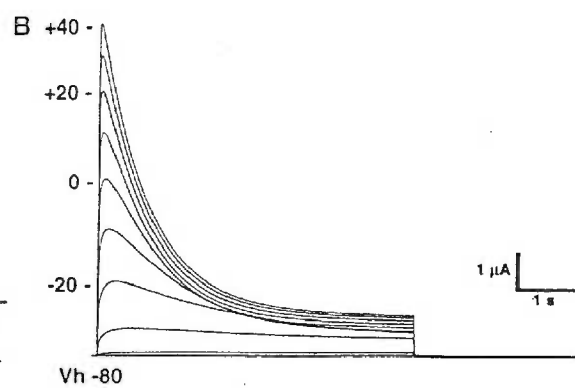
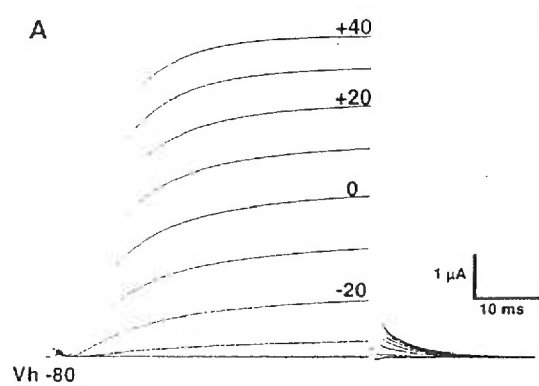


FIGURE 3.4**Inactivation properties of the expressed channels**

Shown are the voltage dependence of the time constant of inactivation (A) and the amount of inactivation (B). Time constants were obtained from single exponential fitted to the decay of the current over 5 s; the amount of inactivation is the difference between the peak current and current remaining after 5 s. Shown in (C) is the time course of recovery from inactivation, determined using pairs of 500 ms pulses to +40 mV separated by various intervals. I1 and I2 are the respective amplitudes of the first and second test pulses.

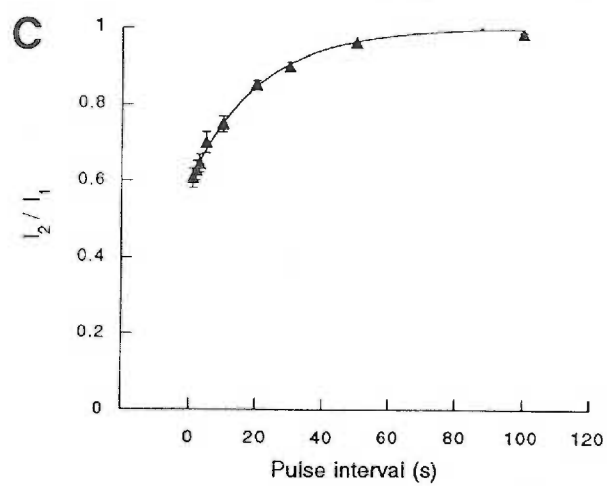
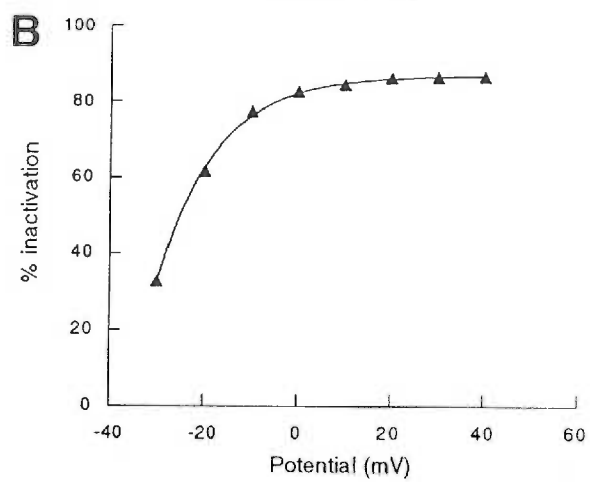
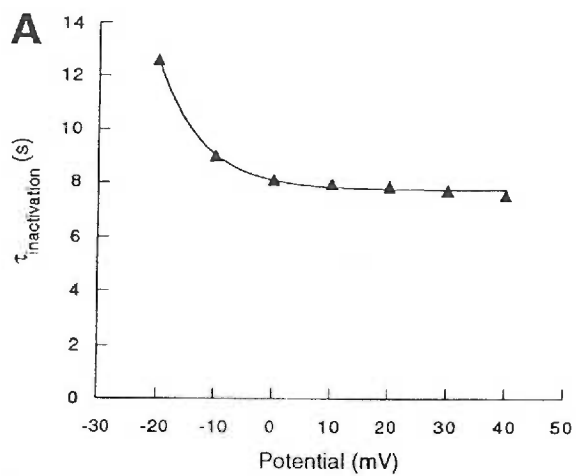


FIGURE 3.5

The effects of blocking drugs on expressed currents

Shown are inhibition curves for the potassium channel blockers 4-AP, TEA and quinine (A), and for the calcium channel blockers verapamil, nifedipine and diltiazem (B). Data points represent the means and standard errors ($n=4$). Fits are to the Hill equation, the parameters of which are given in Table 3.1.

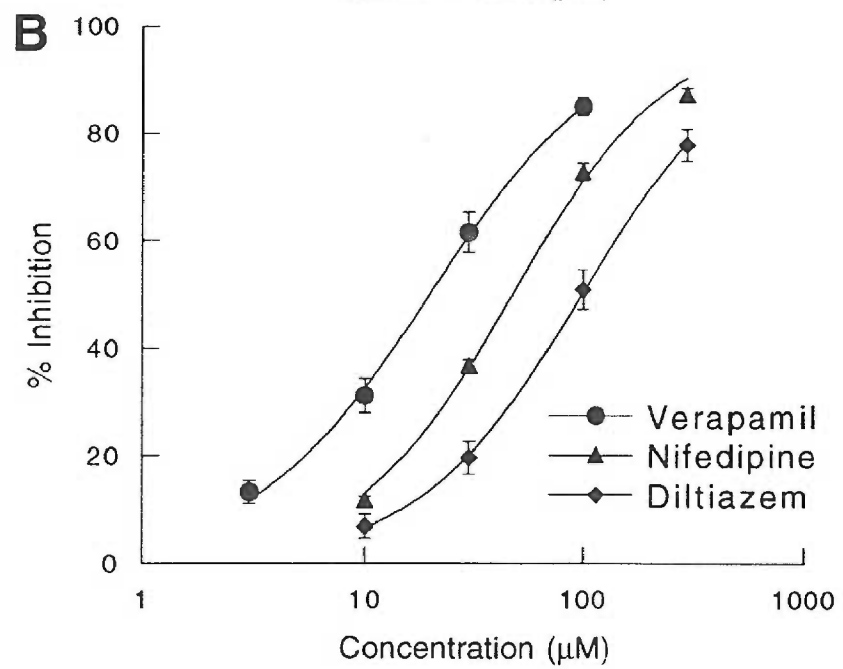
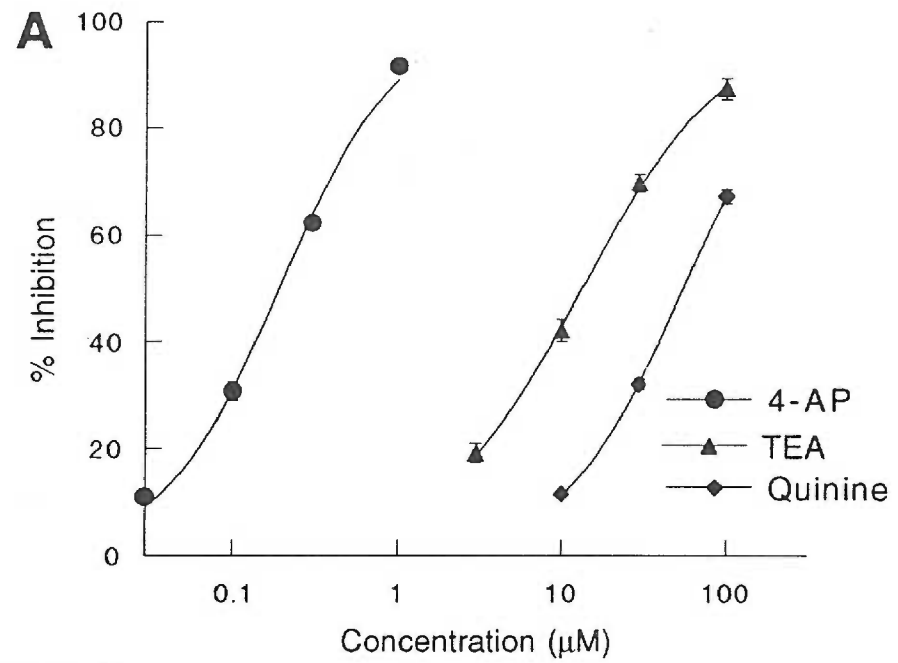


FIGURE 3.6

$[^3\text{H}]$ thymidine incorporation plot of ConA stimulation of human T cells

Human T lymphocytes were plated at a density of $2.5 \times 10^6/\text{ml}$ in the presence of different concentrations of ConA as noted. The cells were incubated for 76 hr with the addition of 1 μCi of $[^3\text{H}]$ thymidine for the last 4 hr. The $[^3\text{H}]$ thymidine incorporation was then determined.

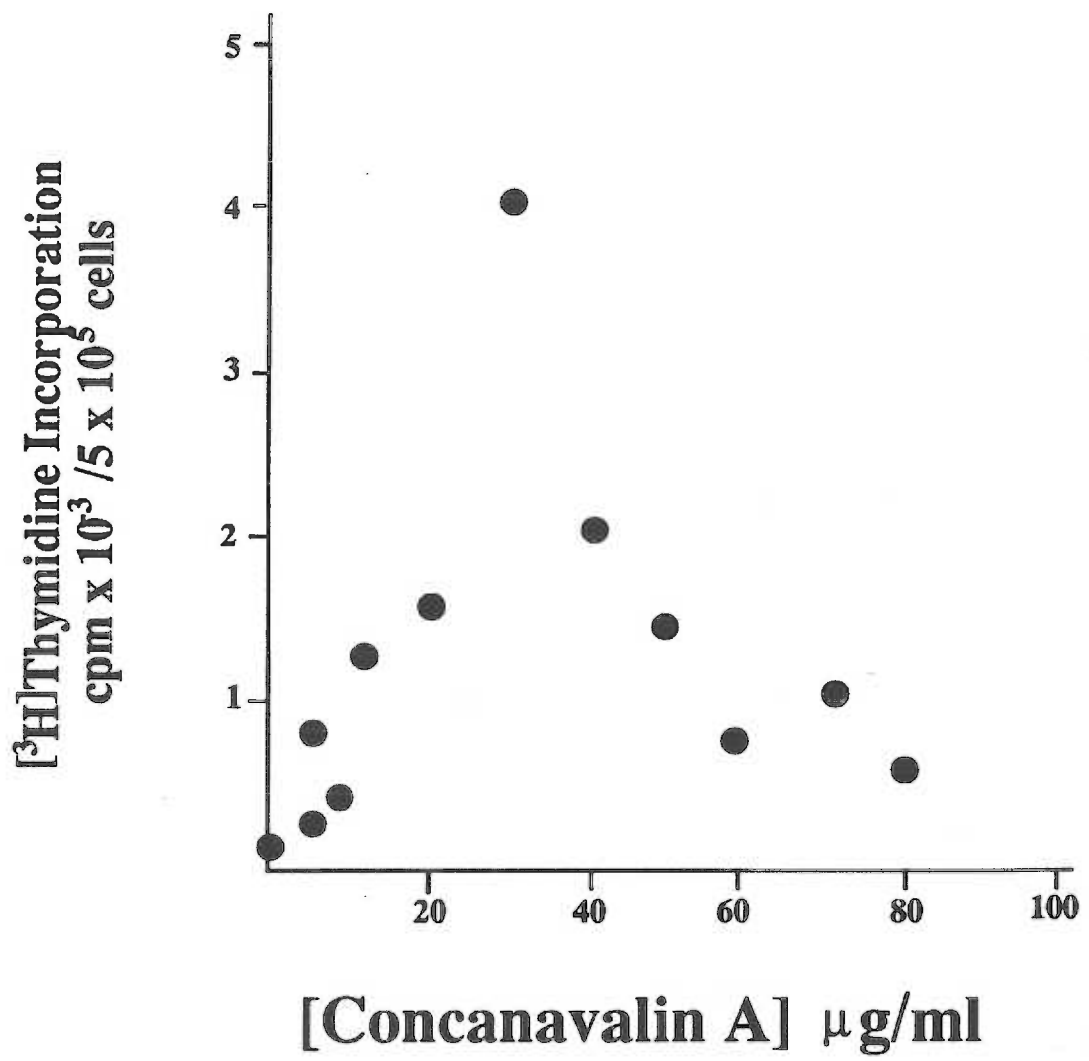


FIGURE 3.7

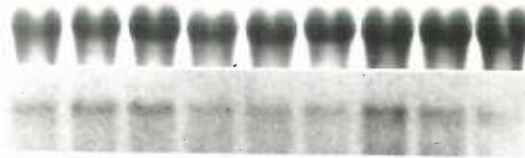
Effects of concanavalin A treatment on cellular levels of HGK5 mRNA in human T lymphocytes

Human T lymphocytes were treated with concanavalin A; concentration and duration of treatment are noted. 20 µg of total RNA was subjected to Northern blot analysis. 28S rRNA was detected by staining with methylene blue. HGK5, cyclophilin and IL-2 receptor mRNA was detected following hybridization with [³²P]-radiolabelled cRNA or DNA probes. 28S rRNA and HGK5 mRNA levels (from these blots, and others) were semi-quantitated by laser densitometry. Following standardization to 28S rRNA levels, relative levels of HGK5 mRNA in stimulated cells were compared to those in non-stimulated cells (lower). The values shown represent the average from two separate experiments utilizing different preparations of human T lymphocytes.

Con A Treatment

concentration ($\mu\text{g/ml}$)
duration (hours)

0 4 40 0 4 40 0 4 40
4 \longrightarrow 8 \longrightarrow 16 \longrightarrow



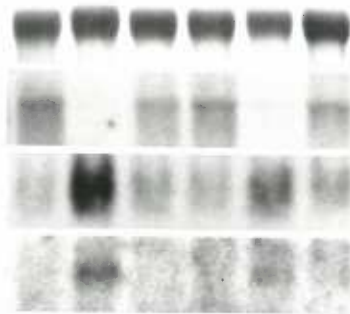
Probe

28S rRNA

HGK5 mRNA

concentration ($\mu\text{g/ml}$)
duration (hours)

0 40 4 0 40 4
48 \longrightarrow 72 \longrightarrow



28S rRNA

HGK5 mRNA

cyclophilin mRNA

IL2 receptor mRNA

Relative Intensity
HGK5 mRNA

$\frac{\text{Stimulated Cells}}{\text{Non-stimulated Cells}}$

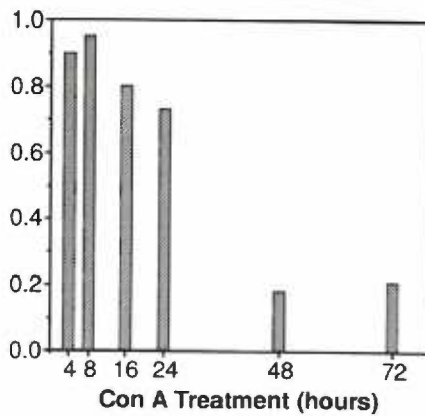


TABLE 3.1

Comparison of functional properties of HGK5 and human T lymphocyte type *n* potassium channels ^a

a HGK5 currents were characterized as described in Figure 3.3. Human type *n* currents were characterized from purified human T lymphocytes using gigaohm-seal patch clamp technology in either a whole cell recording configuration, or an outside-out patch recording configuration. The values shown for the human type *n* current within T cells are taken from the studies described in DeCoursey et al., 1984, 1985; and Cahalan et al., 1985.

b The time constant of recovery of inactivation was determined using pairs of identical pulses to +40 mV from a holding potential of -100 mV. The ratio of the peak currents during the second pulse to the first pulse were fit by a single exponential (HGK5), or double exponential (human T cell).

c Concentration at which there is 50% inhibition of peak current, measured at test potential of 0-10 mV.

d Concentrations of extracellular divalent cations ranged from 0.3 to 3.0 mM for each cation tested. The relative degree of reduction of peak current was then determined within this range of concentrations.

Data given as mean \pm sem (n = 3-5)

	Activation		Inactivation				
	midpoint (mV)	slope (mV)	midpoint (mV)	slope (mV)	t_{inact} (ms)	recovery (s) <i>b</i>	
HGK5	-12.8 ± 0.96	-8.1 ± 0.76	-28.4 ± 0.97	6.1 ± 0.57	786 ± 29	$t = 20$	
human T cell	-35.6	-5.2	-70.6	8.3	-	$t_1 = 10$	

IC_{50} ^c						
	4-AP (mM)	TEA (mM)	Quinine (μM)	Verapamil (μM)	Nifedipine (μM)	Diltiazem (μM)
HGK5	0.19 ± 0.03	13.5 ± 1.2	55 ± 2.0	20.3 ± 2.6	47.8 ± 2.7	105 ± 13
human T cell	0.2	8	14	6	24	60

Reduction of peak current by divalent cations ^d						
Most potent			Least potent			
HGK5	Ni	> Co	> Ba	> Mn	> Ca	Sr
human T cell	Ni	> Co	> Cd	> Mn	> Ca	> Sr

FIGURE 4.1

Amino acid sequence alignment of mouse, rat, and human Kv1.3 potassium channels

The Intelligenetics 'Genalign' algorithm was employed for sequence comparison analysis. mKv1.3 is derived from Chandy et al., 1990; however, there are three amino acid residue corrections based on DNA sequence analysis of a mouse cDNA clone performed in our lab. These sequence changes are represented by deletion of residues ⁴³⁵N and ⁴³⁶N, and substitution of ⁴⁹⁴Q with ⁴⁹⁴H. rKv1.3 is derived from Douglass et al., 1990. hKv1.3 is derived from Cai et al., 1991. 'm', 'r', and 'h' letterings represent mouse, rat, and human sequences, respectively.

mKv1.3 1 MTVVPGDHLLEPEAAGGGGGDPPQGGCgsgggGGGCDRYEPLPPALPAAGEQDCCGERVVI
 |||||||||||||||||||||||||||| ||||||||||||||||||||||||||||
 rKv1.3 1 MTVVPGDHLLEPEAAGGGGGDPPQGGC vsGGGCDRYEPLPPALPAAGEQDCCGERVVI
 |||||||||||||||||| ||| ||||| ||||||||||||||||||
 hKv1.3 1 MTVVPGDHLLEPEvAdGGG aPPQGGC gGGGCDRYEPLPPsLPAAGEQDCCGERVVI

mKv1.3 62 NISGLRFETQLKTLQFPETLLGDPKRRMRYFDPLRNEYFFDRNRPSFDAILYYYQSGGRI
 ||||||||||||||||||||||||||||
 rKv1.3 59 NISGLRFETQLKTLQFPETLLGDPKRRMRYFDPLRNEYFFDRNRPSFDAILYYYQSGGRI
 ||||||||||||||||||||||||||||
 hKv1.3 57 NISGLRFETQLKTLQFPETLLGDPKRRMRYFDPLRNEYFFDRNRPSFDAILYYYQSGGRI

mKv1.3 123 RRPVNVPIDIFSEEIRFYQLGEEAMEKFREDEGFLREEERPLPRRDFQRQVWLLFEYPESS
 ||||||||||||||||||||||||||||
 rKv1.3 120 RRPVNVPIDIFSEEIRFYQLGEEAMEKFREDEGFLREEERPLPRRDFQRQVWLLFEYPESS
 ||||||||||||||||||||||||||||
 hKv1.3 118 RRPVNVPIDIFSEEIRFYQLGEEAMEKFREDEGFLREEERPLPRRDFQRQVWLLFEYPESS

mKv1.3 184 gPARGIAIVSVLVILISIVIFCLETLPEFRDEKDYPASPSQDVFEAANNSTSGApSGASSF
 ||||||||||||||||||||||||||||
 rKv1.3 181 rPARGIAIVSVLVILISIVIFCLETLPEFRDEKDYPASPSQDVFEAANNSTSGAsSGASSF
 |||||||||||||||||| ||| ||| ||||| |||||
 hKv1.3 179 gPARGIAIVSVLVILISIVIFCLETLPEFRDEKDYPASStSQDsFEAAgNSTSGsraGASSF

mKv1.3 245 SDPFFVVELTLCIIWFSFELLVRRFFACPSKATFSRNIMNLIDIVAIIPYFITLGTelaERQG
 ||||||||||||||||||||||||||||
 rKv1.3 242 SDPFFVVELTLCIIWFSFELLVRRFFACPSKATFSRNIMNLIDIVAIIPYFITLGTelaERQG
 ||||||||||||||||||||||||||||
 hKv1.3 240 SDPFFVVELTLCIIWFSFELLVRRFFACPSKATFSRNIMNLIDIVAIIPYFITLGTelaERQG

mKv1.3 306 NGQQAMSLAILRVIRLVRFRIKLSRHSKGLQILGQTLKASMRELGLLIFFLFIGVILFS
 ||||||||||||||||||||||||||||
 rKv1.3 303 NGQQAMSLAILRVIRLVRFRIKLSRHSKGLQILGQTLKASMRELGLLIFFLFIGVILFS
 ||||||||||||||||||||||||||||
 hKv1.3 301 NGQQAMSLAILRVIRLVRFRIKLSRHSKGLQILGQTLKASMRELGLLIFFLFIGVILFS

mKv1.3 367 SAaYFAEADDPSSGFNSIPDAFWAVVTMTTVGYGDMHPVTIGGKIVGSLCAIAGVLTIAL
 || ||||||||||||||||||||||||||||
 rKv1.3 364 SAVYFAEADDPSSGFNSIPDAFWAVVTMTTVGYGDMHPVTIGGKIVGSLCAIAGVLTIAL
 ||||||||| || ||||||||||||||||||||||||
 hKv1.3 362 SAVYFAEADDPtSGFsSIPDAFWAVVTMTTVGYGDMHPVTIGGKIVGSLCAIAGVLTIAL

mKv1.3 428 PVPVIvSNFNIFYHRETEGEEQAQYMHVGSQHLSSSAEELRKARSNSTLSKSEYMVIEEG
 ||||| ||||||||||||||||||||||||||||
 rKv1.3 425 PVPVIISNFNIFYHRETEGEEQAQYMHVGSQHLSSSAEELRKARSNSTLSKSEYMVIEEG
 ||||| |||||||||||||||||| ||||||||||||
 hKv1.3 423 PVPVIvSNFNIFYHRETEGEEQsQYMHVGSQHLSSSAEELRKARSNSTLSKSEYMVIEEG

mKv1.3 489 GMNHSAFPQTPFKTGNSTATCTTNNNPNSCVNIKKIFTDV
 ||||||||||||||||||||||||||||
 rKv1.3 486 GMNHSAFPQTPFKTGNSTATCTTNNNPNSCVNIKKIFTDV
 |||||||||||||||||| ||||||||
 hKv1.3 484 GMNHSAFPQTPFKTGNSTATCTTNNNPNSCVNIKKIFTDV

FIGURE 4.2

Amino acid sequence of hKv1.3 regions used to generate MalE fusion proteins

Region H1 (residues 198 to 242) represents the complete extracellular domain between transmembrane domains S1/S2. Region H2 (residues 478 to 523) represents the final 46 residues at the intracellular carboxy terminus of the channel protein .

Corresponding residues and their location within other members of the mammalian Kv1 subfamily of voltage-gated potassium channels are shown. The species from which the sequence is derived is also noted (r, rat; h, human).

H1

hKv1.3	198	IFCLETLPEFR DEKDY	PAST SQDSFEAAGNSTS	G SRAGA	S	S	FSDP	242
rKv1.1	183	IFCLETLPELK DDKDFT	G	TIHRIDNTTVI YT	SN	I	FTDP	220
rKv1.2	179	SFCLETLPIFR DENED MHG		GGVTFHTYSNST IGYQQ	S	T	S FTDP	221
hKv1.4	323	IFCLETLPEFR DDRDLVMAL		SAGGHGGLLD TSAPHLEN	SGH	TI	FNDP	370
hKv1.5	266	TFCLETLPEFR DERELL	RHPPAPHQPPAPAPGANGSGVMAPP	SGP	TVAPLLPRTLA		DP	323
hKv1.6	190	IFCLETLPQFRVDGRGNNGGVS	RVSPVSRGSQEEEEDEDDSYTFHHG	ITPGEMGTGGSSSLSTLGG	SFFFTDP			262

H2

hKv1.3	478	MVIEEGGMNHSAPP	QTPFKTG NS	T A TCTTN	NPN SCVNI	KK	IFTDV	523
rKv1.1	455	MEIEED MNNSIAHYRQANIR	TG NC	T A TDQ	NCVN KS	K	LLTDV	495
rKv1.2	459	MEIQEGV NNSNEDEFREENLKT	ANC	TLANT	NYVNI T	K	MLTDV	499
hKv1.4	616	MEEGVKE	SLCA KEE KCQAKGDDSE	TDK N	NC S NA	KAVETDV		653
hKv1.5	572	LENADSARRGSCPLEKCNV	K AK	S	N VDLRRSLYALCLDTSR	ETDL		613
hKv1.6	492	TDNGLGKPDFPEAN	RE	R RP	SYLPTP HRAYAEK	R	MLTEV	529

FIGURE 4.3**Characterization of antiserum against MalE - hKv1.3 fusion proteins**

(A) Immunoprecipitation of 58-kDa, ^{35}S radiolabeled in vitro translated hKv1.3.

Lane 1, MalE-H2 antiserum - no preabsorption; Lane 2, MalE-H2 antiserum, preabsorption with the MalE-H2 fusion protein; Lane 3, MalE-H2 antiserum, preabsorption with MalE- β gal fusion protein.

(B) Immunoprecipitation of 65-kDa, ^{125}I surface-labeled mKv1.3 from the SAK8 cell line.

Lane 1, preimmune serum preabsorbed with MalE- β gal; Lane 2, MalE-H2 antiserum preabsorbed with MalE- β gal; Lane 3, MalE-H2 antiserum preabsorbed with MalE-H2. The location of protein molecular weight standards is noted. Arrows indicate the position of the 58-kDa (A), and 65-kDa (B) immunoprecipitated forms of Kv1.3.

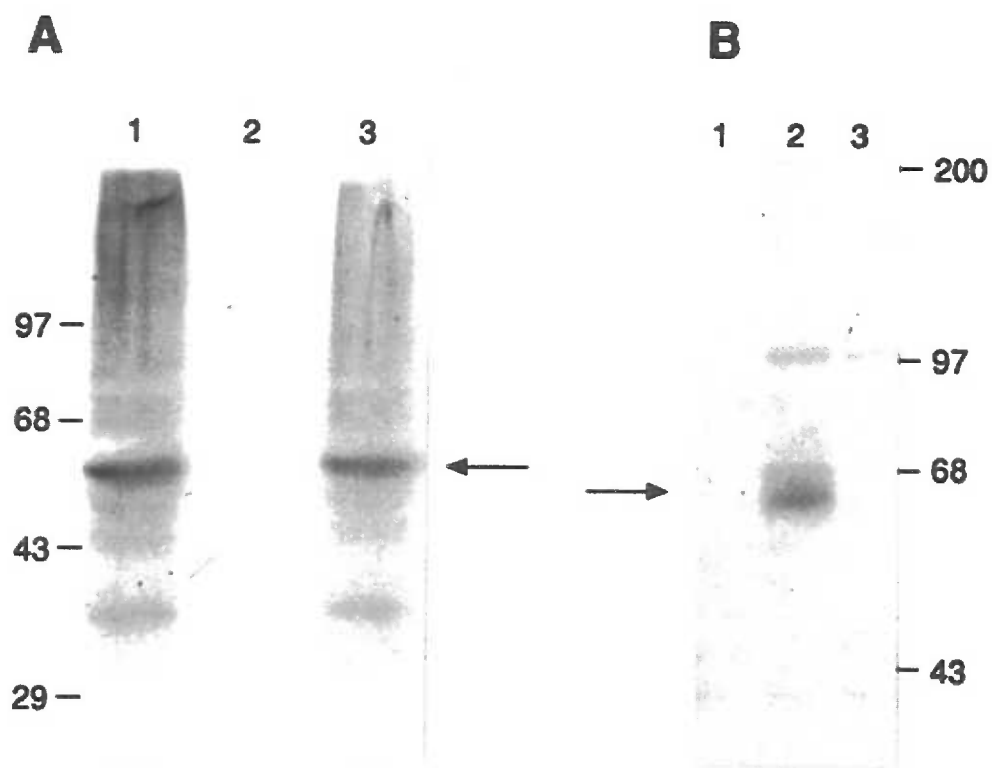


FIGURE 4.4

Immunoprecipitation of 65-kDa, ^{32}P radiolabeled hKv1.3 from metabolically labeled Jurkat cells

Lane 1, preimmune serum preabsorbed with MalE- β gal; Lane 2, MalE-H1 antiserum preabsorbed with MalE- β gal; Lane 3, MalE-H1 antiserum preabsorbed with MalE-H1. The location of protein molecular weight standards is noted. The arrow indicates the position of the 65-kDa immunoprecipitated form of Kv1.3.

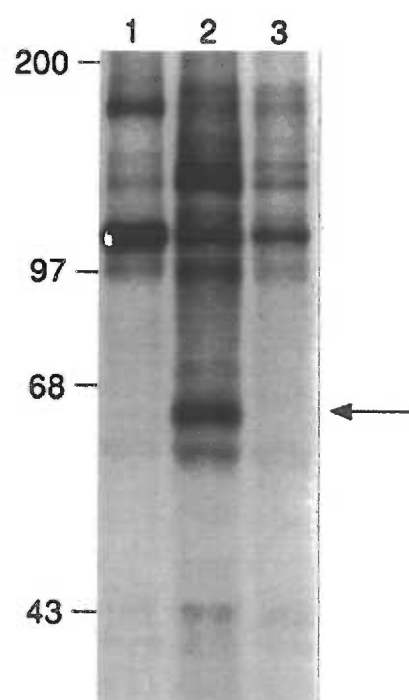


FIGURE 4.5

Phosphoamino acid analysis of 65-kDa, ^{32}P radiolabeled Jurkat hKv1.3 following immunoprecipitation with MalE-H1 antiserum

Radiolabeled immunoprecipitated hKv1.3 (as shown in Figure 4.4, lane 2) was eluted from the gel slice and subjected to phosphoamino acid analysis as described in Experimental Procedures. The region of the resulting autoradiograph localizing radiolabeled phosphoserine is shown. The location of phosphoserine, phosphothreonine and phosphotyrosine standards is also indicated.

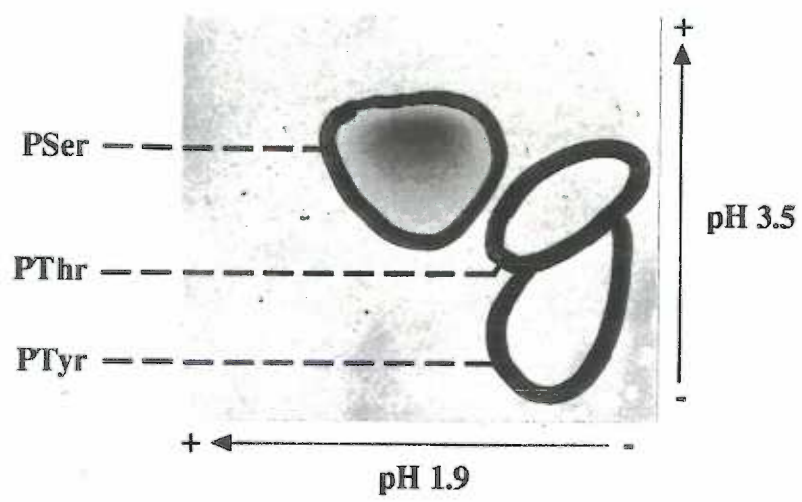


FIGURE 4.6**In vitro phosphorylation/immunoprecipitation of 65-kDa Jurkat hKv1.3 by PKA**

Lanes 1-5 represent Jurkat cell extracts not pre-treated with calf alkaline phosphatase; lanes 6-9 represent cell extracts pre-treated with alkaline phosphatase. Cell extracts in lanes 1 and 6 did not receive exogenous PKA; [γ - 32 P] ATP radiolabeled, immunoprecipitated products result from endogenous kinase activity. All other samples (lanes 2-5, 7-9) were treated with [γ - 32 P] ATP and purified PKA (catalytic subunit) for 30 minutes prior to immunoprecipitation. Immunoprecipitation reactions were as follows: lanes 1, 3, 6 and 8 used MalE-H1 antiserum preabsorbed with MalE- β gal; lanes 4 and 9 used MalE-H1 antiserum preabsorbed with the MalE-H1 fusion protein; lane 5 used MalE-H1 antiserum preabsorbed with the MalE-H2 fusion protein; lanes 2 and 7 used preimmune serum preabsorbed with MalE- β gal. Arrows note the location of the 65-kDa, radiolabeled immunoprecipitated hKv1.3 channel (lanes 1, 3, 5 and 8), as well as an hKv1.3-associated 40-kDa protein (lane 8). The location of protein molecular weight standards is also shown.

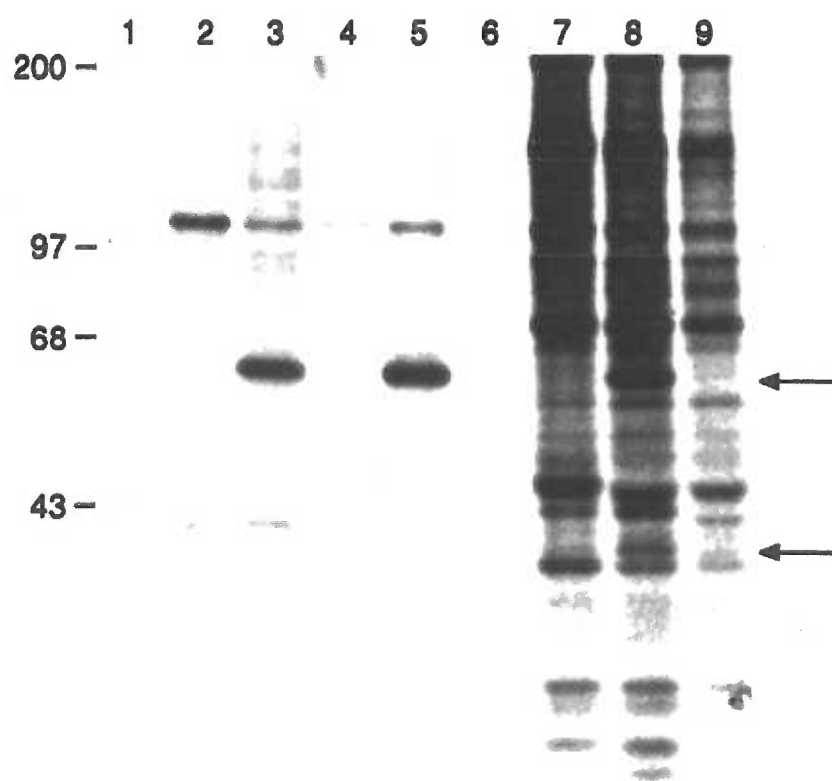


FIGURE 4.7**In vitro phosphorylation/immunoprecipitation of 65-kDa Jurkat hKv1.3 by PKC**

All Jurkat cell extracts were pre-treated with calf alkaline phosphatase. Lanes 1 and 2 are identical to lanes 8 and 9 of Figure 4.6 (PKA-treated extracts), and serve to show the location of radiolabeled 65-kDa Jurkat hKv1.3. Samples in lanes 4-6 were treated with [γ - 32 P] ATP and purified PKC for 20 minutes prior to immunoprecipitation, while the sample in lane 3 did not contain added PKC (representing endogenous kinase activity in the cell extract). Immunoprecipitation reactions were as follows: Lanes 1, 3 and 5 used MalE-H1 antiserum preabsorbed with MalE- β gal; lanes 2 and 6 used MalE-H1 antiserum preabsorbed with the MalE-H1 fusion protein; lane 4 used preimmune serum preabsorbed with MalE- β gal. The arrow notes the location of the 65-kDa, radiolabeled immunoprecipitated hKv1.3 channel (lanes 1 and 5). The location of protein molecular weight standards is also shown.

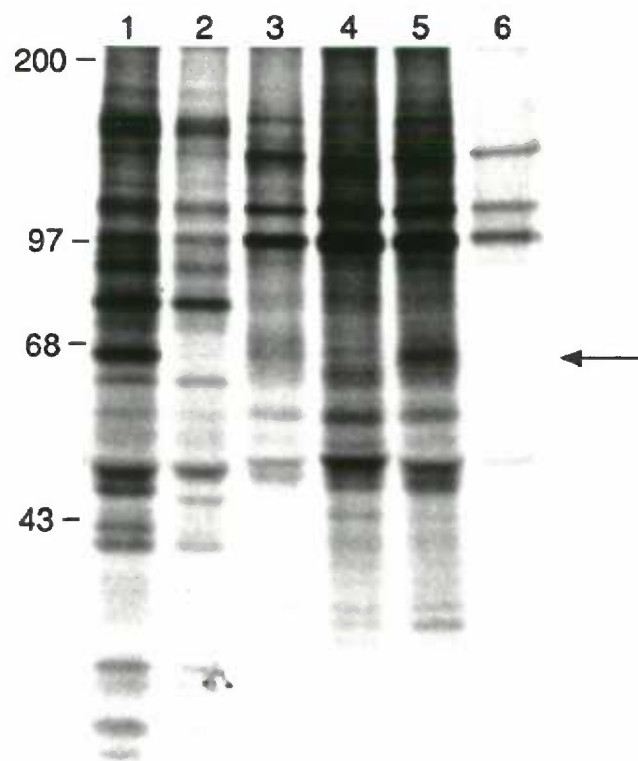


FIGURE 5.1

Amino acid sequence comparison of S4/5 loops between *ShB* (Pongs et al., 1988), hKv1.3, and rKv1.2 (McKinnon, 1989) potassium channels, as well as a list of different mutants.

The bold serine residue represents that subjected to site-directed mutagenesis. The underlined segment denotes a potential PKC consensus recognition sequence. The notations (wt) and (m) refer to wide type and mutant sequences, respectively.

ShB	(wt)	392Ser	380	KGLQILGRTLKAS M RELG
ShB	(m)	392Ala	380	----- A -----
hKv1.3	(wt)	342Ser	330	-----Q---- S -----
hKv1.3	(m)	342Ala	330	-----Q---- A -----
hKv1.3	(m)	342Asp	330	-----Q---- D -----
hKv1.3	(wt)	342Ala->Ser	330	-----Q---- S -----
rKv1.2	(wt)	324Ser	312	-----Q---- S -----
rKv1.2	(m)	324Ala	312	-----Q---- A -----

FIGURE 5.2

Mutation of hKv1.3 ³⁴²Ser to ³⁴²Ala abolishes ionic currents.

Outward potassium currents were elicited by a step to 0 mV for 200 ms from a holding potential of -80 mV. Current amplitudes for ³⁴²Ser (left) ranged from 5-20 mA (n=6). No potassium currents were observed in oocytes injected with ³⁴²Ala RNA (n=16) (center). Currents in oocytes expressing the revertant ³⁴²Ala->Ser RNA (right) exhibited properties indistinguishable from ³⁴²Ser.

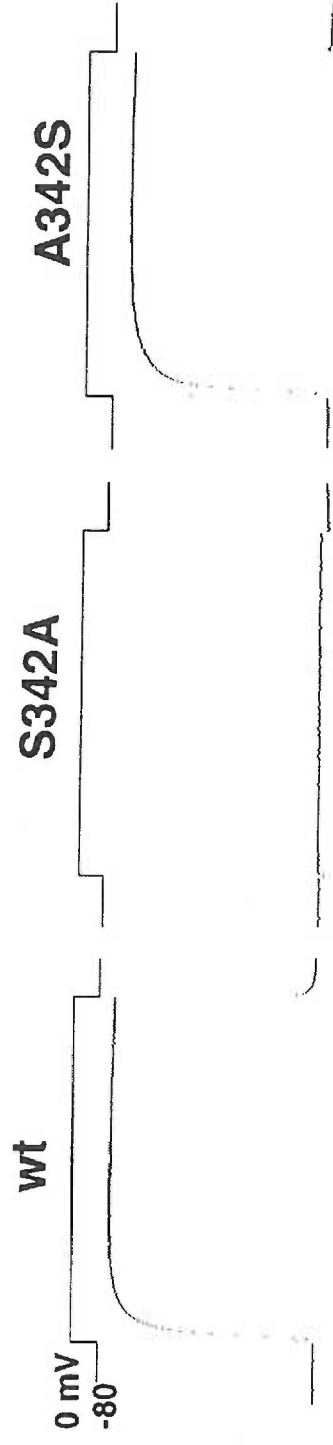


FIGURE 5.3

Gating currents of hKv1.3 ³⁴²Ser and ³⁴²Ala potassium channels.

Gating currents were recorded from oocyte membranes following injection of RNA encoding: A) ³⁴²Ser; B) ³⁴²Ala; or C) Control (uninjected) oocyte membrane.

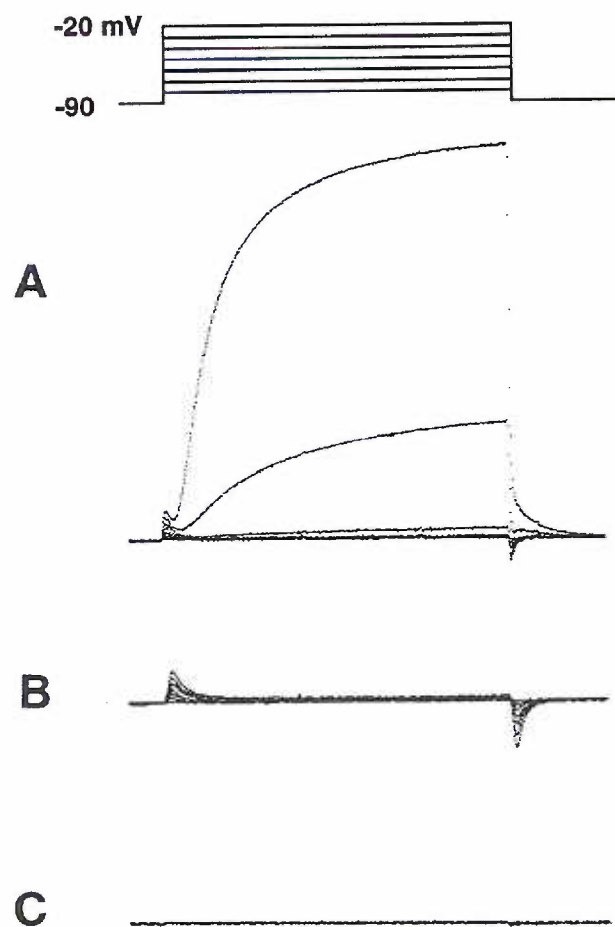


FIGURE 5.4

TEA sensitivity of expressed potassium currents indicates functional polymerization between hKv1.3 ^{342}Ala and ^{399}Tyr subunits.

Data points represent mean \pm s.e.m. for 3-6 oocytes. ^{399}Tyr , $K_d = 1.1$ mM, $n = 0.92$; ^{399}His , $K_d = 20.4$ mM, $n = 0.85$; coinjected $^{342}\text{Ala} + ^{399}\text{Tyr}$, $K_d = 2.3$ mM, $n = 0.76$.

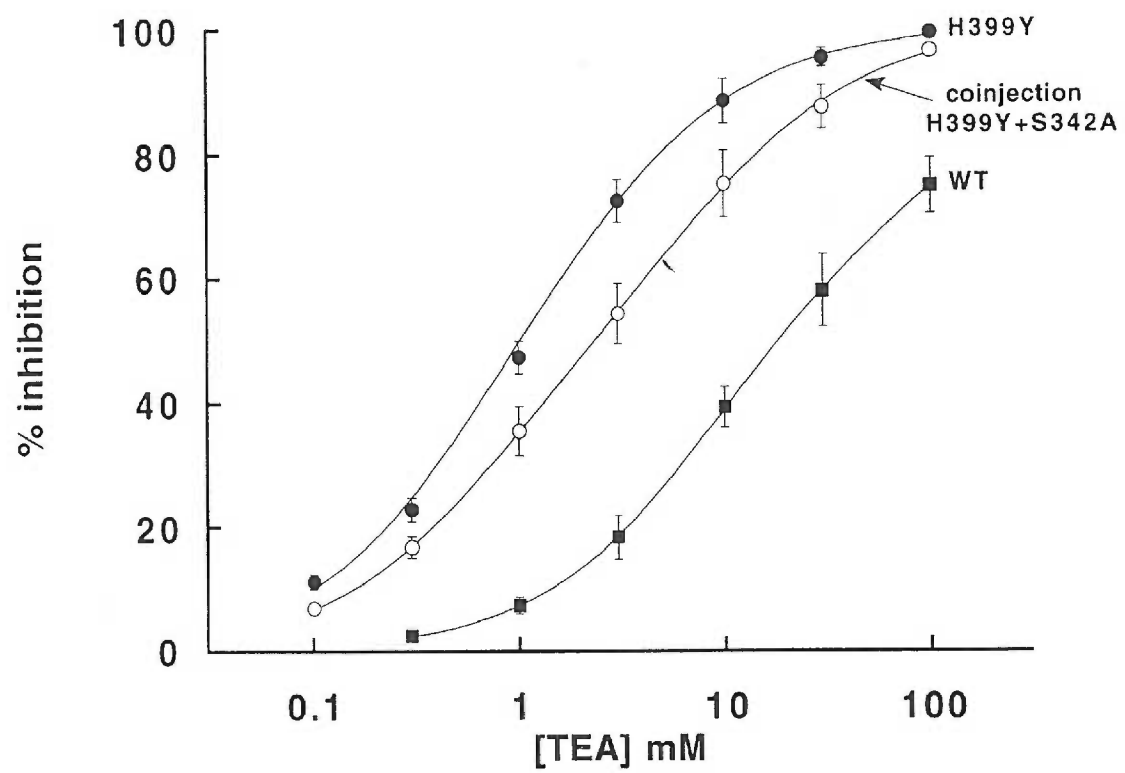


FIGURE 6.1

Amino acid sequence alignment of the S4/5 loops among voltage-gated and calcium-activated potassium channels.

The bold letter represents the highly conserved serine residue located within the PKC consensus sequence (R/K-x-S-x-R/K, where x can be any residue), which is underlined.

References for these sequences are included as dShB (Pongs et al., 1988); rKv1.1 (Baumann et al., 1988); rKv1.2 (McKinnon, 1989); xKv1.2 (Ribera, 1990); hKv1.3 (Cai et al., 1992); rKv1.4 (Stuhmer et al., 1989); rKv1.5 and rKv1.6 (Swanson et al., 1990); dShab, dShaw, and dShal (Wei et al., 1990); rKv2.1 (Frech et al., 1989); mKv3.1 (Yokoyama et al., 1989); rKv3.2 (McCormack et al., 1990); dSlow, which is a calcium-activated potassium channel, (Atkinson et al., 1991). The low-case letter in front of each nomenclature denotes the species from which the amino acid sequence was derived. d, *Drosophila*; x, *Xenopus*; m, mouse; r, rat; and h, human.

dShB	KGLQILGRTLKASMR	ELG
rKv1.1	-----Q-----	---
rKv1.2	-----Q-----	---
xKv1.2	-----Q--N----	---
hKv1.3	-----Q-----	---
rKv1.4	-----H--R----	---
rKv1.5	-----K--Q-----	---
rKv1.6	-----K--Q-----	---
dShab	-----S--F--RN-YK	---
rKv2.1	T---S--F--RR-YN	---
dShaw	S--K--IQ-FR--AK	--T
mKv3.1	V--RV--H--R--TN	-FL
rKv3.2	V--RV--H--R--TN	-FL
dShal	Q--R---Y--- -CAS---	
dSlow	DI--Y-NV --T-SSIR--	